Unraveling the Role of the X Chromosome in Cancer:

Characterization of FOXP3 Isoforms and PR70 in Cutaneous Melanoma

Margaret Redpath, Department of Pathology, McGill University, Montreal

Submitted December 2018

A thesis submitted to McGill University in partial fulfillment of the requirements of the degree of Pathology Doctor of Philosophy

Table of Contents

Page

Abstract

Many cancers have a different incidence, behavior and response to treatment in men and women. Traditionally these sex-specific variations have been attributed to differences in habits, occupational exposures and hormones. More recently it has been recognized that some of the dissimilarities can be attributed to genetics. We were particularly struck by the significant increase in the incidence and mortality of melanoma in men. The objective of this project was to characterize how the X chromosome contributes to this effect. Global analysis of genomic alterations revealed that a somatic loss of one X chromosome in females was significantly associated with a worse prognosis in melanoma. We further showed that it was the inactive X that was lost in all cases. This led to the hypothesis that an activating mutation of an oncogene, or inactivating mutation of a tumor suppressor gene, on the remaining X chromosome in these patients was contributing to tumor aggressiveness. PR70 and FOXP3 were identified as warranting further investigation as candidate X-linked tumor suppressors in melanoma based on their behaviour in other tumor types.

The *PPP2R3B* gene (Xp22.33) encodes for PR70, the regulatory subunit of a protein phosphatase that plays a critical role in cell cycle progression. In melanoma a strong correlation is demonstrated between low levels of PR70 mRNA expression and poor distant metastasis-free survival by multivariate analyses. In line with this, no or low PR70 protein expression is associated with poor overall survival in three independent sample sets of melanoma. Endogenous and exogenous PR70 expression levels are shown to have an inverse correlation with the rate of melanoma cell proliferation. Exogenous PR70 overexpression decreases tumor take and growth in nude mice compared to shRNA-mediated downregulation that increases it.

The *FOXP3* gene (Xp23.11) encodes a transcription factor that is important for T-regulatory cell development. Interestingly, FOXP3 was also found to be expressed in the majority of our melanoma cell lines at both the mRNA and protein level. All five of the known isoforms of FOXP3 were shown to localize to the nucleus in melanoma cell lines and demonstrated isoform- and cell line-specific effects on gene transcription. Both PR70 and FOXP3 are associated with a dose-dependent decrease in melanoma cell proliferation with an accumulation of cells in the G1 phase of the cell cycle. These findings are significant because proliferative rate is one of the strongest independent prognostic factors in melanoma.

De nombreux cancers ont une incidence, un comportement et une réponse au traitement différents chez les hommes et chez les femmes. Traditionnellement, ces variations spécifiques liées au sexe ont été attribuées à des différences entre les sexes dans les habitudes, l'exposition professionnelle et le statut hormonal. Plus récemment, il a été reconnu que certaines de ces différences peuvent être attribuées à la génétique. Nous avons été particulièrement frappés par l'augmentation significative de l'incidence et de la mortalité du mélanome chez l'homme. L'objectif de ce projet était de caractériser la contribution du chromosome X à cet effet. L'analyse globale des altérations génomiques a révélée qu'une perte somatique d'un chromosome X chez les femmes est associée de manière significative à un pronostic plus défavorable du mélanome. Nous avons en outre montré que c'est le X inactif qui est perdu dans tous les cas. Cela a conduit à l'hypothèse qu'une mutation activatrice d'un oncogène, ou une mutation inactivatrice d'un gène suppresseur de tumeur sur le chromosome X restant chez ces patients contribuent à l'agressivité de la tumeur. *PPP2R3B* et *FOXP3* ont été identifiés comme des gènes justifiant une investigation plus poussée en tant que gènes suppresseurs de tumeurs liés au chromosome X dans le mélanome

en raison de leur comportement dans d'autres types de tumeurs. Nous avons démontré que ces gènes sont exprimés dans la majorité de nos lignées cellulaires au niveau de l'ARNm et des protéines. L'expression de *PR70* endogène et exogène est significativement corrélée à une diminution de la prolifération. Dans le mélanome humain, il existe une forte corrélation entre les faibles taux d'expression de l'ARNm du PR70 et la faible survie sans métastase à distance par les analyses multivariées. Dans cette optique, une expression nulle ou faible de la protéine PR70 est associée à une faible survie globale dans trois cohortes indépendantes de mélanome. La surexpression de PR70 exogène diminue la prise de tumeur et la croissance chez les souris nues, contrairement à la baisse de l'expression de PR70 induite par shRNA qui l'augmente. PR70 et le FOXP3 sont tous deux associés à une diminution dose-dépendante de la prolifération cellulaire du mélanome avec une accumulation de cellules dans la phase G1 du cycle cellulaire. Ces résultats sont d'importance *in vivo* car la prolifération est l'un des facteurs pronostiques indépendants les plus forts dans le mélanome.

Acknowledgements

Alan Spatz: Supervision, advice, experimental design, writing of the manuscripts and editing of the thesis.

Leon van Kempen: Supervision, advice, experimental design, writing of the manuscripts and editing of the thesis. Performed cell culture and animal experiments.

Josie Ursini Segal: Advisor

Vassilios Papadopoulos: Advisor

Mounib Elchebly: Advice and provided training in methodology. Performed cell culture and biochemical experiments.

Marie-Noël M'Boutchou: Performed cell culture, flow cytometry and biochemical experiments.

Jonathan Jarry: Performed DNA extraction

Celia Greenwood: Statistical analysis

Kathleen Klein: Statistical analysis

Kishanda Vyboh and Osama Roshdy: Performed flow cytometry experiments

Anke van Rijk: DNA and RNA FISH

Christian Young: Support with the flow cytometry experiments

Richard Scolyer, James Wilmott, Joost van den Oord, Fredrik Pontén, Per-Henrik Edqvist, Dirk Schadendorf: Provided melanoma TMA tissue and clinical data

Ghanem Ghanem: Provided melanoma cell lines.

I received a Doctoral Training Award from the Fonds de Recherche Sante Quebec (FRQS), a CIP Clinical Fellow Award from McGill and a Pathology Graduate Excellence Fellowship from McGill to complete this research.

Contribution to original knowledge

Despite the fact that only a small fraction of all coding and non-coding genes are located on the sex chromosomes, there is growing evidence that the gonosomes are responsible for some of the major differences between the manifestation of disease in men and women. We have shown that two functional X chromosomes are associated with longer distant metastasis-free survival compared to women who have lost an X chromosome or males who only have one. In particular two X-linked genes have been identified that behave as tumor suppressors in melanoma. Exogenous *FOXP3* expression results in a dose-dependent decrease in proliferation in melanoma cells with an accumulation of cells in the G1 phase of the cell cycle. In addition to being an important transcription factor in T-regulatory cell development, we have demonstrated that all of the FOXP3 isoforms localize to the nucleus and show isoform-specific effects of target gene transcription levels in melanoma cells. Furthermore, *PPP2R3B* encodes for PR70 that localizes to the nucleus and cytoplasm and is associated with a decrease in the rate of melanoma cell proliferation *in vitro*, *in vivo* and *ex vivo*. Through dephosphorylation of CDC6, PR70 delays entry into the S-phase of the cell cycle. Furthermore, PR70 is shown to decrease tumor take *in vivo* in mice and to be a strong prognostic factor for distant metastasis-free and overall survival in human melanoma patients.

Chapter 1- Introduction

The X and Y chromosomes are most widely known for their role in determining the sex of an individual. However it is important to realize that the sex chromosomes are found in every cell in our bodies and have an impact on the biology of all of our organs. Besides conditions that are unique to one sex, such as cervical and prostate cancer, many non-sex restricted diseases have a different incidence, symptomatology, progression and response to treatment in men and women. The sex effect in disease is a reflection of a combination of the impact of sex chromosomes and sex steroids on cellular function. In 1993, the National Institutes of Health (NIH) recognized the important role that sex plays in normal physiology and disease by implementing the Revitalization Act requiring scientists to include female participants in human studies. Prior to that change, a lot of the information that was obtained regarding diseases and responses to treatments pertained specifically to males and led to a lack of translation from research to the clinical setting. The repercussion of this investigational bias was that the majority of the drugs that were introduced to the market were later withdrawn due to adverse events in women (Miller, 2014). In an age where personalized medicine is quickly becoming the norm, understanding and recognizing differences between the sexes in terms of the prevalence and behaviour of disease, as well as the responses and risk of side effects to therapy, is critical to tailoring health care to individual patients with optimal results.

Some of the genes that are found in both sexes are controlled by hormone-responsive elements that lead to differences in the direction and/or magnitude of expression of the gene products in males and females. These genes also show differential regulation throughout the lifespan of an individual as the hormonal milieu changes throughout development from a prepubescent to adolescent to adult of reproductive age to post-menopausal/andropausal stage of

life. Other genes, located specifically on the sex chromosomes, can show differential expression in males and females due to differences in the absolute copy number of the gene. Expression levels of genes on the X chromosome can also vary due to the effects of X chromosome inactivation and genetic imprinting related to the inheritance of maternal vs paternal X chromosomes (Wizemann & Pardue, 2001). The pseudoautosomal regions of the sex chromosomes are located at the distal tips of the short and long arms of the X and Y chromosomes. These pseudoautosomal genes are essentially identical as they undergo recombination during meiosis. In contrast, homologous regions on the X and Y chromosomes have genes that are similar, but not identical, as they do not undergo recombination and show genetic divergence from common ancestor sequences.

Early in female development, somatic cells undergo a process of X chromosome inactivation. Whether the maternal or paternal X chromosome is silenced in an individual cell is thought to be due to random selection that leads to mosaic expression of X chromosome alleles throughout the female body. Depending on whether or not the gene is subject to inactivation, females can be homozygous or heterozygous for X-linked genes. In contrast, males are inherently hemizygous for the X-linked genes that do not have paralogues on the Y chromosome. This difference in zygosity, combined with the fact that females are epigenetic/functional mosaics of X-linked genes, gives rise to differences in the incidence and severity of the phenotype of X-linked diseases. Dominant mutant alleles can be fatal to males in utero and thus the disease only manifests in women. For example, mutations in the *IKBKG* gene are lethal in males and result in a relatively benign condition in females called incontinentia pigmenti. Female carriers of a dominant mutation in an X-allele tend to display a milder disease phenotype because this trait is only expressed in cells in which the dominant allele is on the active X. The manifestations of the disease can be further diminished or abrogated in females by selective pressures favoring cells with inactivation

of the mutant allele. In some of the diseases with an increased prevalence in females a non-random, or skewed, pattern of X chromosome inactivation has been observed that is believed to contribute to the pathogenesis of certain diseases such as scleroderma (Ozbalkan et al., 2005).

In the context of cancer, dominant oncogenic mutations are dominant acting in male tumors but only dominant acting in female cells when they are located on the active X. Skewing of X chromosome inactivation can occur because cells with oncogenic mutations on the active X will have a survival advantage over cells with oncogenic mutations that are silenced on the inactive X. Alternatively, negative selection of cells with wild type tumor suppressor genes located on the active X chromosome will occur in females with heterozygous loss of function mutations in recessive X-linked tumor suppressor genes. This results in skewing of X chromosome inactivation because compared to cells with the wild type allele being silenced on the inactive X, these cells will have intact mechanisms that suppress proliferation and/or induce apoptosis. Since men only have one X chromosome, recessive X-linked tumor suppressor genes behave in a dominant fashion for them because a single mutation is sufficient for loss of function of a tumor suppressor protein.

With time the relative expression of the maternal and paternal genes can be skewed if there are selective pressures or growth advantages that are distinct between the two alleles. In the harsh conditions created by tumors skewing of X chromosome inactivation can be exacerbated by the positive selection of clones that have traits that help the cells survive longer or proliferate faster in oxygen or nutrient deprived environments. In Wilms tumor for example, mutations of the X-linked gene *WTX* have been found in sporadic tumors in males and females with heterozygous mutations in females selectively targeting the active X-chromosome in all cases (Rivera et al., 2007). Similarly in breast cancer, mutations in an X-linked tumor suppressor gene, *FOXP3,* have been

shown to occur exclusively in the active X with skewed inactivation of the wildtype allele (Zuo et al., 2007).

Some X-linked tumor suppressor genes can provide a protective advantage to females by increasing their baseline expression by escaping inactivation. Approximately 15% of genes on the X-chromosome escape inactivation under normal conditions. Depending on the gene, the tissue involved, and the individual, this can lead to expression of genes from the inactive X that range from low amounts to levels comparable to the active X. Which genes escape, and to what degree, has been shown to differ between females and cell types. In addition to the genes that regularly escape inactivation, spontaneous reactivation of single X-linked genes is estimated to occur with a frequency of $<10^{-8}$ in somatic cells. In breast cancer cells the rate of reactivation has been observed to be significantly higher due to a decreased density of Xist RNA on the inactive X that is associated with decreased histone methylation, decreased promotor methylation, increased histone acetylation and an increased presence of RNA polymerase II. This results in transcription of genes from the inactive X that normally do not escape inactivation (Chaligne et al., 2015). Interestingly, this epigenetic instability of tumor cells also results in silencing of some genes that normally escape X chromosome inactivation. Even low level differences in the expression of certain genes, such as those encoding transcription factors, can have profound effects on downstream targets that lead to significant, physiologically relevant changes in cellular function. X-linked genes can affect a variety of cell functions through their involvement in cell metabolism, development, growth, protein synthesis, coagulation, innate immunity, adiposity, blood pressure and apoptosis.

These mechanisms of X chromosome imprinting, inactivation and skewing undoubtedly contribute to some of the differences in the behaviour of diseases in men and women, but to what

degree is not yet known. Lupus, pulmonary hypertension, migraines and Raynaud's disease are just a few examples of conditions with a strikingly increased prevalence in females. Examples of disease with an increased prevalence in males include autism, schizophrenia, myocarditis and heart failure with reduced ejection fraction. One category of disease where males are at a particular disadvantage is cancer. Men are at an increased risk of developing cancer in general and have a particularly high relative risk of acquiring head and neck carcinoma, Kaposi sarcoma, bladder and esophageal cancers. Data from 60 countries was compiled and men were found to have an increased incidence of cancer in 32 out of the 35 anatomic sites that were analyzed (Edgren, Liang, Adami, & Chang, 2012). While differences in smoking and alcohol consumption habits and occupational exposures to benzenes, ionizing radiation and toxic metals have been shown to explain some of the sex-related differences in cancer incidence, there is also evidence that genomic factors play a significant role. Exome sequencing data in tumor types that are more common in males revealed six genes that are more prone to loss of function mutations or DNA copy number loss in male cancers (Dunford et al., 2017). Interestingly all of these genes are located in the non-pseudoautosomal region of the X chromosome and many were previously shown to behave as tumor suppressor genes. Tumors can circumvent the protective effect of an autosomal or gonosomal tumor suppressor gene through chromosome loss, coding mutations causing inactivated or truncated proteins, non-coding mutations affecting transcriptional or translational regulation and epigenetic changes. Additionally X-linked tumor suppressor genes can become inactivated through mechanisms such as skewing of X-inactivation or aberrant inactivation of individual genes.

In females the X chromosome is one of the most frequently aneuploid chromosomes in cancer, suggesting that aberrant expression of X-linked genes is important for tumor survival

(Dunford et al., 2017). The first objective of this project is to investigate if there are gains or losses of the X chromosome in melanoma and whether these changes affect the active or inactive X. X-linked tumor suppressor genes have the potential to provide relative protection from tumor initiation and progression in females with two X-chromosomes, which may also explain why men are at an increased risk of both developing melanoma and dying from it. So in addition to analyzing genomic alterations and X-inactivation status, the aim of this research is to identify specific X-linked tumor suppressor genes. *PPP2R3B* is a gene located at Xp22.33 that caught our attention because its protein product is PR70, a regulatory subunit of a protein phosphatase that is a negative regulator of DNA replication, cell cycle progression and mRNA translation. It has the potential to be a powerful tumor suppressor through a dual mechanisms of inhibition of the initiation of transcription through dephosphorylation of CDC6 and blocking of cell cycle progression through dephosphorylation of Rb. Genes associated with replication, including replication of origins firing and separation of sister chromatids, have been reproducibly shown to predict metastasis and death (Spatz, Stock, Batist, & van Kempen, 2010). We decided to study how PR70 behaves in melanoma because it has the potential of being a strong, prognostic factor that can shape future therapies.

FOXP3 is another promising candidate gene on the X chromosome that is worth investigating in melanoma because it has been shown to behave as a tumor suppressor in several different types of cancer. FOXP3 is a transcription factor that downregulates the expression of important oncogenes in breast and prostate cancer. Some of these oncogenes, such as c-Myc, are commonly activated in melanoma so FOXP3 has the potential to act as a tumor suppressor in melanoma as well. In other cancers FOXP3 has been shown to have tumor promoting properties through its interaction with the immune environment. This is not surprising given that FOXP3 is an important transcription factor in lymphocyte differentiation. FOXP3 expression in T-

lymphocytes generates a T-regulatory phenotype with the upregulation of cell surface markers that signal other inflammatory cells to calm down. These signals are essential for preventing autoimmune disease and are normally turned on at the end of an inflammatory response when effector cells are no longer required. It is worth investigating if FOXP3 expression in melanoma cells can lead to expression of chemokines, cytokines or cell surface markers that can help the tumor cells escape immunosurveillance. This could be achieved by directly suppressing the local inflammatory cells, by preventing recruitment of effector cells or by summoning T-regulatory cells for protection. If FOXP3 has the potential to modulate the tumor infiltrating cells in melanoma this could have a major impact on tumor survival and response to treatment. Many of the newer melanoma therapies involve stimulating the immune system so FOXP3 has the potential to be an important predictive biomarker of response to treatment.

The main objective of this project is to better understand how the X chromosome contributes to the strong sex effect that is observed in cutaneous melanoma. This will be achieved by taking an in depth look at the biology of melanoma with a global analysis of genomic alterations, X-inactivation status and the characterization of two potential X-linked tumor suppressor genes in detail, *FOXP3* and *PPP2R3B*.

Chapter 2- Review of relevant literature

Compared to woman, males are at an increased risk of developing most types of cancer. Likewise, females with Turner syndrome, who like men have only one normal copy of the X chromosome, are also at a significantly increased risk of developing malignancies in general and melanoma in particular (Ji, Zöller, Sundquist, & Sundquist, 2016). In contrast, males with Klinefelter syndrome, who have an increased number of X chromosomes, are found to be relatively protected from the development of solid tumors. Because women with Turner syndrome often develop premature dysfunction of their ovaries and men with Klinefelter syndrome often have small testes, these naturally occurring models of altered numbers of X chromosomes are imperfect paradigms for teasing out the relative contributions of sex hormones and sex chromosomes in cancer biology.

A model was recently developed to investigate the impact of sex chromosomes and sex hormones on the development and progression of cancer by uncoupling the sex chromosome complement in a mouse from the development of gonads and production of sex-specific hormones (Kaneko & Li, 2018). By moving the *SRY* gene from the Y chromosome to an autosome, they were able to generate four different scenarios: a genetic XY mouse with testes, an XX mouse with testes, an XX mouse with ovaries and an XY mouse with ovaries. When these mice were exposed to a bladder cancer inducing chemical they showed that an XY genotype and the presence of testes were both independently associated with an increased risk of developing bladder cancer and dying from it. They further identified *KDM6A* as an X-linked tumor suppressor that has a protective effect in their mouse model and is associated with a better prognosis in humans using clinical data extracted from The Cancer Genome Atlas. *KDM6A* has also been shown to act as a tumor suppressor in lymphoma and mutations are associated with multiple myeloma, esophageal

squamous cell carcinoma, renal clear cell carcinoma, myeloid leukemia, glioblastoma, breast, colorectal and pancreatic cancer (Li et al., 2018; Van Haaften et al., 2009; Bailey et al., 2016). Many other groups have been interested in finding tumor suppressor genes that contribute to the increased incidence and worse prognosis of cancer in men. Exome sequencing data of tumors that have a higher incidence in men were screened for mutations that occur more frequently in men and six X-linked genes were identified *ATRX, CNKSR2, DDX3X, KDM5C, KDM6A* and *MAGEC3* (Dunford et al., 2017). Mutations in many of these genes have been found in a variety of cancers, some of which showed tumor suppressive effects.

As previously discussed, we chose to focus our attention on *PPP2R3B* as a potential tumor suppressor in melanoma. This gene is located on the pseudoautosomal region of the sex chromosomes (Xp22.3, Yp11.3) and encodes for a protein called PR70 that is a member of Protein Phosphatase 2A (PP2A) family. PP2A is an important family of phosphatases in human cells and its dysregulation has been associated with the development of cancer, autoimmune disease, neurodegenerative disorders and cardiovascular disease (Meeusen & Janssens, 2018; Sharabi, Kasper, & Tsokos, 2018; O'Connor, Perl, Leonard, Sangodkar, & Narla, 2018). Mechanisms of PP2A inhibition in disease include genetic mutations, promotor methylation, post-translational modifications, endogenous inhibitor proteins and exogenous viral inhibitory proteins (Kauko & Westermarck, 2018). PP2A has an effect on several important pathways including cell growth, metabolism, cell cycle progression, migration, proliferation and survival.

The PP2A family is comprised of a group of heterotrimeric proteins that are formed by different combinations of the 3 subunits. The core dimer of the holoenzyme functions as a serine/threonine phosphatase and consists of a structural scaffolding subunit A and a catalytic subunit C. The regulatory subunit B provides substrate specificity to the holoenzyme and affects

subcellular localization. It is encoded by a diverse set of genes that have been grouped into four non-homologous families: B, B', B'' and B'''. Post translation modifications of the core dimer affect its affinity for particular B subunits and allows for tissue specific control of the phosphatase (Perrotti & Neviani, 2013). PR70 is an X-linked member of the B'' family that has been shown to direct phosphatase activity towards targets that are involved in DNA replication (CDC6) and cell cycle progression (pRB) (Davis, Yan, Martinez, & Mumby 2008; Magenta et al., 2008). Some of the regulatory B subunits are quickly degraded when they are not associated with the A and C subunits, whereas others are more stable in the free form. PR70 has been shown to stable in its unbound state and to maintain its ability to bind to CDC6 even when it is not associated with the A/C dimer (Davis et al., 2008). This highlights the opposing roles that PR70 overexpression can have on its protein targets; when associated to the A/C dimer it can lead to dephosphorylation but as a free protein it can exert a dominant negative effect by binding to its target and preventing recruitment of the PP2A heterotrimer. It is not known how PR70 behaves in cancers, including melanoma.

FOXP3 is another X-linked protein whose action in melanoma is unknown. Female mice that have germline heterozygous mutations of *FOXP3* are at increased risk of developing multiple spontaneous malignancies with a 90% incidence of cancer by two years of age. Analysis of the mammary carcinomas that developed in these mice showed skewed X chromosome inactivation such that the X containing the wild-type *FOXP3* allele was inactivated in all cases (Zuo et al., 2007). In human males a single mutation in *FOXP3* has been shown to be equally debilitating with prostate cancers often harboring somatic *FOXP3* deletions or missense mutations that lead to reduced expression levels compared to benign prostatic epithelial cells in the same patient (Wang

et al., 2009). To better understand the potential role of FOXP3 in melanoma an in depth look at the structure and regulation of FOXP3 is required.

The dual role of the X-linked *FoxP3* gene in human cancers.

Publication: Redpath, M., Xu, B., van Kempen, L. C., & Spatz, A. (2011). *Molecular Oncology*, *5*(2), 156–163.

Contributions of authors: Margaret Redpath, Bin Xu, Leon van Kempen and Alan Spatz contributed to the writing of this manuscript.

"After decades of continuous failures, ipilumimab - which blocks cytotoxic T-lymphocyte-associated antigen 4 (CTLA-4) was recently demonstrated to improve overall survival in patients with previously treated metastatic cutaneous melanoma. Ipilimumab, with or without a gp100 vaccine, was associated with improved survival as compared with gp100 alone (Hodi et al., 2010). This is the first ever reported positive phase 3 trial in advanced melanoma. Ipilumimab blocks CTLA-4 and this blockade may improve survival by modifying the intratumoral effector/regulatory cell ratio, thus highlighting the importance of regulatory T-lymphocytes (T_{Reg}) for melanoma progression *in vivo*. $CD4^+$ T_{Reg} express the transcription factor forkhead box P3 (Foxp3), which is essential for their normal development and function (Fontenot and Rudensky, 2005). Antigenic stimulation of conventional CD4+ T cells in the presence of transforming growth factor-β (TGF-β) induces FoxP3 expression and the acquisition of suppressor function (Amarnath et al., 2007; Chen and Konkel, 2010; Fantini et al., 2004; Floess et al., 2007; Fu et al., 2004; Horwitz et al., 2008; Huber et al., 2009; Huter et al., 2008; Kawamoto et al., 2010; Marie et al., 2005; Samanta et al., 2008; Schramm et al., 2004; Zheng et al., 2006; Zhou et al., 2008a, 2010). It has been clearly established that stable FoxP3 expression is required to maintain suppressive

properties of T_{Reg} cells (Blache et al., 2009). Although it is necessary for the continued suppressive action of functional T_{Reg} cells, FoxP3 expression alone is not sufficient to accurately identify functional T_{Reg} cells because post-translational changes in discrete residues of the protein can lead to loss of function (Li and Greene, 2008). The regulation of FoxP3 expression is essential to modulating immune surveillance through the regulatory T-cell lineage. The *FoxP3* gene has a dual role as it is also an X-linked tumor suppressor gene (TSG) in several solid tumors. Whether it is a TSG in melanoma has yet to be determined. Understanding the regulation and function of the *FoxP3* gene is therefore crucial to better understanding the biology of melanoma.

1. Structure of the *FoxP3* gene and regulation by transcription factors

The *FoxP3* gene is located on the X chromosome (chr) at Xp11.23 and is submitted to X chr inactivation (Bennett et al., 2001; Wang et al., 2009). The gene contains 11 coding exons (exons 1-11) and 3 non coding exons (Bennett et al., 2001). The two 5' non coding exons (-2a and -2b) are spliced into a common non coding exon (-1) (Floess et al., 2007; Kaur et al., 2010; Smith et al., 2006). The -2b and -1 exons encompass regulatory *cis*-elements. (Lal and Bromberg, 2009; Lopes et al., 2007). It should be noticed that several reports refer to exon -1 as exon 1 and name the exons differently from 1 to 12. An AA insertion in exon 8 leads to the *scurfy* phenotype in mice. (Bennett et al., 2001). About 60% of patients with an *IPEX* syndrome-immune dysfunction, polyendocrinopathy, enteropathy, X-linked syndrome have missense mutations in exons 9, 10, and 11 which encode the forkhead domain (Bennett et al., 2001; Harbuz et al., 2010; Owen et al., 2003; Rubio-Cabezas et al., 2009; Torgerson et al., 2007).

The FoxP3 protein is highly conserved (Lal et al., 2009; Sadlon et al., 2010; Zheng et al., 2010). It is critical to the understanding of FoxP3 function to realize that human cells express three FoxP3 isoforms (Aarts-Riemens et al., 2008; Allan et al., 2005; Kaur et al., 2010; Smith et al.,

2006; Ziegler, 2006). The longest form resembles the murine FoxP3, whereas the other two are unique to humans. FoxP3ΔE2 lacks exon 2, which is part of the repressor domain in the FoxP3 protein. Compared to full length FoxP3, expression of FoxP3ΔE2 in human $CD4^{+}CD25^{-}FoxP3^{-}$ T cells leads to more IL-2 secretion and proliferation in response to T-cell receptor (TCR) stimulation (Allan et al., 2005). It has been proposed that FoxP3ΔE2 acts as a dominant negative isoform (Li et al., 2007; Xu et al., 2010). Human T_{Regs} can also express a third isoform that lacks both exon 2 and exon 7 (Kaur et al., 2010). The absence of exon 7, which encodes a leucine zipper motif, in the FoxP3ΔE2Δ7 isoform abrogates the suppressive function of T_{Regs} (Kaur et al., 2010). This emphasizes the importance of distinguishing the FoxP3, FoxP3ΔE2, and FoxP3ΔE2Δ7 isoforms to accurately sub-type T_{Regs}.

Conservative noncoding sequences (CNS) are located within 500 base pairs 5' to the transcription start site and serve as a proximal promoter region (Zhang et al., 2008). It contains TATA, GC, and CAAT boxes that, when mutated, lead to decreased FoxP3 activity (Mantel et al., 2006). This region also contains binding sites for important transcription factors, such as nuclear factor of activated T cells (NFAT), activator protein-1 (AP-1), and Sp-1 that play a role in anti-CD3/CD28-driven FoxP3 expression (Kim, 2009; Zheng et al., 2010). The 5' intron 2, located between exon -2a and exon -1, contains a CNS and is referred to as the intronic enhancer, whereas the CNS situated 5 kb upstream of the transcriptional start site is referred to as the upstream enhancer (Lal et al., 2009). The proximal promoter is able to bind with STAT5 and is dependent on IL-2Rβ signalling (Burchill et al., 2007). It has been recently suggested that STAT5 is required for FoxP3 expression (Burchill et al., 2007). The second enhancer region (3' CNS enhancer) locates to +4301 to +4500 as identified by luciferase reporter assays in Jurkat cells (Wu et al., 2006). This enhancer region contains a CREB/ATF (activating transcription factor) motif that is

capable of binding CREB and maintaining FoxP3 expression and thus a stable T_{Reg} population (Kim and Leonard, 2007). Binding sites for STAT5 and STAT3 that mediate signalling of inflammatory cytokines, including IL-2, IL-6, IL-21, and IL-27, are also located within this enhancer region (Zorn et al., 2006). It seems that both STAT5 and STAT3 bind to the same target site, while STAT3 binds with a much lower affinity. Recently, using mice with specific deletions of the conservative regions, Zheng et al. have identified another pioneer CNS (Zheng et al., 2009). It locates to intron 4, which is between exons 1 and 2, binds c-Rel, and acts to potently increase the number of T_{Regs} in the thymus and periphery.

In Th1, the IFN-γ-induced protein interferon regulatory factor 1 binds to the FoxP3 proximal promoter and inhibits FoxP3 expression (Ouaked et al., 2009). In Th2, IL-4 inhibits FoxP3 expression in peripheral naive $CD4^{+}CD25^{-}$ T cells by stimulating phosphorylation of STAT6, which binds between exons -2b and -1 and inhibits TGF-β-induced FoxP3 expression (Takaki et al., 2008). TGF-β and IL-4 cosignalling induces IL-9 secretion, leading to the newly identified $IL\text{-}9^{+}IL\text{-}10^{+}FoxP3^{-}$(Th9) subset (Vang et al., 2008).

Polymorphisms of the *FoxP3* gene, including single nucleotide polymorphisms (SNP) and microsatellite polymorphisms have been reported in multiple case-control and cohort studies, mostly in patients with autoimmune diseases or cancers and their controls (Lin et al., 2011). Reported polymorphisms include SNPs in the promoter region, SNPs in the intron regions, SNPs downstream of the coding regions, and microsatellite polymorphism (GT)n in the promoter region, and TC(n) in the intron region (Lan et al., 2010). While most of the polymorphisms seem to be clinically irrelevant, a few alleles do show weak clinical correlation with autoimmune diseases, including SNPs in primary biliary cirrhosis and psoriasis, and (TC)n microsatellite polymorphisms

in autoimmune thyroid disease (Inoue et al., 2010; Wang et al., 2010a). Overall, there is a lack of convincing evidence to suggest that any FoxP3 polymorphism is clinically significant.

2. Epigenetic regulation of FoxP3 expression

It is well-established that methylation of CpG sequences inhibits acetylation of histones and binding of transcription factors to DNA, thus resulting in quiescent genes. Demethylation of CpG sequences and acetylation of histones, on the other hand, are features of active genes. Such epigenetic modifications are also observed in the FoxP3 gene. The methylation status of the CpG residues in the proximal promoter region plays an essential role in FoxP3 expression (Janson et al., 2008). Demethylation induced by treatment with 5-aza-2'-deoxycytidine (Aza) leads to FoxP3 expression in human NK cells (Lal et al., 2009; Moon et al., 2009). Ten to forty-five percent of the CpG sites in the FoxP3 proximal promoter are methylated in naive $CD4^+CD25^-$ T cells, whereas all are demethylated in natural T_{Regs} (Lal and Bromberg, 2009; Polansky et al., 2008). TGF-β induces demethylation of CpG at this site in $CD4^+CD25^-$ T cells (Lal et al., 2009). Multiple CpG sequences have been identified in the FoxP3 gene, from 5' to 3' as follows: i) within an upstream CNS, 5-6000 bp 5' to the transcription starting site; ii) within the intronic enhancer, and iii) within intron 10, between exons 7 and 8 (Floess et al., 2007; Hansmann et al., 2010; Lal et al., 2009; Polansky et al., 2010; Zheng et al., 2010). The intronic enhancer contains a Runx1 binding sequence. When the enhancer is demethylated (i.e. activated), it can be occupied by a FoxP3, Runx1, and core-binding factor-β complex (Zhang et al., 2008).

TGF-β induces FoxP3 expression in peripheral naive $CD4^+CD25^-$ T cells. In addition to TGF-β receptor-induced SMAD3 signaling for T_{Reg} generation, TGF-β signaling may also act via TIEG1 and the E3 ubiquitin ligase *itch* in a ubiquitin-dependent pathway (Venuprasad et al., 2008). TGF-β also inhibits the phosphorylation of ERK leading to inhibition of DNA methyltransferase

(DNMT) expression; and inhibition of DNMT with siRNA or DNMT inhibitors leads to FoxP3 expression in $CD4^+$ T cells, suggesting that inhibition of DNMT activity plays an important role in FoxP3 expression (Luo et al., 2008).

The inflammatory cytokine IL-6 suppresses the development and function of T_{Regs}. (Lal et al., 2009). Actually, IL-6 both induces DNMT1 expression and enhances its activity. IL-6 induces STAT3-dependent methylation of the upstream FoxP3 enhancer by DNMT1 in T_{Regs}, leading to repression of FoxP3 (Wang et al., 2007). Preactivated $CD4^+CD25^-$ T cells or $CD4^+CD25^-CD44^{hi}$ memory T cells express very little FoxP3 after TGF-β stimulation. This is probably the result of high levels of DNMT1 activity in these cells because inhibition of DNMT with Aza or deficiency of DNMT1 in T cells leads to FoxP3 expression, suggesting that regulation of FoxP3 is tightly controlled by epigenetic modifications in activated $CD4^+$ T cells (Lal et al., 2009).

Natural T_{Regs} possess demethylated CpGs at the FoxP3 locus and show stable *FoxP3* expression, whereas TGF-β induced T_{Regs} show methylated CpGs and do not maintain constitutive FoxP3 expression after restimulation in the absence of TGF-β (Baron et al., 2007; Floess et al., 2007; Lal and Bromberg, 2009; Polansky et al., 2008). It has been reported that a fraction of the $FoxP3^+CD4^+$ natural T_{Regs} adoptively transferred into lymphopenic mice are converted into $FoxP3^-$ T cells (Bruinsma et al., 2010). Under inflammatory conditions, $FoxP3^+$ T_{Regs} lose FoxP3 expression and thus suppressive function in an IL-6-dependent manner (Lal et al., 2011). IL-6 and TCR signalling induce down-regulation of FoxP3 expression and lead to development of Th17 cells (Maitra et al., 2009). One mode of action of IL-6 is to induce remethylation of CpG DNA at the upstream enhancer and thus down-regulates FoxP3 expression in natural T_{Regs} (Lal et al., 2009). Epigenetic inheritance during the cell cycle is crucial in maintaining chromatin structure in cell

lineages. But the extrinsic and intrinsic signals that regulate CpG DNA methylation and perpetuate the H3 methylation level at the FoxP3 locus from one cell cycle to another are not yet understood.

3. Mechanisms of impaired regulation by $CD4^+CD25^+FoxP3^+$ regulatory T cells in human autoimmune diseases

T_{Reg} cells, defined by the expression of CD4, CD25 and FoxP3, have a central role in protecting an individual from autoimmunity. This role was first identified in mice in which the absence or depletion of T_{Regs} resulted in the development of autoimmune gastritis, thyroiditis, diabetes and inflammatory bowel disease (IBD) (Ochs et al., 2007). Subsequently, numerous studies in animal models of autoimmunity showed that defects in $CD4^+CD25^+FoxP3^+$ T_{Regs} contribute to the development of autoimmunity and that the disease could be reversed by the adoptive transfer of T_{Regs} (Buckner, 2010). The importance of T cell regulation in human disease is highlighted by the severe inflammation and autoimmunity that occurs in individuals who suffer from IPEX. These individuals develop a broad range of autoantibodies causing insulin-dependent diabetes, thyroiditis, eczema, hemolytic anemia and IBD. In the absence of a bone marrow transplant, IPEX patients die at an early age (Wildin and Freitas, 2005).

In mouse models, the concept that inadequate numbers of T_{Regs} may contribute to autoimmunity is supported by the occurrence of aggressive autoimmunity in scurfy mice and is indirectly implied by the successful treatment of autoimmunity in mice through the adoptive transfer of wild-type T_{Regs} (Komatsu and Hori, 2007). In addition, there is evidence from mouse models that, under the appropriate conditions, T_{Regs} can be induced in the periphery, and that these T_{Regs} may prevent the development of autoimmunity. Multiple factors influence the homeostasis and induction of T_{Regs} in the periphery, including CD28, IL-2, TGF-β and dendritic cells (DCs) (Buckner, 2010; Buckner and Ziegler, 2008).

Evidence that an inadequate number of T_{Regs} leads to autoimmunity in humans is most clearly shown in patients with IPEX, who completely lack T_{Regs} as a result of a mutation in *FoxP3* (Lal and Bromberg, 2009). However, most patients with autoimmune disease probably have a more modest reduction in T_{Regs}. In these common diseases, the challenge is to determine whether the number of T_{Regs} is inadequate at the site of inflammation and whether this is due to systemic factors or factors in the local tissue milieu (Buckner, 2010). In human disease, the task of enumerating T_{Regs} has been complicated by the presence of multiple T_{Reg} subsets and the lack of a cell marker that is unique to T_{Regs}. Type 1 regulatory T (T_R1) cells are induced in the periphery and suppress T cell proliferation through the production of interleukin-10 (IL-10) and TGF-β. TR1 cells do not have a unique cell marker but are identified by their production of IL-10 and absence of pro-inflammatory cytokines (Roncarolo and Gregori, 2008; Veldman et al., 2009). T helper 3 (T_H3) cells are a regulatory T cell population that originates in the periphery and mediates suppression through the secretion of TGF-β; similar to T_R1 cells, they do not have a unique cell surface marker (Carrier et al., 2007). $CD4^+CD25^+FoxP3^+$ T_{Regs} can be divided into two groups: thymus-derived natural T_{Reg} cells and periphery-induced adaptive T_{Reg} cells. Both populations express FoxP3 and suppress immune responses through contact-dependent mechanisms and the production of soluble factors, including the cytokines TGF-β, IL-10 and IL-35 (Buckner, 2010). Thymus derived $CD4^+CD25^+FoxP3^+$ T_{Reg} cells are stable with respect to retaining regulatory function and FoxP3 expression in the periphery. They are unique in that their FoxP3 locus is demethylated and they express the transcription factor Helios (Fujimoto et al., 2011; Thornton et al., 2010). Adaptive T_{Reg} cells can be induced in the periphery from a $CD4^+FoxP3^-$ T cell population following T cell receptor stimulation in the presence of TGF-β (Mahic et al., 2008). It has now become clear that the $FoxP3^+$ T cell population is composed of several populations that

are defined by the expression of CD25, CD45RA and FoxP3. Miyara et al. defined these populations as a naive T_{Reg} cell population that is $CD25^{hi}CD45RA^{+}FoxP3^{hi}$, an effector T_{Reg} cell population that is $CD25^{hi}CD45RA^{-}FoxP3^{hi}$ and a non-regulatory $FoxP3^{+}$ population that is $CD25^{hi}CD45RA^{-}FoxP3^{low}$ (Miyara and Sakaguchi, 2011; Miyara et al., 2009). Another difficulty is the extent to which the peripheral blood reflects the global number of T_{Regs} in the body and, more specifically, their number in inflamed tissues.

T_{Regs} were first defined on the basis of their expression of CD25, which forms part of the high-affinity IL-2 receptor. Unfortunately, the definition of T_{Regs} based on the level of CD25 expression has not been consistently reported in the literature, making comparisons between studies difficult. Furthermore, CD25 is also expressed by recently activated T cells, resulting in the inclusion of $CD4^{+}CD25^{+}$ effector T cells in the T_{Reg} population (Buckner, 2010). With the discovery that expression of FoxP3 plays a central role in the differentiation and maintenance of T_{Regs}, the use of flow cytometry-based analysis of FoxP3 expression in T cells became the gold standard for defining T_{Regs}. However, it then became evident that FoxP3 can also be expressed by effector T cells following activation, thus any assessment of T_{Regs} number or function is likely tainted by inclusion of recently activated effector T cells in the T_{Regs} population. Furthermore, as FoxP3 is a nuclear protein, assessment of its expression in T cells requires fixation and permeabilization of the cells, resulting in an inability to obtain viable cells for further functional analysis. In the past few years, additional markers, such as CD127 have been identified that assist in the distinction of effector T cells from T_{Regs} and facilitate the experimental purification of T_{Regs} (Simonetta et al., 2010).

In the context of anti-CTLA-4 melanoma therapy, a major challenge is to measure resistance of effector T cells to suppression. The resistance of effector T cells to T_{Regs} has been

observed in several animal models of autoimmunity (Chen et al., 2010; Schneider et al., 2008). In these models, inflammation and tissue destruction progress despite the presence of functional T_{Regs} at the site of inflammation. Such findings suggest that a resistance of effector T cells to T_{Regs} may contribute to autoimmunity. Whether this might be of interest to predict response to anti-CTLA-4 therapy needs further investigation.

4. *FoxP3* as an X-linked tumor suppressor gene

Foxp3 is expressed in epithelial cells from various organs such as breast, thymus, prostate and lung. Importantly, mice that are heterozygous for *FoxP3* mutations spontaneously develop mammary carcinomas at a high frequency (Chen et al., 2008). Genetic analyses in both mice and humans revealed that *Foxp3* is an important X-linked tumor suppressor in breast and in prostate cancer (Gupta et al., 2007; Karanikas et al., 2008; Katoh et al., 2010; Kiniwa et al., 2007; Ladoire et al., 2011; Li et al., 2011; Liu and Zheng, 2007; Mahmoud et al., 2010; Merlo et al., 2009; Valdman et al., 2010; Wang et al., 2009, 2010b; Yokokawa et al., 2008; Zuo et al., 2007a, 2007b). Mice with germline *FoxP3* mutations are substantially more prone to developing both spontaneous and carcinogen-induced mammary carcinomas (Zuo et al., 2007b). The role of the *FoxP3* gene in mammary carcinogenesis has been supported by several lines of evidence. The *FoxP3* gene is expressed in normal breast epithelia but is down-regulated in mammary cancer. Ectopic expression of *FoxP3* in a variety of breast cancer cell lines resulted in cell cycle arrest and cessation of cell growth (Zuo et al., 2007a). Moreover, FoxP3 directly regulates transcription of *ErbB2*, *Skp2* and *CDKN1A* (p21) (Katoh et al., 2010). Frequent chromosomal deletions and somatic mutations of the *FoxP3* gene were detected in human cancer samples including cutaneous melanomas (Fujii et al., 2010; Karanikas et al., 2008). There is a down-regulation of FoxP3 protein in cancer cells compared to normal breast epithelia. The *FoxP3* gene also plays an important role in prostate

epithelia. Among human prostate cancers, frequent chromosomal deletions, somatic mutations and epigenetic silencing of the *FoxP3* gene were found (Li et al., 2011; Wang et al., 2009, 2010b). Since the *FoxP3* gene is located on the X chromosome, a genetic/epigenetic single-hit results in inactivation of this gene in males, escaping the Knudson model (Spatz et al., 2004). Immunohistochemistry revealed that FoxP3 expression is significantly down-regulated in cancer cells when compared to normal prostate glands (Valdman et al., 2010). Moreover, mice with prostate-specific ablations of FoxP3, $FoxP3^{fl/y}$; $PB\text{-}Cre^{+}$, developed prostatic hyperplasia and prostatic intraepithelial neoplasm (PIN) that are putative pre-cancerous lesions of the prostate (Ebelt et al., 2009; Wang et al., 2009). In human samples, FoxP3 expression in PINs are down-regulated compared to adjacent normal prostate glands, which suggests that the inactivation of the *FoxP3* gene plays an important role in the initial stage of prostatic carcinogenesis (Ebelt et al., 2009).

Another interesting aspect of FoxP3 abnormalities is that some types of cancers predominantly express splice variants of the FoxP3 protein in addition to those occurring in non-transformed cells (FoxP3, FoxP3ΔE2, and FoxP3ΔE2Δ7). In cutaneous melanomas, and in some breast and ovarian cancers, and malignant T cells of Sezary syndrome, specific splice variants of the FoxP3, such as ΔE3, ΔE3-4, ΔE3/8 and ΔE8, were reported to be preferably expressed (Kaur et al., 2010; Smith et al., 2006) The Δ3-4 splice variant results in a truncated FoxP3 with a premature stop codon, and therefore might contribute to the malignant progression of cells (Wang et al., 2009). Whereas FoxP3 has been shown to up-regulate CTLA-4 expression, it is not known whether different variants in the primary melanoma are associated with different responses to ipilimumab at a later stage.

Expression of the oncogene *c-MYC* has been demonstrated to be directly repressed by FoxP3 in prostate epithelia (Wang et al., 2009). Overexpression of c-MYC contributes to more aggressive and poorly differentiated cancer phenotypes and has been involved in the biology of melanoma. c-MYC is a sequence-specific transcription factor and an important player in various cellular processes including cell cycle and apoptosis; processes which are also dysregulated in cancer cells with high c-MYC expression levels. C-MYC directly activates CDK4 and CCND2 expression, while indirectly repressing CDK inhibitors such as *CDKN1A* (p21) and *CDKN2B* (p15) expression (Wang et al., 2011). Moreover, c-MYC directly upregulates *eIF4E* and *eIF2α*; both of which are the rate-limiting effectors of cell cycle.

HER2 is a member of the transmembrane receptor tyrosine kinases and is involved in the regulations of various cellular functions such as cell growth and survival. The cytoplasmic portion of HER2 is phosphorylated at conserved tyrosine residues and these phosphorylated tyrosines can serve as binding sites for adapters which link HER2 to its downstream pathways or targets such as PI3K-Akt and MAPK-Erk. Both *HER2* gene amplification and loss of nuclear *FoxP3* contribute to HER2 overexpression in breast cancer samples (Mahmoud et al., 2010; Zhou et al., 2008b). FoxP3 can repress transcription of HER2 in human breast cancers by binding directly to the *ERBB2* gene promoter (Zhou et al., 2008b). Since *in vitro* HER2 overexpression nullifies the ability of FoxP3 to inhibit cell growth, repression of HER2 may be critical for the tumor suppressor function of FoxP3 in the breast epithelial cells (Zuo et al., 2007a). Maybe this can partially explain why circulating $CD4^{+}CD25^{+}FoxP3^{+}$ T_{Regs} decrease in breast cancer patients after vaccination with a modified MHC class II HER2/neu peptide (Gates et al., 2010). Recently it has been demonstrated that the influence of FoxP3 was dependent on the molecular sub-type of breast cancer. Indeed,

FoxP3 expression in cancer cells may be a marker of good prognosis in HER2-overexpressing tumors and of poor prognosis in other molecular sub-types of breast cancer (Ladoire et al., 2011).

High levels of expression of SKP2 have been reported in a wide variety of cancers including melanoma (Katagiri et al., 2006; Rose et al., 2011). SKP2 is an important player in the ubiquitin-dependent degradation of $p27^{KIP1}$, a CDK inhibitor especially of Cyclin-E/CDK2 and Cyclin-A/CDK2 (Katagiri et al., 2006; Rose et al., 2011). SKP2 is robustly expressed during S and G2 phases of the cell cycle and regulates p27 degradation, thus facilitating progression of the cell cycle. It has been demonstrated that FoxP3 directly represses *SKP2* expression in human and mouse mammary epithelial cells (Zuo et al., 2007a). FoxP3 occupies the *Skp2* promoter and represses promoter activity of the locus (Zuo et al., 2007a). FoxP3 directly regulates key molecules of cell cycle regulation, which further supports the notion that *FoxP3* is an important tumor suppressor.

Previous reports have revealed that FoxP3 forms complexes with Rel family transcription factors NFAT and NFκB, and FoxP3 blocks their ability to activate *Il-2* and *INFγ* transcription (Ruan et al., 2009; Soligo et al., 2011). By making a repressive FoxP3:NFAT complex, FoxP3 inhibits NFAT:AP-1 complex at the *Il-2* promoter (Kim, 2009). FoxP3 could also weaken the DNA binding activity of AP-1 (Lee et al., 2008). AML1/RUNX1, which activates endogenous *Il-2* and *IFNγ* expression in $CD4^+$ T cells, is reported to make a complex with FoxP3. (Hancock and Ozkaynak, 2009; Ono et al., 2007). AML1/RUNX1 could bind to the *Il-2* enhancer with FoxP3 and exert optimal repression of *Il-2* in T_{Regs} (Ono et al., 2007).

5. Conclusion

The *FoxP3* gene has important functions as a tumor suppressor gene in human carcinomas and recent data suggests it plays a role in melanoma as well. At the same time, this gene directly commands the natural regulatory T cells that have been demonstrated to be an effective target for melanoma therapy. Thus an interesting issue is whether FoxP3 gene is a friend or a foe for melanoma therapy. Perhaps gaining better insight about the roles of aberrantly spliced variants will be the first step in answering this question. Although molecular mechanisms have not yet been clarified, some agents have been reported to increase FoxP3 in cancer cells. Anisomycin could induce the transcription of *FoxP3* in various breast cancer cell lines, resulting in significantly repressed cell growth *in vitro* and in xenografts *in vivo* (Liu et al., 2009). In breast and colon cancer cell lines, FoxP3 expression is directly regulated by p53. Doxorubicin, which activates p53, dramatically activates FoxP3 transcription *in vitro* (Jung et al., 2010). Maybe the restoration of FoxP3 functions in melanoma cells with low FoxP3 expression or ΔE3/ΔE3ΔE4 variants combined with anti-CTLA-4 therapy could have potential as a novel therapeutic strategy. Identification of these variants could also be of help in discovering the first predictive biomarker for anti-CTLA-4 therapy. It will also likely enable improved development of effective combinations of immunotherapy and targeted therapy.

REFERENCES

Aarts-Riemens, T., Emmelot, M.E., Verdonck, L.F., Mutis, T., 2008. Forced overexpression of either of the two common human Foxp3 isoforms can induce regulatory T cells from CD4(+) CD25(-) cells. Eur. J. Immunol. 38, 1381-1390.

Allan, S.E., Passerini, L., Bacchetta, R., Crellin, N., Dai, M., Orban, P.C., Ziegler, S.F., Roncarolo, M.G., Levings, M.K., 2005. The role of 2 FOXP3 isoforms in the generation of human $CD4^+$ Tregs. J. Clin. Invest. 115, 3276-3284.

Amarnath, S., Dong, L., Li, J., Wu, Y., Chen, W., 2007. Endogenous TGF-beta activation by reactive oxygen species is key to Foxp3 induction in TCR-stimulated and HIV-1-infected human $CD4^+CD25^-$ T cells. Retrovirology 4, 57.

Baron, U., Floess, S., Wieczorek, G., Baumann, K., Grutzkau, A., Dong, J., Thiel, A., Boeld, T.J., Hoffmann, P., Edinger, M., Turbachova, I., Hamann, A., Olek, S., Huehn, J., 2007. DNA demethylation in the human FOXP3 locus discriminates regulatory T cells from activated FOXP3(+) conventional T cells. Eur. J. Immunol. 37, 2378-2389.

Bennett, C.L., Brunkow, M.E., Ramsdell, F., O'Briant, K.C., Zhu, Q., Fuleihan, R.L., Shigeoka, A.O., Ochs, H.D., Chance, P.F., 2001. A rare polyadenylation signal mutation of the FOXP3 gene (AAUAAA–>AAUGAA) leads to the IPEX syndrome. Immunogenetics 53, 435-439.

Blache, C., Adriouch, S., Calbo, S., Drouot, L., Dulauroy, S., Arnoult, C., Le Corre, S., Six, A., Seman, M., Boyer, O., 2009. Cutting edge: CD4-independent development of functional $FoxP3^+$ regulatory T cells. J. Immunol. 183, 4182e4186.

Bruinsma, M., Wils, E.J., Lowenberg, B., Cornelissen, J.J., Braakman, E., 2010. The impact of

CD4(+)Foxp3(+) Treg on immunity to murine cytomegalovirus after bone marrow transplantation depends on the peripheral or thymic source of T cell regeneration. Transpl. Immunol.

Buckner, J.H., 2010. Mechanisms of impaired regulation by CD4(+) CD25(+)FOXP3(+) regulatory T cells in human autoimmune diseases. Nat. Rev. Immunol. 10, 849-859. Buckner, J.H., Ziegler, S.F., 2008. Functional analysis of FOXP3. Ann. N. Y. Acad. Sci. 1143, 151-169.

Burchill, M.A., Yang, J., Vogtenhuber, C., Blazar, B.R., Farrar, M.A., 2007. IL-2 receptor beta-dependent STAT5 activation is required for the development of $Foxp3^{+}$ regulatory T cells. J. Immunol. 178, 280-290.

Carrier, Y., Yuan, J., Kuchroo, V.K., Weiner, H.L., 2007. Th3 cells in peripheral tolerance. I. Induction of Foxp3-positive regulatory T cells by Th3 cells derived from TGF-beta T cell-transgenic mice. J. Immunol. 178, 179-185.

Chen, G.Y., Chen, C., Wang, L., Chang, X., Zheng, P., Liu, Y., 2008. Cutting edge: broad expression of the FoxP3 locus in epithelial cells: a caution against early interpretation of fatal inflammatory diseases following in vivo depletion of FoxP3-expressing cells. J. Immunol. 180, 5163-5166.

Chen, W., Konkel, J.E., 2010. TGF-beta and 'adaptive' Foxp3(+) regulatory T cells. J. Mol. Cell Biol. 2, 30-36.

Chen, X., Hamano, R., Subleski, J.J., Hurwitz, A.A., Howard, O.M., Oppenheim, J.J., 2010. Expression of costimulatory TNFR2 induces resistance of $CD4^{+}FoxP3^{-}$ conventional T cells to suppression by $CD4^{+}FoxP3^{+}$ regulatory T cells. J. Immunol. 185, 174-182.

Ebelt, K., Babaryka, G., Frankenberger, B., Stief, C.G., Eisenmenger, W., Kirchner, T.,

Schendel, D.J., Noessner, E., 2009. Prostate cancer lesions are surrounded by FOXP3$^-$, PD-1$^+$ and B7-H1$^+$ lymphocyte clusters. Eur. J. Cancer 45, 1664-1672.

Fantini, M.C., Becker, C., Monteleone, G., Pallone, F., Galle, P.R., Neurath, M.F., 2004. Cutting edge: TGF-beta induces a regulatory phenotype in CD4$^+$CD25$^-$ T cells through Foxp3 induction and down-regulation of Smad7. J. Immunol. 172, 5149-5153.

Floess, S., Freyer, J., Siewert, C., Baron, U., Olek, S., Polansky, J., Schlawe, K., Chang, H.D., Bopp, T., Schmitt, E., Klein- Hessling, S., Serfling, E., Hamann, A., Huehn, J., 2007. Epigenetic control of the foxp3 locus in regulatory T cells. PLoS Biol. 5, e38.

Fontenot, J.D., Rudensky, A.Y., 2005. A well adapted regulatory contrivance: regulatory T cell development and the forkhead family transcription factor Foxp3. Nat. Immunol. 6, 331-337.

Fu, S., Zhang, N., Yopp, A.C., Chen, D., Mao, M., Zhang, H., Ding, Y., Bromberg, J.S., 2004. TGF-beta induces Foxp3$^+$ T-regulatory cells from CD4$^+$ CD25$^-$ precursors. Am. J. Transplant. 4, 1614-1627.

Fujii, H., Arakawa, A., Kitoh, A., Miyara, M., Kato, M., Kore-Eda, S., Sakaguchi, S., Miyachi, Y., Tanioka, M., Ono, M., 2010. Perturbations of both non-regulatory and regulatory FOXP3(+) T cells in patients with malignant melanoma. Br. J. Dermatol.

Fujimoto, M., Nakano, M., Terabe, F., Kawahata, H., Ohkawara, T., Han, Y., Ripley, B., Serada, S., Nishikawa, T., Kimura, A., Nomura, S., Kishimoto, T., Naka, T., 2011. The influence of excessive IL-6 production *in vivo* on the development and function of Foxp3$^+$ regulatory T cells. J. Immunol. 186, 32-40.

Gates, J.D., Clifton, G.T., Benavides, L.C., Sears, A.K., Carmichael, M.G., Hueman, M.T.,

Holmes, J.P., Jama, Y.H., Mursal, M., Zacharia, A., Ciano, K., Khoo, S., Stojadinovic, A., Ponniah, S., Peoples, G.E., 2010. Circulating regulatory T cells ($CD4^+CD25^+FOXP3^+$) decrease in breast cancer patients after vaccination with a modified MHC class II HER2/neu (AE37) peptide. Vaccine 28, 7476-7482.

Gupta, S., Joshi, K., Wig, J.D., Arora, S.K., 2007. Intratumoral FOXP3 expression in infiltrating breast carcinoma: its association with clinicopathologic parameters and angiogenesis. Acta Oncol. 46, 792-797.

Hancock, W.W., Ozkaynak, E., 2009. Three distinct domains contribute to nuclear transport of murine Foxp3. PLoS One 4, e7890.

Hansmann, L., Schmidl, C., Boeld, T.J., Andreesen, R., Hoffmann, P., Rehli, M., Edinger, M., 2010. Isolation of intact genomic DNA from FOXP3-sorted human regulatory T cells for epigenetic analyses. Eur. J. Immunol. 40, 1510-1512.

Harbuz, R., Lespinasse, J., Boulet, S., Francannet, C., Creveaux, I., Benkhelifa, M., Jouk, P.S., Lunardi, J., Ray, P.F., 2010. Identification of new FOXP3 mutations and prenatal diagnosis of IPEX syndrome. Prenat. Diagn. 30, 1072-1078.

Hodi, F.S., O'Day, S.J., McDermott, D.F., Weber, R.W., Sosman, J.A., Haanen, J.B., Gonzalez, R., Robert, C., Schadendorf, D., Hassel, J.C., Akerley, W., van den Eertwegh, A.J., Lutzky, J., Lorigan, P., Vaubel, J.M., Linette, G.P., Hogg, D., Ottensmeier, C.H., Lebbe, C., Peschel, C., Quirt, I., Clark, J.I., Wolchok, J.D., Weber, J.S., Tian, J., Yellin, M.J., Nichol, G.M., Hoos, A., Urba, W.J., 2010. Improved survival with ipilimumab in patients with metastatic melanoma. N. Engl. J. Med. 363, 711-723.

Horwitz, D.A., Zheng, S.G., Wang, J., Gray, J.D., 2008. Critical role of IL-2 and TGF-beta in

generation, function and stabilization of $Foxp3^{+}CD4^{+}$ Treg. Eur. J. Immunol. 38, 912-915.

Huber, S., Stahl, F.R., Schrader, J., Luth, S., Presser, K., Carambia, A., Flavell, R.A., Werner, S., Blessing, M., Herkel, J., Schramm, C., 2009. Activin a promotes the TGF-beta-induced conversion of $CD4^{+}CD25^{-}$ T cells into $Foxp3^{+}$ induced regulatory T cells. J. Immunol. 182, 4633-4640.

Huter, E.N., Punkosdy, G.A., Glass, D.D., Cheng, L.I., Ward, J.M., Shevach, E.M., 2008. TGF-beta-induced $Foxp3^{+}$ regulatory T cells rescue scurfy mice. Eur. J. Immunol. 38, 1814-1821.

Inoue, N., Watanabe, M., Morita, M., Tomizawa, R., Akamizu, T., Tatsumi, K., Hidaka, Y., Iwatani, Y., 2010. Association of functional polymorphisms related to the transcriptional level of FOXP3 with prognosis of autoimmune thyroid diseases. Clin. Exp. Immunol. 162, 402-406.

Janson, P.C., Winerdal, M.E., Marits, P., Thorn, M., Ohlsson, R., Winqvist, O., 2008. FOXP3 promoter demethylation reveals the committed Treg population in humans. PLoS One 3, e1612.

Jung, D.J., Jin, D.H., Hong, S.W., Kim, J.E., Shin, J.S., Kim, D., Cho, B.J., Hwang, Y.I., Kang, J.S., Lee, W.J., 2010. Foxp3 expression in p53-dependent DNA damage responses. J. Biol. Chem. 285, 7995-8002.

Karanikas, V., Speletas, M., Zamanakou, M., Kalala, F., Loules, G., Kerenidi, T., Barda, A.K., Gourgoulianis, K.I., Germenis, A.E., 2008. Foxp3 expression in human cancer cells. J. Transl. Med. 6, 19.

Katagiri, Y., Hozumi, Y., Kondo, S., 2006. Knockdown of Skp2 by siRNA inhibits melanoma

cell growth in vitro and *in vivo*. J. Dermatol. Sci. 42, 215-224.

Katoh, H., Zheng, P., Liu, Y., 2010. Signalling through FOXP3 as an X-linked tumor suppressor. Int. J. Biochem. Cell Biol. 42, 1784-1787.

Kaur, G., Goodall, J.C., Jarvis, L.B., Hill Gaston, J.S., 2010. Characterisation of Foxp3 splice variants in human $CD4^+$ and $CD8^+$ T cells-identification of Foxp3Delta7 in human regulatory T cells. Mol. Immunol. 48, 321-332.

Kawamoto, K., Pahuja, A., Hering, B.J., Bansal-Pakala, P., 2010. Transforming growth factor beta 1 (TGF-beta1) and rapamycin synergize to effectively suppress human T cell responses via upregulation of $FoxP3^+$ Tregs. Transpl. Immunol. 23, 28-33.

Kim, C.H., 2009. FOXP3 and its role in the immune system. Adv. Exp. Med. Biol. 665, 17-29.

Kim, H.P., Leonard, W.J., 2007. CREB/ATF-dependent T cell receptor-induced FoxP3 gene expression: a role for DNA methylation. J. Exp. Med. 204, 1543-1551.

Kiniwa, Y., Miyahara, Y., Wang, H.Y., Peng, W., Peng, G., Wheeler, T.M., Thompson, T.C., Old, L.J., Wang, R.F., 2007. $CD8^+$ $Foxp3^+$ regulatory T cells mediate immunosuppression in prostate cancer. Clin. Cancer Res. 13, 6947-6958.

Komatsu, N., Hori, S., 2007. Full restoration of peripheral $Foxp3^+$ regulatory T cell pool by radioresistant host cells in scurfy bone marrow chimeras. Proc. Natl. Acad. Sci. U S A 104, 8959-8964.

Ladoire, S., Arnould, L., Mignot, G., Coudert, B., Rebe, C., Chalmin, F., Vincent, J., Bruchard, M., Chauffert, B., Martin, F., Fumoleau, P., Ghiringhelli, F., 2011. Presence of Foxp3 expression in tumor cells predicts better survival in HER2-overexpressing breast cancer patients treated with neoadjuvant chemotherapy. Breast Cancer Res. Treat. 125, 65-72.

Lal, G., Bromberg, J.S., 2009. Epigenetic mechanisms of regulation of Foxp3 expression. Blood 114, 3727-3735.

Lal, G., Yin, N., Xu, J., Lin, M., Schroppel, S., Ding, Y., Marie, I., Levy, D.E., Bromberg, J.S., 2011. Distinct inflammatory signals have physiologically divergent effects on epigenetic regulation of foxp3 expression and treg function. Am. J. Transplant. 11, 203-214.

Lal, G., Zhang, N., van der Touw, W., Ding, Y., Ju, W., Bottinger, E.P., Reid, S.P., Levy, D.E., Bromberg, J.S., 2009. Epigenetic regulation of Foxp3 expression in regulatory T cells by DNA methylation. J. Immunol. 182, 259-273.

Lan, Y., Tang, X.S., Qin, J., Wu, J., Qin, J.M., 2010. Association of transcription factor FOXP3 gene polymorphism with genetic susceptibility to systematic lupus erythematosus in Guangxi Zhuang population. Zhonghua YiXue YiChuanXue ZaZhi 27, 433-436.

Lee, S.M., Gao, B., Fang, D., 2008. FoxP3 maintains Treg unresponsiveness by selectively inhibiting the promoter DNA-binding activity of AP-1. Blood 111, 3599-3606.

Li, B., Greene, M.I., 2008. Special regulatory T-cell review: FOXP3 biochemistry in regulatory T cells-how diverse signals regulate suppression. Immunology 123, 17-19.

Li, R., Perez, N., Karumuthil-Melethil, S., Prabhakar, B.S., Holterman, M.J., Vasu, C., 2007. Enhanced engagement of CTLA-4 induces antigen-specific $CD4^{+}CD25^{+}Foxp3^{+}$ and $CD4^{+}CD25^{-}$ TGF-beta 1^{+} adaptive regulatory T cells. J. Immunol. 179, 5191-5203.

Li, W., Wang, L., Katoh, H., Liu, R., Zheng, P., Liu, Y., 2011. Identification of a tumor suppressor Relay between the FOXP3 and the Hippo pathways in breast and prostate cancers. Cancer Res.

Lin, Y.C., Lee, J.H., Wu, A.S., Tsai, C.Y., Yu, H.H., Wang, L.C., Yang, Y.H., Chiang, B.L.,

2011. Association of single-nucleotide polymorphisms in FOXP3 gene with systemic lupus erythematosus susceptibility: a case-control study. Lupus 20, 137-143.

Liu, Y., Wang, Y., Li, W., Zheng, P., 2009. Activating transcription factor 2 and c-Jun-mediated induction of FoxP3 for experimental therapy of mammary tumor in the mouse. Cancer Res. 69, 5954-5960.

Liu, Y., Zheng, P., 2007. FOXP3 and breast cancer: implications for therapy and diagnosis. Pharmacogenomics 8, 1485-1487.

Lopes, J.E., Soper, D.M., Ziegler, S.F., 2007. Foxp3 is required throughout the life of a regulatory T cell. Sci. STKE ., pe36.

Luo, X., Zhang, Q., Liu, V., Xia, Z., Pothoven, K.L., Lee, C., 2008. Cutting edge: TGF-beta-induced expression of Foxp3 in T cells is mediated through inactivation of ERK. J. Immunol. 180, 2757-2761.

Mahic, M., Henjum, K., Yaqub, S., Bjornbeth, B.A., Torgersen, K.M., Tasken, K., Aandahl, E.M., 2008. Generation of highly suppressive adaptive CD8(+)CD25(+)FOXP3(+) regulatory T cells by continuous antigen stimulation. Eur. J. Immunol. 38, 640-646.

Mahmoud, S.M., Paish, E.C., Powe, D.G., Macmillan, R.D., Lee, A.H., Ellis, I.O., Green, A.R., 2010. An evaluation of the clinical significance of FOXP3(+) infiltrating cells in human breast cancer. Breast Cancer Res. Treat.

Maitra, U., Davis, S., Reilly, C.M., Li, L., 2009. Differential regulation of Foxp3 and IL-17 expression in CD4 T helper cells by IRAK-1. J. Immunol. 182, 5763-5769.

Mantel, P.Y., Ouaked, N., Ruckert, B., Karagiannidis, C., Welz, R., Blaser, K., Schmidt-Weber, C.B., 2006. Molecular mechanisms underlying FOXP3 induction in human T cells. J. Immunol. 176, 3593-3602.

Marie, J.C., Letterio, J.J., Gavin, M., Rudensky, A.Y., 2005. TGF-beta1 maintains suppressor function and Foxp3 expression in $CD4^{+}CD25^{+}$ regulatory T cells. J. Exp. Med. 201, 1061-1067.

Merlo, A., Casalini, P., Carcangiu, M.L., Malventano, C., Triulzi, T., Menard, S., Tagliabue, E., Balsari, A., 2009. FOXP3 expression and overall survival in breast cancer. J. Clin. Oncol. 27, 1746-1752.

Miyara, M., Sakaguchi, S., 2011. Human FoxP3(+)CD4(+) regulatory T cells: their knowns and unknowns. Immunol. Cell Biol.

Miyara, M., Yoshioka, Y., Kitoh, A., Shima, T., Wing, K., Niwa, A., Parizot, C., Taflin, C., Heike, T., Valeyre, D., Mathian, A., Nakahata, T., Yamaguchi, T., Nomura, T., Ono, M., Amoura, Z., Gorochov, G., Sakaguchi, S., 2009. Functional delineation and differentiation dynamics of human $CD4^{+}$ T cells expressing the FoxP3 transcription factor. Immunity 30, 899-911.

Moon, C., Kim, S.H., Park, K.S., Choi, B.K., Lee, H.S., Park, J.B., Choi, G.S., Kwan, J.H., Joh, J.W., Kim, S.J., 2009. Use of epigenetic modification to induce FOXP3 expression in naive T cells. Transplant. Proc. 41, 1848-1854.

Ochs, H.D., Gambineri, E., Torgerson, T.R., 2007. IPEX, FOXP3 and regulatory T-cells: a model for autoimmunity. Immunol. Res. 38, 112-121.

Ono, M., Yaguchi, H., Ohkura, N., Kitabayashi, I., Nagamura, Y., Nomura, T., Miyachi, Y., Tsukada, T., Sakaguchi, S., 2007. Foxp3 controls regulatory T-cell function by interacting with AML1/Runx1. Nature 446, 685-689.

Ouaked, N., Mantel, P.Y., Bassin, C., Burgler, S., Siegmund, K., Akdis, C.A., Schmidt-Weber,

C.B., 2009. Regulation of the foxp3 gene by the Th1 cytokines: the role of IL-27-induced STAT1. J. Immunol. 182, 1041-1049.

Owen, C.J., Jennings, C.E., Imrie, H., Lachaux, A., Bridges, N.A., Cheetham, T.D., Pearce, S.H., 2003. Mutational analysis of the FOXP3 gene and evidence for genetic heterogeneity in the immunodysregulation, polyendocrinopathy, enteropathy syndrome. J. Clin. Endocrinol. Metab. 88, 6034-6039.

Polansky, J.K., Kretschmer, K., Freyer, J., Floess, S., Garbe, A., Baron, U., Olek, S., Hamann, A., von Boehmer, H., Huehn, J., 2008. DNA methylation controls Foxp3 gene expression. Eur.J. Immunol. 38, 1654-1663.

Polansky, J.K., Schreiber, L., Thelemann, C., Ludwig, L., Kruger, M., Baumgrass, R., Cording, S., Floess, S., Hamann, A., Huehn, J., 2010. Methylation matters: binding of Ets-1 to the demethylated Foxp3 gene contributes to the stabilization of Foxp3 expression in regulatory T cells. J. Mol. Med. 88, 1029-1040.

Roncarolo, M.G., Gregori, S., 2008. Is FOXP3 a bona fide marker for human regulatory T cells? Eur. J. Immunol. 38, 925-927.

Rose, A.E., Wang, G., Hanniford, D., Monni, S., Tu, T., Shapiro, R.L., Berman, R.S., Pavlick, A.C., Pagano, M., Darvishian, F., Mazumdar, M., Hernando, E., Osman, I., 2011. Clinical relevance of SKP2 alterations in metastatic melanoma. Pigment Cell Melanoma Res. 24, 197-206.

Ruan, Q., Kameswaran, V., Tone, Y., Li, L., Liou, H.C., Greene, M.I., Tone, M., Chen, Y.H., 2009. Development of Foxp3(+) regulatory t cells is driven by the c-Rel enhanceosome. Immunity 31, 932-940.

Rubio-Cabezas, O., Minton, J.A., Caswell, R., Shield, J.P., Deiss, D., Sumnik, Z., Cayssials, A.,

Herr, M., Loew, A., Lewis, V., Ellard, S., Hattersley, A.T., 2009. Clinical heterogeneity in patients with FOXP3 mutations presenting with permanent neonatal diabetes. Diabetes Care 32, 111-116.

Sadlon, T.J., Wilkinson, B.G., Pederson, S., Brown, C.Y., Bresatz, S., Gargett, T., Melville, E.L., Peng, K., D'Andrea, R.J., Glonek, G.G., Goodall, G.J., Zola, H., Shannon, M.F., Barry, S.C., 2010. Genome-wide identification of human FOXP3 target genes in natural regulatory T cells. J. Immunol. 185, 1071-1081.

Samanta, A., Li, B., Song, X., Bembas, K., Zhang, G., Katsumata, M., Saouaf, S.J., Wang, Q., Hancock, W.W., Shen, Y., Greene, M.I., 2008. TGF-beta and IL-6 signals modulate chromatin binding and promoter occupancy by acetylated FOXP3. Proc. Natl. Acad. Sci. U S A 105, 14023-14027.

Schneider, A., Rieck, M., Sanda, S., Pihoker, C., Greenbaum, C., Buckner, J.H., 2008. The effector T cells of diabetic subjects are resistant to regulation via $CD4^+$ $FOXP3^+$ regulatory T cells. J. Immunol. 181, 7350-7355.

Schramm, C., Huber, S., Protschka, M., Czochra, P., Burg, J., Schmitt, E., Lohse, A.W., Galle, P.R., Blessing, M., 2004. TGF-beta regulates the $CD4^+CD25^+$ T-cell pool and the expression of Foxp3 *in vivo*. Int. Immunol. 16, 1241-1249.

Simonetta, F., Chiali, A., Cordier, C., Urrutia, A., Girault, I., Bloquet, S., Tanchot, C., Bourgeois, C., 2010. Increased CD127 expression on activated $FOXP3^+CD4^+$ regulatory T cells. Eur. J. Immunol. 40, 2528-2538.

Smith, E.L., Finney, H.M., Nesbitt, A.M., Ramsdell, F., Robinson, M.K., 2006. Splice variants of human FOXP3 are functional inhibitors of human $CD4^+$ T-cell activation. Immunology 119, 203-211.

Soligo, M., Camperio, C., Caristi, S., Scotta, C., Del Porto, P., Costanzo, A., Mantel, P.Y., Schmidt-Weber, C.B., Piccolella, E., 2011. CD28 costimulation regulates FOXP3 in a RelA/NFkappaB-dependent mechanism. Eur. J. Immunol. 41, 503-513.

Spatz, A., Borg, C., Feunteun, J., 2004. X-chromosome genetics and human cancer. Nat. Rev. Cancer 4, 617-629.

Takaki, H., Ichiyama, K., Koga, K., Chinen, T., Takaesu, G., Sugiyama, Y., Kato, S., Yoshimura, A., Kobayashi, T., 2008. STAT6 Inhibits TGF-beta1-mediated Foxp3 induction through direct binding to the Foxp3 promoter, which is reverted by retinoic acid receptor. J. Biol. Chem. 283, 14955-14962.

Thornton, A.M., Korty, P.E., Tran, D.Q., Wohlfert, E.A., Murray, P.E., Belkaid, Y., Shevach, E.M., 2010. Expression of Helios, an Ikaros transcription factor family member, differentiates thymic-derived from peripherally induced Foxp3^{+} T regulatory cells. J. Immunol. 184, 3433-3441.

Torgerson, T.R., Linane, A., Moes, N., Anover, S., Mateo, V., Rieux- Laucat, F., Hermine, O., Vijay, S., Gambineri, E., Cerf- Bensussan, N., Fischer, A., Ochs, H.D., Goulet, O., Ruemmele, F.M., 2007. Severe food allergy as a variant of IPEX syndrome caused by a deletion in a noncoding region of the FOXP3 gene. Gastroenterology 132, 1705-1717.

Valdman, A., Jaraj, S.J., Comperat, E., Charlotte, F., Roupret, M., Pisa, P., Egevad, L., 2010. Distribution of Foxp3-, CD4- and CD8-positive lymphocytic cells in benign and malignant prostate tissue. APMIS 118, 360-365.

Vang, K.B., Yang, J., Mahmud, S.A., Burchill, M.A., Vegoe, A.L., Farrar, M.A., 2008. IL-2, -7, and -15, but not thymic stromal lymphopoeitin, redundantly govern CD4^{+}Foxp3^{+} regulatory T cell development. J. Immunol. 181, 3285-3290.

Veldman, C., Pahl, A., Hertl, M., 2009. Desmoglein 3-specific T regulatory 1 cells consist of two subpopulations with differential expression of the transcription factor Foxp3. Immunology 127, 40-49.

Venuprasad, K., Huang, H., Harada, Y., Elly, C., Subramaniam, M., Spelsberg, T., Su, J., Liu, Y.C., 2008. The E3 ubiquitin ligase Itch regulates expression of transcription factor Foxp3 and airway inflammation by enhancing the function of transcription factor TIEG1. Nat. Immunol. 9, 245-253.

Wang, C., Lisanti, M.P., Liao, D.J., 2011. Reviewing once more the c-myc and Ras collaboration: converging at the cyclin D1-CDK4 complex and challenging basic concepts of cancer biology. Cell Cycle 10, 57-67.

Wang, D., Zhang, H., Liang, J., Gu, Z., Zhou, Q., Fan, X., Hou, Y., Sun, L., 2010a. $CD4^+$ $CD25^+$ but not $CD4^+$ $Foxp3^+$ T cells as a regulatory subset in primary biliary cirrhosis. Cell Mol. Immunol. 7, 485-490.

Wang, L., Liu, R., Ribick, M., Zheng, P., Liu, Y., 2010b. FOXP3 as an X-linked tumor suppressor. Discov. Med. 10, 322-328.

Wang, L., Liu, R., Li, W., Chen, C., Katoh, H., Chen, G.Y., McNally, B., Lin, L., Zhou, P., Zuo, T., Cooney, K.A., Liu, Y., Zheng, P., 2009. Somatic single hits inactivate the X-linked tumor suppressor FOXP3 in the prostate. Cancer Cell 16, 336-346.

Wang, R., Han, G., Wang, J., Song, L., Chen, G., Xu, R., Yu, M., Qian, J., Shen, B., Li, Y., 2007. The role of STAT3 in antigen-IgG inducing regulatory CD4(+)Foxp3(+)T cells. Cell Immunol. 246, 103-109.

Wildin, R.S., Freitas, A., 2005. IPEX and FOXP3: clinical and research perspectives. J. Autoimmun. 25 (Suppl), 56-62.

Wu, Y., Borde, M., Heissmeyer, V., Feuerer, M., Lapan, A.D., Stroud, J.C., Bates, D.L., Guo, L., Han, A., Ziegler, S.F., Mathis, D., Benoist, C., Chen, L., Rao, A., 2006. FOXP3 controls regulatory T cell function through cooperation with NFAT. Cell 126, 375-387.

Xu, L., Kitani, A., Stuelten, C., McGrady, G., Fuss, I., Strober, W., 2010. Positive and negative transcriptional regulation of the Foxp3 gene is mediated by access and binding of the Smad3 protein to enhancer I. Immunity 33, 313-325.

Yokokawa, J., Cereda, V., Remondo, C., Gulley, J.L., Arlen, P.M., Schlom, J., Tsang, K.Y., 2008. Enhanced functionality of $CD4^{+}CD25(high)FoxP3^{+}$ regulatory T cells in the peripheral blood of patients with prostate cancer. Clin. Cancer Res. 14, 1032-1040.

Zhang, F., Meng, G., Strober, W., 2008. Interactions among the transcription factors Runx1, RORgammat and Foxp3 regulate the differentiation of interleukin 17-producing T cells. Nat. Immunol. 9, 1297-1306.

Zheng, Q., Xu, Y., Liu, Y., Zhang, B., Li, X., Guo, F., Zhao, Y., 2009. Induction of Foxp3 demethylation increases regulatory $CD4^{+}CD25^{+}$ T cells and prevents the occurrence of diabetes in mice. J. Mol. Med. 87, 1191-1205.

Zheng, S.G., Wang, J.H., Stohl, W., Kim, K.S., Gray, J.D., Horwitz, D.A., 2006. TGF-beta requires CTLA-4 early after T cell activation to induce FoxP3 and generate adaptive $CD4^{+}CD25^{+}$ regulatory cells. J. Immunol. 176, 3321-3329.

Zheng, Y., Josefowicz, S., Chaudhry, A., Peng, X.P., Forbush, K., Rudensky, A.Y., 2010. Role of conserved non-coding DNA elements in the Foxp3 gene in regulatory T-cell fate. Nature 463, 808-812.

Zhou, L., Lopes, J.E., Chong, M.M., Ivanov II, , Min, R., Victora, G.D., Shen, Y., Du, J.,

Rubtsov, Y.P., Rudensky, A.Y., Ziegler, S.F., Littman, D.R., 2008a. TGF-beta-induced Foxp3 inhibits T(H)17 cell differentiation by antagonizing RORgammat function. Nature 453, 236-240.

Zhou, X., Kong, N., Zou, H., Brand, D., Li, X., Liu, Z., Zheng, S.G., 2010. Therapeutic potential of TGF-beta-induced CD4(+) Foxp3(+) regulatory T cells in autoimmune diseases. Autoimmunity.

Zhou, Z., Song, X., Li, B., Greene, M.I., 2008b. FOXP3 and its partners: structural and biochemical insights into the regulation of FOXP3 activity. Immunol. Res. 42, 19-28.

Ziegler, S.F., 2006. FOXP3: of mice and men. Annu. Rev. Immunol. 24, 209-226.

Zorn, E., Nelson, E.A., Mohseni, M., Porcheray, F., Kim, H., Litsa, D., Bellucci, R., Raderschall, E., Canning, C., Soiffer, R.J., Frank, D.A., Ritz, J., 2006. IL-2 regulates FOXP3 expression in human $CD4^{+}CD25^{+}$ regulatory T cells through a STAT-dependent mechanism and induces the expansion of these cells *in vivo*. Blood 108, 1571-1579.

Zuo, T., Liu, R., Zhang, H., Chang, X., Liu, Y., Wang, L., Zheng, P., 2007a. FOXP3 is a novel transcriptional repressor for the breast cancer oncogene SKP2. J. Clin. Invest. 117, 3765-3773.

Zuo, T., Wang, L., Morrison, C., Chang, X., Zhang, H., Li, W., Liu, Y., Wang, Y., Liu, X., Chan, M.W., Liu, J.Q., Love, R., Liu, C.G., Godfrey, V., Shen, R., Huang, T.H., Yang, T., Park, B.K., Wang, C.Y., Zheng, P., 2007b. FOXP3 is an X-linked breast cancer suppressor gene and an important repressor of the HER-2/ErbB2 oncogene. Cell 129, 1275-1286."

Chapter 3- Characterization of PR70 in melanoma

Published as:

van Kempen LC, Redpath M, Elchebly M, Klein KO, Papadakis AI, Wilmott JS, Scolyer RA, Edqvist PH, Pontén F, Schadendorf D, van Rijk AF, Michiels S, Dumay A, Helbling-Leclerc A, Dessen P, Wouters J, Stass M, Greenwood CM, Ghanem GE, van den Oord J, Feunteun J, Spatz A. The protein phosphatase 2A regulatory subunit PR70 is a gonosomal melanoma tumor suppressor gene. *Sci Transl Med*. 2016 Dec 14;8 (369):369ra177.

Contribution of authors:

Margaret Redpath: Designed the immunohistochemical experiments, optimized the antibodies, performed immunohistochemical analyses and data interpretation, as well as confocal microscopy, cell culture, protein and DNA extraction, clinical database management and preparation of the manuscript. Presented this work at two conferences with oral presentations entitled “PR70, A Novel Melanoma Tumor Suppressor” at the EORTC Melanoma Group Conference in May 2013 and “The Protein Phosphatase 2 Subunit of PR70 is a Novel Tumor Suppressor Gene” at the Paris Melanoma Conference in May 2013 earning an “Outstanding Abstract Award”.

Leon van Kempen: Designed the in vitro and in vivo cell culture, DNA and RNA FISH, and biochemical experiments as well as *PPP2R3B* mutation analysis; performed cell culture and animal experiments and data interpretation; and contributed to the writing of the manuscript.

Mounib Elchebly: Performed cell culture, animal and biochemical experiments as well as data interpretation

Kathleen Oros Klein: performed statistical analyses

Celia Greenwood: performed statistical analyses

Stefan Michiels: performed statistical analyses

Andreas Papadakis: Biochemical experiments and data interpretation.

James Wilmott: Provided melanoma tissue and/or clinical data

Richard Scolyer: Provided melanoma tissue and/or clinical data

Joost van den Oord: Provided melanoma tissue and/or clinical data

Fredrik Pontén: Provided melanoma tissue and/or clinical data

Per-Henrik Edqvist: Provided melanoma tissue and/or clinical data

Dirk Schadendorf: Provided melanoma tissue and/or clinical data

Jasper Wouters: Provided melanoma tissue and/or clinical data

Marguerite Stass: Provided melanoma tissue and/or clinical data

Anke van Rijk: Performed DNA and RNA FISH experiments and data analysis.

Jean Feunteun: Designed the aCGH experiments and performed data interpretation.

Ghanem Ghanem: Generated and characterized the melanoma cell lines.

Anne Dumay: Performed the aCGH analyses.

Anne Helbling-Leclerc: Performed the aCGH analyses.

Alan Spatz: Designed the immunohistochemical experiment, aCGH and FISH analyses of the X chromosome status, and analysis of the PR70-ROF interaction; performed data interpretation; and contributed to the writing of the manuscript.

"Male gender is independently and significantly associated with poor prognosis in melanoma of all clinical stages. The biological underpinnings of this sex difference remain largely unknown, but we hypothesized that gene expression from gonosomes (sex chromosomes) might play an important role. We demonstrate that loss of the inactivated X chromosome in melanomas arising in females is strongly associated with poor distant metastasis–free survival, suggesting a dosage benefit from two X chromosomes. The gonosomal protein phosphatase 2 regulatory subunit B, beta (PPP2R3B) gene is located on the pseudoautosomal region (PAR) of the X chromosome in females and the Y chromosome in males. We observed that, despite its location on the PAR that predicts equal dosage across genders, *PPP2R3B* expression was lower in males than in females and was independently correlated with poor clinical outcome. *PPP2R3B* codes for the PR70 protein, a regulatory substrate-recognizing subunit of protein phosphatase 2A. PR70 decreased melanoma growth by negatively interfering with DNA replication and cell cycle progression through its role in stabilizing the cell division cycle 6 (CDC6)–chromatin licensing and DNA replication factor 1 (CDT1) interaction, which delays the firing of origins of DNA replication. Hence, PR70 functionally behaves as an X-linked tumor suppressor gene.

INTRODUCTION

In recent years, major advances in the understanding of melanoma have been directly translated into new active targeted therapies and have improved clinical management of this disease. Immunological checkpoint inhibitors and targeted agents such as selective inhibitors of the B-Raf proto-oncogene, serine/threonine kinase (BRAF), and mitogen-activated protein kinase kinase have demonstrated their impact on prolonged survival in metastatic melanomas (1, 2). However, in both instances, only a subset of patients experienced a long-term benefit. This bottleneck underlines the importance of identifying key molecular events associated with melanoma

progression and of better understanding the biological substrates of phenotypic variables that affect disease outcome (3).

A striking finding in cutaneous melanoma is the importance of gender as a strong and independent prognostic indicator for survival at all stages of the disease. A recent meta-analysis of 2734 melanoma patients demonstrated an adjusted hazard ratio (HR) of male gender for 5-year disease-specific survival (DSS) of 0.85 (0.77 to 0.95) that persists even after metastasis to distant sites [adjusted HR for 2-year DSS in stage IV patients, 0.81 (0.72 to 0.92)] (4, 5). This implicates sex-related characteristics that influence melanoma progression and survival. We hypothesized that differences in the dosage of gonosomal gene products contribute to the sex effect in melanoma. X chromosome inactivation is a process that entails chromosome-wide transcriptional silencing and involves large-scale remodeling of its three-dimensional (3D) structure under the control of the X-inactive specific transcript (Xist) long noncoding RNA. Inactivation of one X chromosome in female cells nearly equalizes gene expression between mammalian males and females. However, this process is incomplete, leaving at least 15% of the ~1100 X-linked genes expressed at higher levels in females than in males (6). Expression of the escaping alleles on the inactive X (Xi) chromosome is frequently lower than that of the corresponding alleles on the active X (Xa) chromosome (7, 8). In addition, impaired X inactivation can lead to either the uncovering of activated oncogenes or gene-dosage effects on tumor suppressor genes (TSGs) in a non-Knudsonian manner, such as loss of one TSG allele being sufficient to initiate tumorigenesis (9). Therefore, one can postulate that X-linked TSGs that escape inactivation might play an important role in cell biology and that impairment of these genes or alteration in their regulation could be critical events in tumor progression.

Here, we explore whether molecular events associated with the X chromosome inactivation interact with melanoma progression. We also specifically study the role of *PPP2R3B* as a new X-linked melanoma TSG.

RESULTS

Loss of the Xi chromosome is associated with poor prognosis in females

We performed an analysis of global genomic aberrations in a series of 49 primary melanomas (33 female and 16 male patients). Unsupervised hierarchical clustering using Ward's method and Euclidean distances resulted in three clusters (fig. S1 and table S1). Overall, loss of one X chromosome in females ($P = 0.009$, log-rank; Fig. 1A) and the presence of the Y chromosome in males ($P = 0.014$, log-rank) correlated with poor DMFS (≤3 years).

To first test the frequency of X loss, we subjected tissue microarrays (TMAs) containing multiple cores of 177 melanoma metastases from female patients to centromeric X DNA fluorescence in situ hybridization (FISH). Loss of centromeric X was observed in 44 of 177 cases (~25%). We next asked whether this loss preferentially affected the Xi. Consecutive sections of the TMAs were hybridized with probes detecting *Xist* RNA as a means of marking the epigenetically silenced X chromosome (Fig. 1B). Xist RNA FISH demonstrated the absence of Xi in 41 of 44 cases (93.1%), which indicated a significant skewing toward the loss of Xi ($P < 0.001$, Fisher's exact test). In the group of 133 melanoma cases with no X loss, two active copies of X were observed in 42 cases. Therefore, loss of the Xi chromosome was observed in 83 cases (46.8%), either by X chromosome loss (23.1%), Xa duplication, or loss of X inactivation (23.7%), as observed in breast and ovarian cancer (10). In 33 of 177 cases with known follow-up, when one

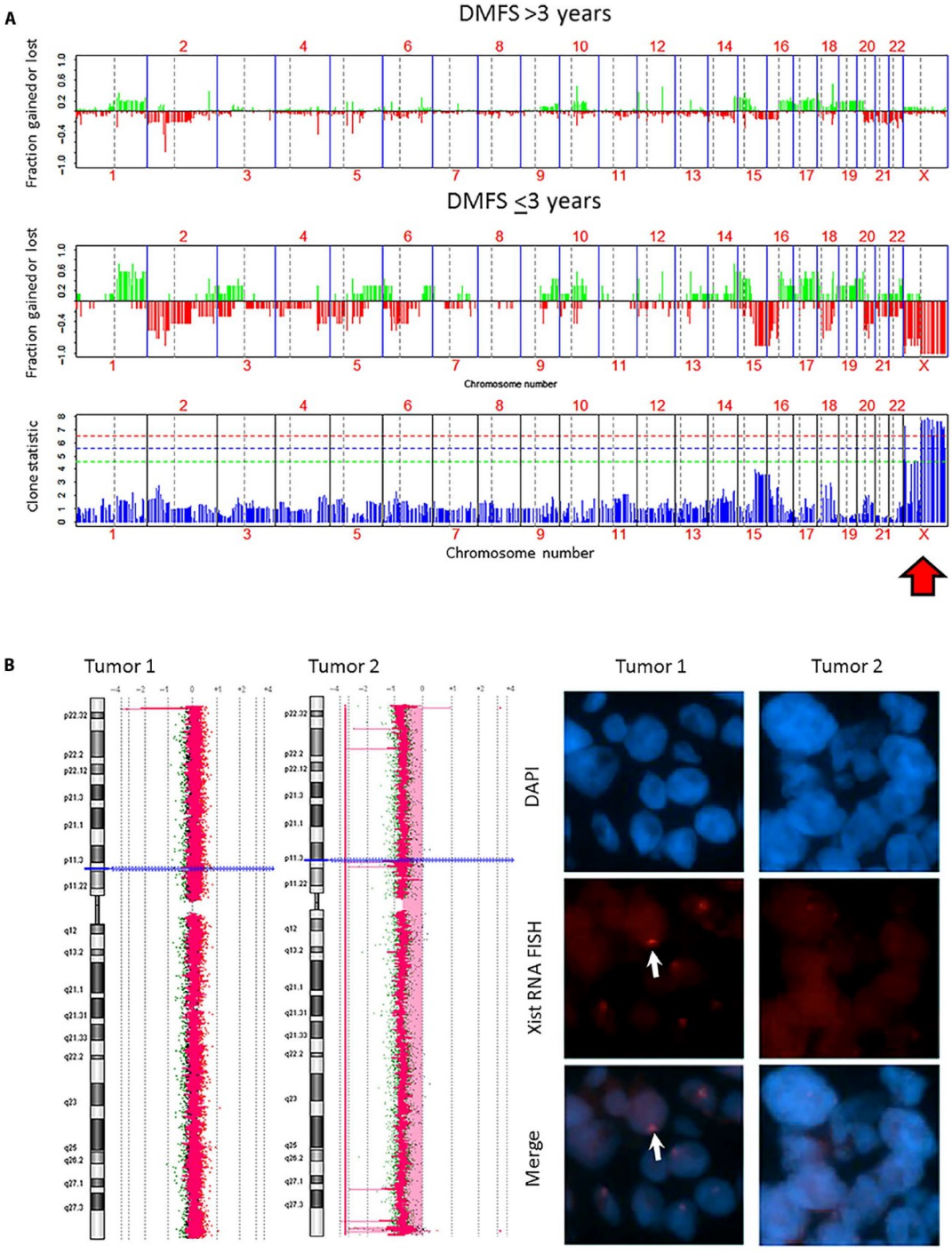

Fig. 1. Loss of Xi chromosome is strongly associated with decreased distant metastasis–free survival (DMFS). **(A)** Array-based comparative genomic hybridization revealed a significant correlation between loss of X and poor 3-year distant metastasis–free survival. The loss of one X chromosome in females ($P = 0.009$, log-rank) and the presence of the Y chromosome in males ($P = 0.014$, log-rank) correlated with poor DMFS (≤3 years). The arrow indicates X chromosome. **(B)** In cases where the tumor showed evidence of X loss (for example, tumor 2; left panel), the loss always involved the Xi, as visualized by the loss of the Xist cloud by RNA FISH (tumor 2; right panel). The white arrow indicates one of multiple nuclei with a cloud of Xist RNA located at the nuclear envelope and is indicative for Xi ($P < 0.001$, Fisher's exact test). DAPI, 4′,6-diamidino-2-phenylindole.

of the two X chromosomes was lost, it was always Xi (n = 11), correlating with poor DMFS (P = 0.01, log-rank).Thus, loss of Xi in melanoma was frequently observed and correlated with poor DMFS for women.

PPP2R3B expression and PR70 protein dosage correlate with melanoma survival and gonosomal status

Loss of the Xi chromosome reduces the protein expression levels of genes that escape inactivation. In the case of TSGs, this reduced expression might determine the adverse effect of X chromosome loss on clinical outcomes. Males with Y chromosome loss also have an adverse prognosis, and postzygotic, mosaic loss of Y is associated with increased cancer risk and shorter survival (11). Most genes within the pseudoautosomal region (PAR) and inactivation-escaping region on X have a functional copy on the Y chromosome (12); this suggests that genes that have an impact on cancer prognosis are located on both the X and Y chromosomes and are expressed on the Xi, most likely within the PAR. Previous genome-wide expression studies demonstrate the importance of dysregulation in the firing of DNA replication in melanoma prognosis (13). Therefore, we focused our attention on genes that are shared by the X and Y chromosomes, those that escaped X chromosome inactivation (6, 14), and those that encode proteins that might be involved replication origin firing (ROF). *PPP2R3B* (Xp22.3, Yp11.3, PAR1) was the only gene that met all three criteria.

PPP2R3B encodes 1 of the ~15 possible regulatory subunits of the heterotrimeric protein phosphatase 2A (PP2A) holoenzyme (15). The PP2A complex is a key serine/threonine phosphatase that regulates multiple signals in mammalian cells. For example, PP2A is a negative regulator of several signaling pathways that promote cell growth, proliferation, and survival, including the phosphoinositide-3-kinase and the mitogen-activated protein/extracellular signal–

regulated kinase family of kinases. Quantitative polymerase chain reaction (qPCR) analysis of *PPP2R3B* mRNA expression in a series of 49 primary melanomas revealed a strong correlation between low levels of expression and poor DMFS ($P = 0.001$, log-rank, univariate analysis; fig. S2A). When expression was analyzed as a continuous variable in a Cox regression analysis, a stronger significance was obtained ($P = 0.0007$), suggesting a dose-dependent correlation between reduced *PPP2R3B* expression and short DMFS.

Immunohistochemical study of PR70 expression in an independent series of 339 (143 female and 196 male patients) tissue samples from primary melanomas revealed that increased PR70 protein expression was associated with improved survival (Fig. 2, A and B, and fig. S2B). Mean overall survival for patients with high (2+ and 3+) PR70-expressing tumors was 2.4-fold higher compared to those with PR70-negative (0) or weakly positive (1+) tumors: 10.2 years [95% confidence interval (CI), 8.8 to 11.9] and 4.3 years (95% CI, 3.1 to 5.6), respectively (Fig. 2B). Five-year overall survival for PR70 high tumors was 65% versus 32% for PR70 low tumors ($P < 0.001$, log-rank; Fig. 2B). We also found an association of PR70 expression with sex (P=0.03, Mann-Whitney *U* test), with lower expression levels being detected in tumors from male patients. This was surprising because one would expect similar expression of PAR genes in both males and females because PARs are homologous in X and Y chromosomes.

Next, we assessed whether decreased *PPP2R3B* expression correlated with specific loss of the Xi allele. *Xist* RNA FISH was performed in parallel with nascent *PPP2R3B* mRNA FISH. Parallel analysis of Xi and nascent *PPP2R3B* mRNA expression suggested that loss of *Xist* correlated with the loss of biallelic nascent *PPP2R3B* RNA expression (Fig. 2C). Samples with biallelic expression displayed a higher signal intensity of the spot away from the nuclear membrane and therefore likely originated from the Xa. This is consistent with the known reduction in

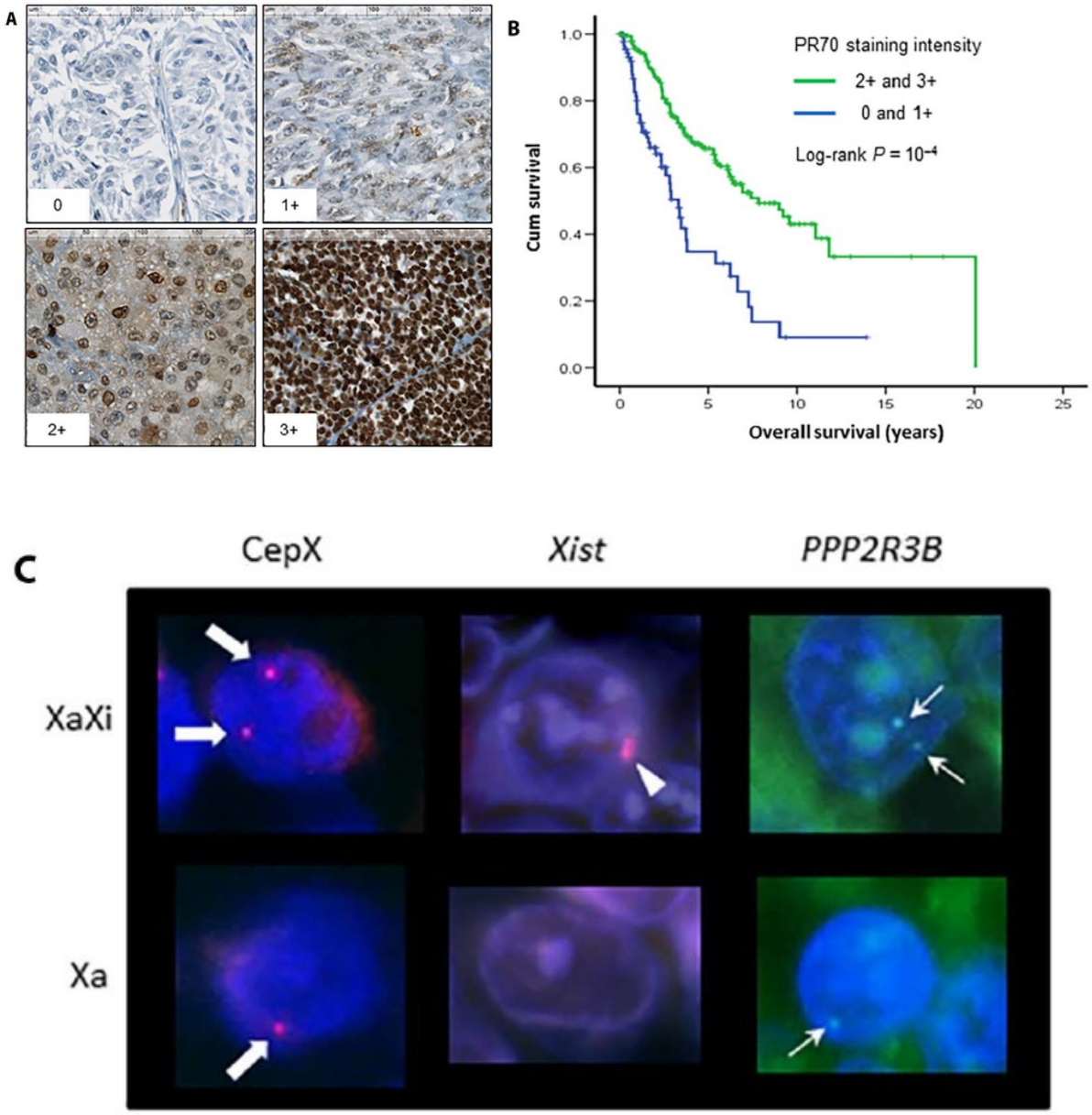

Fig. 2. Loss of PR70 and *PPP2R3B* expression correlates with poor overall survival. (A) Representative images for the semiquantitative scoring of PR70 expression. The description of the scoring system is described in Materials and Methods. **(B)** Loss of PR70 expression (combined absent and weak expression) significantly correlated with poor overall survival. Consecutive sections of the TMAs were hybridized with probes detecting Xist RNA to mark the epigenetically silenced X chromosomes. Xist RNA FISH was used to detect the absence or presence of Xi. Cum, cumulative. **(C)** Loss of Xi resulted in the loss of one actively transcribed *PPP2R3B* allele, as visualized by X chromosome centromere DNA FISH (CepX), Xist FISH (Xist), and nascent *PPP2R3B* RNA FISH (*PPP2R3B*) on formalin-fixed, paraffin-embedded melanomas.

transcriptional activity of the inactivation-escaping allele on Xi compared to the allele on Xa (14). Collectively, these data demonstrate a close correlation between the level of PR70 in melanoma cells and the severity of the disease and suggest that the PR70 expression level is determined, in part, by the copy number of the *PPP2R3B* gene in females and lower *PPP2R3B* gene expression in males.

***PPP2R3B* is not frequently mutated in melanoma**

In the classic model of TSG inactivation, both alleles are inactivated by two independent events that can be of different natures, including inactivating mutations, deletions, or epigenetic silencing. To test whether any of these events targeted the *PPP2R3B* gene, we analyzed existing genomic data for melanoma tissue and melanoma cell lines. DNA sequences of 122 paired samples of tumor and germline DNA from melanoma patients were extracted from the Melanoma Genome Sequencing Project (data set phs000452.v1.p1) in the National Center for Biotechnology Information (NCBI) Genotypes and Phenotypes Database. A total of 331 intronic and exonic single-nucleotide variants (SNVs) were identified. No somatic mutations (SNVs or indels) were found in the coding region of *PPP2R3B*, at the intron-exon boundaries, or within the 1000–base pair promoter region upstream of the canonical ATG that codes for the first methionine amino acid. Furthermore, single-nucleotide polymorphism (SNP) frequencies were compared to those in the 1000 Genomes database (www.internationalgenome.org/), and melanoma patients did not reveal an enrichment of specific SNPs compared to healthy individuals, making it unlikely that germline *PPP2R3B* variants confer melanoma susceptibility. We also sequenced the *PPP2R3B* coding region in the following materials: 10 pairs of lymph node metastases (>80% of tumor cells) and reactive lymph nodes (all females), 10 early passage melanoma cell lines and the tumors from which they were derived (all females), and an additional 20 primary melanomas from males and

females. No mutations other than those listed in the Supplementary Materials and fig. S3 were identified in the *PPP2R3B* gene. A recently published whole-exome sequencing study on six cell lines derived from melanoma metastases likewise did not identify nonsynonymous SNVs, potentially altering the protein sequence (16). From these data, it can be concluded that the frequency of an inactivating mutation of *PPP2R3B* is less than 0.6% (1 of the total 167 melanoma samples for which *PPP2R3B* sequence data were available) and that germline SNVs within *PPP2R3B* are unlikely to explain the loss of expression of *PPP2R3B* in melanoma.

PR70 attenuates melanoma growth in vitro

qPCR analyses of *PPP2R3B* expression in a panel of nine low passage melanoma cell lines derived from lymph node metastases revealed a correlation between high *PPP2R3B* expression and increased cell doubling time as measured using MTT [3-(4,5-dimethylthiazol-2-yl)-2,5-diphenyltetrazolium bromide] assay ($P < 0.001$, Pearson correlation, $r = 0.940$; Fig. 3A). Because mutations in the *BRAF*, *NRAS*, or *TP53* gene are often present in melanomas, we studied whether there was a correlation between *PPP2R3B* expression and mutations in these genes. No association was observed between *PPP2R3B* expression and *BRAF*, *NRAS*, or *TP53* mutation status. The MM73, MM102, and MM117 cell lines derived from human metastatic melanomas expressed low levels of endogenous *PPP2R3B*, and so we transfected them each with a *PPP2R3B* expression construct to analyze the gene's effect on cancer cell line growth in 2D and 3D cultures and *in vivo* in mice. Stable cell lines could be derived only from the MM117 cell line. Notably, the range of *PPP2R3B* overexpression in the derived cell lines was within physiologically relevant levels similar to those in MM98, a cell line with high endogenous PR70 expression. $MM117^{PPP2R3B}$ cells expressing high levels of PR70 (Fig. 3B) displayed a more rounded phenotype in 2D cultures (fig. S4A), a decrease in the fraction of cells in the G2-M phase cells in flow cytometry analyses, and

a 40% increase in cell doubling time as measured by MTT assay (fig. S4B). We also examined whether the observed correlation between high PR70 and reduced proliferation *in vitro* extended to tissue samples. To this end, we analyzed 172 primary melanomas for PR70 expression and assessed mitotic rate with the mitosis marker phosphohistone H3 (PH3) on consecutive tissue sections. We found an increased fraction of M phase melanoma cells in tissues with low PR70 expression ($P = 0.002$; Wilcoxon signed-rank test).

MM117 melanoma cells with forced PR70 expression were not able to form solid spheres on a layer of agar 72 hours after seeding (Fig. 3C). In long-term soft agar assays, forced expression of PR70 impaired the capacity to form colonies (Fig. 3D) but without impairing the distribution of the diameter of the spheroids that did develop (fig. S4C). The correlation between PR70 expression levels, the ability of MM117 cells to form solid spheres, and their clonogenic capacity (Fig. 3, B to D) suggested a dose-dependent phenotypic effect of PR70 expression. We next assessed the effect of knocking down PR70 expression using short hairpin RNA (shRNA) targeting *PPP2R3B* in three independently isolated nevus cell lines, which repeatedly resulted in cell death (fig. S5A). However, using the same shRNA targeting *PPP2R3B*, we succeeded to generate stable MM57 melanoma cells with reduced PR70 expression ($MM57^{shPPP2R3B}$) (Fig. 3E). These *PPP2R3B* knockdown cells displayed an increased cytoplasmic volume compared to control cells and occasional multinucleated cells, which were not observed in the control cell population (fig. S5B). The $MM57^{shPPP2R3B}$ cells were able to form solid spheroids on soft agar (fig. S5B) and displayed increased clonogenic capacity on soft agar (Fig. 3F). These observations, together with the ex vivo data (Fig. 2B and fig. S2), demonstrate that PR70 loss promotes tumor progression in melanoma but is not tumorigenic in nevus cells.

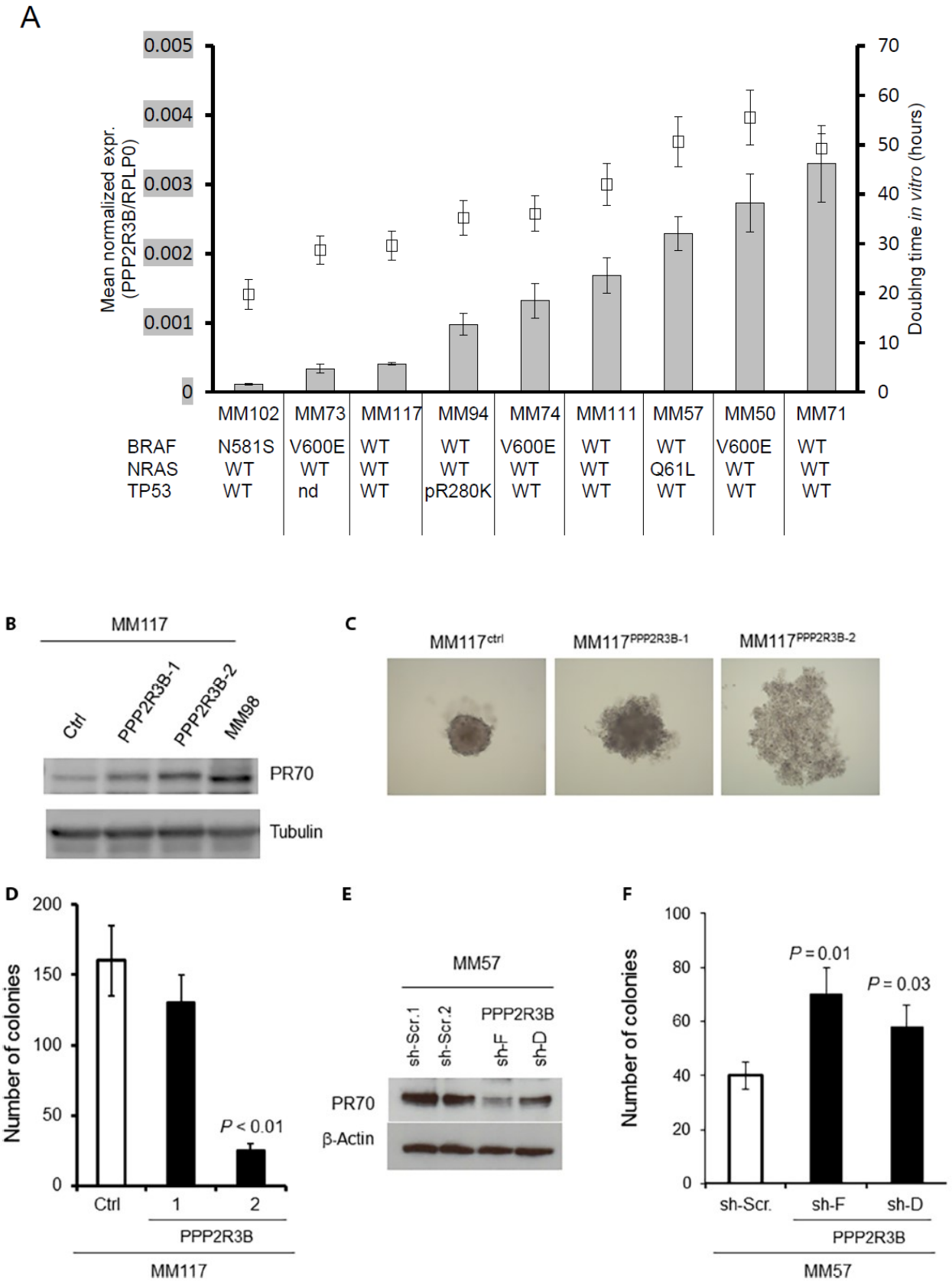
A
Mean normalized expr. (PPP2R3B/RPLP0)
0.005
0.004
0.003
0.002
0.001
0
Doubling time in vitro (hours)
70
60
50
40
30
20
10
0
MM102 MM73 MM117 MM94 MM74 MM111 MM57 MM50 MM71
BRAF N581S V600E WT WT V600E WT WT V600E WT
NRAS WT WT WT WT WT WT Q61L WT WT
TP53 WT nd WT pR280K WT WT WT WT WT
B
MM117
Ctrl
PPP2R3B-1
PPP2R3B-2
MM98
PR70
Tubulin
C
MM117ctrl
MM117PPP2R3B-1
MM117PPP2R3B-2
D
Number of colonies
200
150
100
50
0
P < 0.01
Ctrl
1
2
PPP2R3B
MM117
E
MM57
sh-Scr.1
sh-Scr.2
PPP2R3B
sh-F
sh-D
PR70
β-Actin
F
Number of colonies
100
80
60
40
20
0
P = 0.01
P = 0.03
sh-Scr.
sh-F
sh-D
PPP2R3B
MM57

Fig. 3. PPP2R3B expression decreased colony-forming capacity of early passage melanoma cells. (A) High *PPP2R3B* expression in melanoma cells as measured by qPCR correlated with an increased doubling time of melanoma cells *(P* < 0.001, Pearson correlation, *r* = 0.940). Expression was determined by quantitative real-time PCR for *PPP2R3B*, which was normalized to the ribosomal protein lateral stalk subunit P0 (*RPLP0*). Cell doubling time was determined by MTT assay. Mutation status of *BRAF* [wild-type (WT), N581S, or V600E], *NRAS* (WT or Q61L), and *TP53* [WT, R280K, or not determined (nd)] for the cell lines is as indicated. **(B)** Ectopic expression of PR70 inMM117 generated three independent stable clones labeled control (Ctrl; low expression), *PPP2R3B*-1 (intermediate expression), and *PPP2R3B*-2 (high expression). Western blot analysis confirmed that ectopic expression of PR70 in MM117 cells is comparable to endogenous levels observed in MM98, a PR70 high cell line. Tubulin was used as a loading control. **(C)** A spheroid formation assay revealed that intercellular adhesion of MM117 cells is reduced with increasing PR70 expression. **(D)** High PR70 expression reduced the clonogenic capacity of MM117 in soft agar. **(E)** Western blot analysis confirmed reduced PR70 expression after stable expression of two independent hairpins targeting *PPP2R3B* (sh-F and sh-D) in MM57 cells. Two independent scramble sequences (Scr.1 and Scr.2) were used as controls. **(F)** Reduced PR70 expression increased the clonogenic capacity of MM57 cells in soft agar.

PR70 expression reduces melanoma tumorigenicity

The poor prognostic value associated with the loss of PR70 expression in melanoma and the growth inhibitory effect of its expression in *in vitro* models suggests that PR70 has a tumor suppressor function. This hypothesis was supported by a reduction in the formation of tumors ("tumor take") after subcutaneous injection of control and altered MM117 cells in mice. Control $MM117^{ctrl}$ cells displayed 87% tumor take compared to 30% for $MM117^{PPP2R3B\text{-}1}$ cells ($P = 0.02$, Mann-Whitney U test) and 20% for $MM117^{PPP2R3B\text{-}2}$ cells ($P = 0.005$, Mann-Whitney U test) (Fig. 4A). The said hypothesis was also supported by the decreased growth rate of $MM117^{PPP2R3B}$ tumors that did develop, relative to control $MM117^{ctrl}$ tumors (fig. S6).

Immunohistochemical quantification of melanoma cells in the M phase using PH3 immunohistochemistry (Fig. 4B) revealed that the density of mitotic cells was reduced to half in $MM117^{PPP2R3B}$ tumors as compared to $MM117^{ctrl}$ tumors (2.2% versus 4.2%, respectively; P=0.008, Mann-Whitney U test; Fig. 4C). Conversely, subcutaneously injected $MM57^{sh\text{-}ctrl}$ cells (4×10^6) resulted in xenograft growth in 2 of the 10 injected mice (20%), but knockdown of PR70 expression ($MM57^{sh\text{-}PPP2R3B}$) increased tumor take to 40% (2 of 5 injected mice) and 60% (3 of 5 injected mice) with two different shPPP2R3B constructs (Fig. 4D). However, the *in vivo* growth

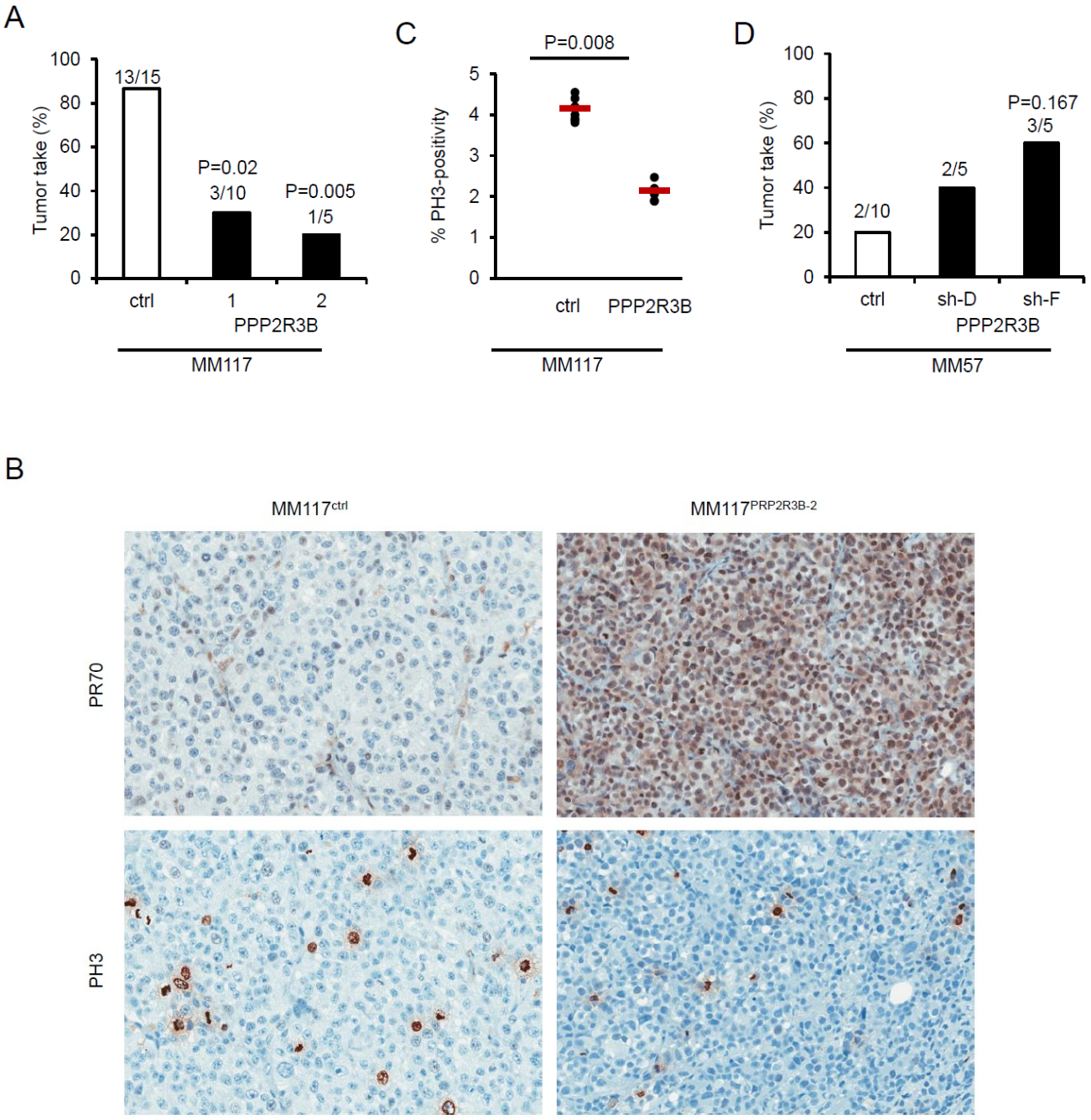

Fig. 4. PR70 expression decreased tumorigenicity in mice. (A) Ectopic PR70 expression in MM117 cells (*PPP2R3B*-1 and *PPP2R3B*-2) reduced their tumorigenicity after subcutaneous injection. **(B)** MM117 xenograft with high PR70 expression demonstrated reduced proliferation as compared to control (left panel), as visualized by immunohistochemical detection of the mitosis marker PH3 indicated by the brown staining. **(C)** Quantification of PH3-positive melanoma cells confirmed the inverse correlation between PR70 expression and proliferation. **(D)** MM57 with silenced PR70 expression (shPPP2R3B-D and shPPP2R3B-F) demonstrated increased tumor take after subcutaneous injection.

profile of these cells was not strikingly different compared to that of $MM57^{sh\text{-}ctrl}$ cells (fig. S7). The fact that knockdown of PR70 induced colony formation of MM57 cells and tumor take *in vivo* and cell death in nevus cells suggests that PR70 effects are context-dependent.

Collectively, these data demonstrated that PR70 expression has a tumor growth suppressive effect on melanoma cells and that loss of its expression is associated with a poor prognosis. The fact that (i) the effect on survival is associated with levels of *PPP2R3B* mRNA and PR70 protein expression and (ii) the *PPP2R3B* gene is not frequently mutated in cutaneous melanoma points to a dose-dependent effect on tumor growth.

PR70 stabilizes the CDC6-CDT1 interaction and controls the firing of origins of DNA replication

PP2A/PR70 has been reported to increase expression of the cell division cycle 6 (CDC6) protein, which is essential for DNA replication, possibly as a result of the increased stability of CDC6 mediated by PR70 dephosphorylation of its NH_2 terminus (17). The phosphorylation of chromatin-bound CDC6 by the cyclin-dependent kinase 2 (CDK2) and CDC6's subsequent release and dissociation of its interaction with chromatin licensing and DNA replication factor 1 (CDT1) is a critically important step in the initiation of the firing of replication origins (summarized in fig. S8) (18). Reduced PR70 expression could, therefore, impair CDC6 dephosphorylation and disrupt the CDT1-CDC6 interaction and its inhibitory effect on the ROF and cell cycle progression. Furthermore, PR70 has been implicated in the regulation of cell cycle progression through dephosphorylation of the tumor suppressor retinoblastoma protein (pRb) (19); this can potentially reduce the G_1-S cell cycle transition as a result of increased sequestration of the transcription factor E2F to nonphosphorylated pRb. Therefore, we investigated whether PR70 could regulate the firing of replication origins through a modification of the CDC6-CDT1 interaction.

In MM117 melanoma cells, PR70 overexpression indeed delayed the G_1-S transition. Whereas PR70 overexpression did not affect the exit of cells from the G_2-M phase into G_1 after the release from a nocodazole induced M phase arrest, PR70 overexpression did result in an accumulation of cells in G_1 and a delayed entry into the S phase (Fig. 5A and fig. S9). We also observed a correlation between pRb phosphorylation status and PR70 expression and between pRb dephosphorylation and PR70 overexpression, in line with the previously observed pRb-dephosphorylating activity of PR70 (fig. S10) (19). Because PR70 has also been reported to dephosphorylate CDC6 (17), and because CDC6 phosphorylation results in dissociation of the CDC6-CDT1 complex from DNA and subsequent firing of DNA replication (20–22), we next addressed whether PR70 overexpression stabilizes the CDC6-CDT1 complex in MM117. Coimmunoprecipitation experiments in MM117 did not demonstrate a PR70-induced difference in CDC6-CDT1 interactions in nonsynchronized cells, but a strong increase in the amount of CDC6-CDT1 complex was observed in cells that expressed high levels of PR70 18 hours after the release from a nocodazole arrest (Fig. 5B). This observation is consistent with the accumulation of cells in G1 and delayed entry into the S phase and thus supports the hypothesis that PR70 delays cell cycle progression by preventing the firing of origins of DNA replication. Further evidence that PR70 can delay activation of DNA replication was provided by chromatin association assays. Eighteen hours after the release of MM117 cells in culture from a nocodazole arrest, we observed higher amounts of CDT1, CDC6, and minichromosome maintenance 10 (MCM10) that remained associated with chromatin in PR70-overexpressing cells compared to control cells (Fig. 5C).When PR70 was knocked down in MM57 cells, we observed a decrease in total and chromatin-associated CDT1and CDC6 (Fig. 5D). These data suggest that PR70 can attenuate progression from G1 to S by limiting the firing of origins of DNA replication. The delay in firing is further supported by our

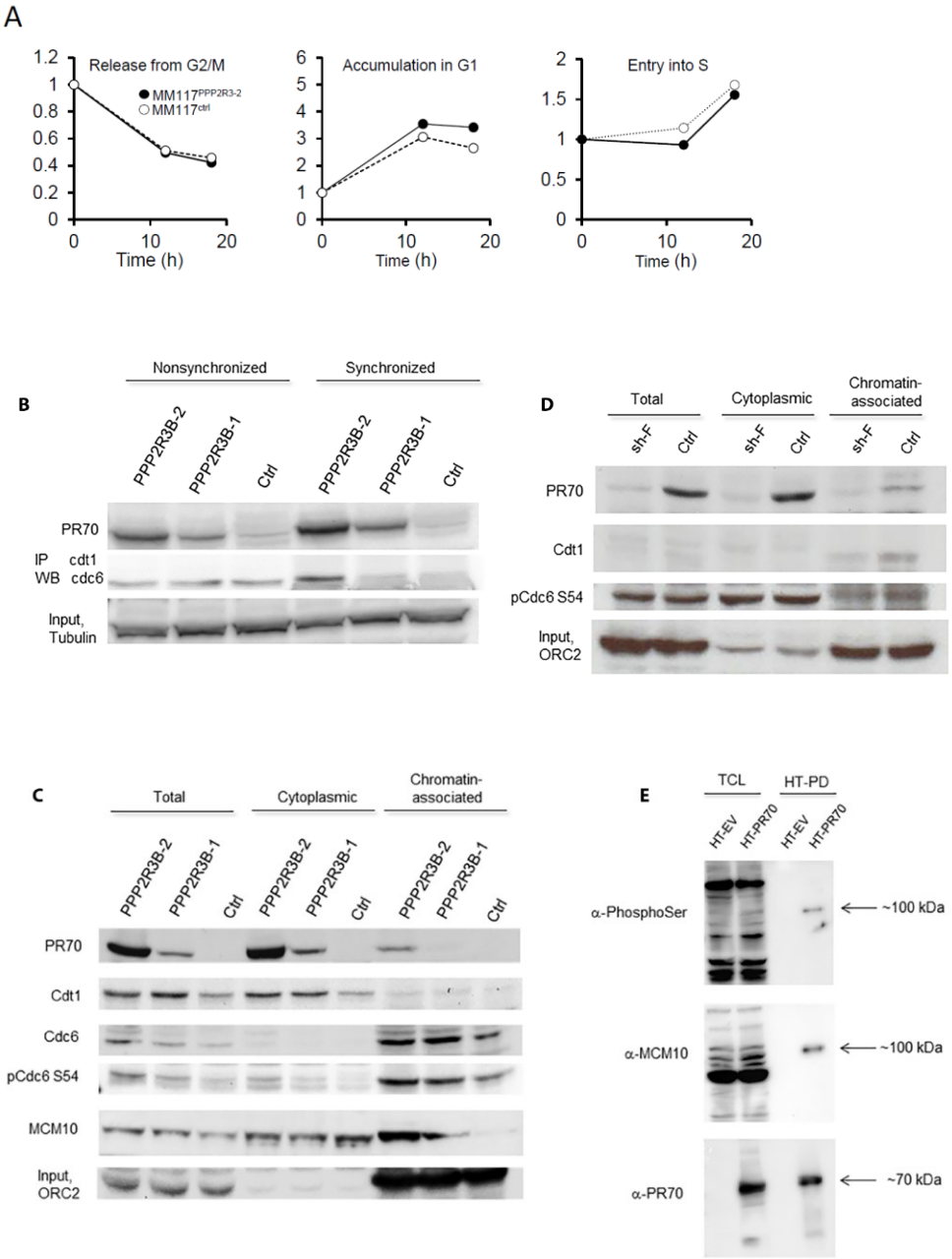

Fig. 5. PR70 attenuated the G1-S transition. (A) Bromodeoxyuridine (BrdU)/propidium iodide (PI) flow cytometry analyses revealed an accumulation of cells in G1 and delayed entry in the S phase after release from a nocodazole arrest. A representative graph of one of three experiments is shown. **(B)** Ectopic expression of PR70 inMM117 generated three independent stable clones labeled control (Ctrl; low expression), *PPP2R3B*-1 (intermediate expression), and *PPP2R3B*-2 (high expression). Immunoprecipitation (IP) and Western blotting (WB) revealed that PR70 stabilized the formation of the CDT1-CDC6 complex after release from a nocodazole arrest. **(C)** Chromatin association assays confirmed that PR70 can bind to chromatin and that this correlates with increased binding of the CDT1-CDC6-MCM10 complex. Immunoblotting for the chromatin-associated origin of replication complex 2 (ORC2) demonstrated correct fractionation. **(D)** Reduced PR70 expression via sh-F decreased the binding of PR70, CDT1, and CDC6 to chromatin. **(E)** HaloTag pull-down of PR70 in HEK293T cells. Cells were transfected with empty vector (HT-EV) or vector-encoding Halo-tagged PR70 (HT-PR70), and total cell lysates (TCL) and HaloTag pull-down samples (HT-PD) were immunoblotted for the indicated proteins.

observation that PR70 interacts with the phosphorylated MCM10 protein in human embryonic kidney (HEK) 293T cells (Fig. 5E). MCM10 is required for DNA synthesis during genome duplication and is the essential factor that recruits CDC45 to the replication complex and initiates origin melting and DNA replication (23).

DISCUSSION

Sex is a strong prognostic factor for melanoma survival at all stages of disease (4, 5), but the molecular mechanisms underpinning these associations remain poorly understood. Here, we demonstrated an important role for a new gonosomal melanoma tumor suppressor, *PPP2R3B*/PR70, in the firing of origins of replication and melanoma progression. Moreover, we show that the effect of *PPP2R3B*/PR70 is determined by its expression level and by X chromosome status in females.

We previously hypothesized a non-Knudsonian model of X-linked TSG inactivation or oncogene activation in tumors. This model takes into account the specific genetics of the X chromosome inactivation in females, including whether the gene does or does not escape inactivation (9). This model predicts that, in males, a mutation that affects a nonpseudoautosomal X-linked TSG requires a single hit. By contrast, the genetics differs in females. In the case of a gene that escapes inactivation, both copies must be affected for a complete loss of function. By contrast, for genes subject to inactivation, a single hit on the active allele would result in a complete loss of function in females. This model has since been confirmed in several in vivo situations in humans [for example, mutation of the *WTX* gene that does not escape X inactivation in a subset of Wilms tumors (24) and somatic inactivating mutations in the demethylase-encoding *UTX* gene, which escapes X inactivation in a wide range of solid tumors (25)]. Our current study demonstrates a dose-dependent tumor suppressive effect of a nonmutated X-linked gene that escapes X

chromosome inactivation and therefore provides supportive evidence for the continuum model for TSGs (26). This model states that the level of gene expression, rather than the gene's mutation status, determines the antitumor effect of a tumor suppressor protein.

Different levels of X-linked gene expression in males and females are determined not only by transcriptional activity but also by the gender-dependent differential regulation of their expression. Array-based gene expression analyses in peripheral blood cells revealed striking differences in baseline expression levels of X-linked genes in males and females as well as differences in the up-regulation and down-regulation of expression after acute stress, such as an acute ischemic stroke (27). Differences in gender-biased gene expression are not restricted to gonosomes, as demonstrated by network analyses of gene expression profiles and transcription factor binding assays in chronic obstructive pulmonary disease patients (28). Our analyses demonstrate that loss of the Xi chromosome significantly correlated with poor clinical outcome, whereas other chromosomal aberrations do not. Therefore, loss of this chromosome appears to more strongly drive the malignant phenotype than do other alterations at the genome level in melanoma.

About 15% of all genes on the Xi chromosome escape inactivation and can potentially contribute to melanoma-promoting gene-dosage effects. We have demonstrated that one of these escaping genes, *PPP2R3B*, is a critical regulator of the firing of origins of replication in a dose-dependent manner and regulates cell proliferation, one of the most significant prognostic factors of melanoma (3). Last, we observed that *PPP2R3B* expression is lower in male patients with melanoma and on the Xi allele in female patients, therefore opening a new avenue to better understand gender differences in this disease.

In a genome-wide expression study of thick primary melanomas, we previously demonstrated a role for the dysregulation of genes involved in the firing of DNA replication origins in melanoma progression (13). Gene expression signatures that are associated with cell proliferation (13) and enhanced expression of proteins involved in the initiation of DNA replication (such as CDK2) (29) and DNA unwinding (such as MCM helicases 4 and 6) (13) have a strong prognostic value for predicting disease progression and melanoma patient survival. The firing of origins of DNA replication is tightly regulated to duplicate DNA only once during the S phase, thus preventing aneuploidy, and the expression and phosphorylation of CDC6 plays an important role in this process. The observed increase in CDC6 expression in melanoma cells with forced PR70 expression is most likely a consequence of PR70-induced dephosphorylation of pRb [fig. S10 and (19)]. Dephosphorylation of pRb at the start of the G1 phase results in dissociation of the pRb-E2F complex, after which, free E2F directly drives the expression of CDC6 (30). Previously published data (21) in addition to our own data (Fig. 5) demonstrate that PR70 also directs the dephosphorylating activity of PP2A, which prevents the release of E2F and subsequent induction of CDC6 expression in G1. In parallel, PP2A/PR70 prevents the release of the CDT1-CDC6 complex from chromatin (Fig. 5, B to D), thereby delaying the initiation of DNA replication induced by the cyclin A–CDK2 protein complex during the early S phase.

It is important to note that the tumor suppressive function of PR70 is not the only activity that is reduced when the Xi chromosome is lost. Therefore, the cumulative effect of silencing-escaping X-linked genes on melanoma cell biology remains unknown.

MATERIALS AND METHODS

Study design

The aim of the study was to study the impact of molecular events associated with the X chromosome inactivation on melanoma progression and to explore the functions of the X-linked *PPP2R3B/PR70* TSG in human clinical samples, in xenografts, and in melanoma cell lines. Primary tumors and metastases were evaluated by microscopic techniques. Tumor cell markers, cell proliferation, and X chromosome status were monitored with routine histology, immunohistochemistry, FISH, cell proliferation assay, flow cytometry, spheroid formation assay, and soft agar colony formation assay. *PPP2R3B* functions and protein interactions were explored ex vivo and in vitro in melanoma cell lines by immunohistochemistry, immunoblotting, HaloTag pull-down, and chromatin-binding assays. For in vivo experiments, human melanoma cell lines were grafted under the skin of 5- to 6-week-old mice; the mice were sacrificed when moribund because of tumor burden. Gene expression was studied by qPCR.

Tumor specimens

Frozen primary tumor samples (snap-frozen and stored at −70°C) from melanoma patients (33 females and 16 males) with well-documented follow-up data were retrieved from the pathology archive at the University Hospitals Leuven (Leuven, Belgium). These tissues are part of a larger collection of samples that were previously used to identify a set of 254 genes whose expression correlates with DMFS at 4 years. All tissues were reviewed by two expert melanoma pathologists (J.v.d.O. and A.S.). The clinical and histopathological characteristics are summarized in table S1. Pairs of lymph node metastasis and noninvolved lymph nodes and 20 additional primary melanomas were retrieved from the Leuven pathology archive for PPP2R3B mutation analysis.

TMAs of primary melanoma were obtained from the Department of Dermatology, University Hospital Essen (Essen, Germany); the Department of Tissue Pathology and Diagnostic Oncology, the Royal Prince Alfred Hospital, the University of Sydney (Sydney, Australia); the

Department of Immunology, Genetics, and Pathology, Uppsala University (Sweden); and the Laboratory of Translational Cell and Tissue Research, University of Leuven (Leuven, Belgium). The TMAs of melanoma metastasis from females were generated by the Laboratory of Translational Cell and Tissue Research, University of Leuven. Informed consents and institutional review board approval were obtained as per the protocols of the different institutes.

Array-based comparative genomic hybridization

The frozen tissue samples for array CGH (aCGH) were retrieved from the pathology archives at the University Hospitals Leuven. At the time of sampling, representative parts from primary and metastatic lesions were snap-frozen in liquid nitrogen–cooled isopentane and stored at −80°C until used. Sampling, storage, and use of these samples were performed according to requirements of the local ethical committee. DNA and RNA were prepared from the same frozen tissue samples. First, RNA was extracted from 20 to 40 frozen tissue sections (10 mm) each containing >70% of melanoma cells using the Qiagen RNEasy Mini Kit, followed by DNA extraction from the flow-through phase of the RNA extraction procedure. The DNA was purified using the ChargeSwitch Forensic DNA Purification Kit protocol (Invitrogen). Concentration and purity of DNA and RNA were determined by using the NanoDrop 100ND-1000 Spectrometer (Thermo Fisher Scientific).

DNA was enzymatically digested by Alu I and Rsa I, quantified, and concentrated when necessary. Fragmented DNA (500 ng) was labeled by random priming for 1 hour. Sample DNA was labeled with Cy5-dUTP (deoxyuridine triphosphate), and commercial DNA (Promega) of the same sex was labeled with Cy3-dUTP. After 40 hours of hybridization at 65°C, the Agilent 244K high-density oligoarrays (G4411B) were washed with Agilent Wash Buffers 1 and 2 and dried with a nitrogen pulse gun. Scan of arrays was performed on an Agilent G2565 BA scanner (Agilent) with a resolution of 5mm, using 100% of the photomultiplicator power for both signals.

Acquisition of spot intensities, rank-mode normalization, and log2-based ratios computation were performed using Feature Extraction v9.1.3.1 (Agilent Software). An in-house filter discarding a defined list of probes with erratic values was applied (methods should be published later). Calls for gains and losses of genomic parts were performed using the ADM-2 algorithm of CGH Analytics v3.4 (Agilent Software) with the following parameters: threshold, 6; minimum probes, 2; and minimum base-2 logarithm (log2), 0.25. Log2 values of each defined segment were then re-affected to each probe it handles.

The public data set of the melanoma bacterial artificial chromosome–based aCGH study GSE2631 (31) was retrieved from Gene Expression Omnibus (www.ncbi.nlm.nih.gov/geo/). Calls for gains and losses of genomic parts were performed on these data using the package DNA copy (32), with the "undo" method active and the "undoSD" value set to 1.4. The frequency plots were obtained using the aCGH package v1.10.0 under the R statistical language (www.r-project.org). The hierarchical clustering of samples was performed under R, using Euclidean distances and Ward's collection method. The stability testing of the resulting dendrogram was performed using the pvclust (v1.3.0) package for R (33).

The comparison of populations and their aberrations according to clinical annotations were performed using *t* test on each probe. Corresponding plots were generated using aCGH.

Because genomic probes are, by definition, linked by their position on the genome, false discovery rate (FDR) computation methods for *P* value adjustment are not efficient on data provided by high-density CGH oligoarrays. Thus, FDR adjustment of *P* values was performed on these data using the Benjamini-Hochberg method, but raw P values were used for significance filtering.

Quantitative polymerase chain reaction

The reporting on the qPCR method adheres to the MIQE (Minimum information for publication of quantitative real-time PCR experiments) guidelines (34). The absence of DNA contamination and RNA integrity that was extracted from the frozen tissues was assessed on a Bioanalyzer (Agilent Technologies). RNA integrity numbers higher than 7.5 and, in most cases, higher than 9 were obtained. Complementary DNA (cDNA) was synthesized from 1 mg of total RNA using TaqMan Reverse Transcription Reagent (Life Technologies) using random hexamers according to the manufacturer's instructions in a final volume of 10 µl. cDNA was diluted 10 times with water, and 5 µl of the diluted cDNA was used for subsequent qPCR performed using TaqMan hydrolysis probes according to the manufacturer's instructions via manual mixing of the reagents. The following hydrolysis probe was used for the quantification of *PPP2R3B* expression: Hs00203045_m1, RefSeq NM_013239.4, exon spanning primers, exon boundary 7–8, assay location 1302, and amplicon length 61. As a reference gene, a hydrolysis probe (Hs99999902_m1, exon junction primer, RefSeq NM_001002.3, exon boundary 3–3, assay location 268, and amplicon length 105) toward RPLP0 was used. qPCR was performed on an Applied Biosystems 7500 Fast Real-Time PCR System in a final volume of 20 µl in a 96-well format with the following cycling parameters: 50°C for 2 min, 95°C for 10 min, followed by 40 cycles of 95°C for 15 s and 60°C for 1min. Preliminary standard curve experiments using cDNA created from tissue in which *PPP2R3B* was expressed demonstrated that the slope, r^2 of the calibration curves, and amplification efficiency (E) of *PPP2R3B* and RPLP0 were −3.410, 0.99, and 96.45%, and −3.375, 1.00, and 97.83%, respectively. Quantification cycle (Cq) values for "no input" control was >40 for both targets in all assays.

The range of RPLP0 Cq values was 23.7 to 32.9 with an intraexperimental coefficient of variation (CV) of 0.02 to 1.24%. The range of *PPP2R3B* Cq values was 28.9 to 33.9 with a CV of 0.01 to 0.9%. For each sample, normalized expression was determined and adjusted for the different amplification efficiencies (E) according to $(E_{target})\ \Delta Cq^{target\ (control\text{-}sample)}/(Eref)\Delta Cq^{ref(control\text{-}sample)}$.

NCBI Genotypes and Phenotypes Database, data set phs000452.v1.p1

The Melanoma Research Project files were downloaded from the Sequence Read Archives at the NCBI. SAMtools was used to extract aligned reads for chrX:294,668-348,790 spanning the regulatory and transcription region of the *PPP2R3B* gene. The function mpileup from SAMtools was used for SNP and INDEL calling, using the 1000 Genomes build GRCh37 as the reference genome.

The frequency of SNVs at each position for all individuals was calculated independently for the tumors and the matched blood samples. The following criteria were used for each call for inclusion in the frequency calculation: read depth of at least 4, a quality control call above 20, and the presence of the variant allele in greater than 12.5% of the reads. The frequency of each variant was then compared in tumor, matched blood, and the reference genome.

PR70 immunohistochemistry

PR70 immunohistochemistry followed the REMARK (Reporting Recommendations for Tumor Marker Prognostic Studies) guidelines (35). Tissue samples were cut at 4 μm, placed on SuperFrost/Plus slides (Thermo Fisher Scientific), and dried overnight at 37°C. The slides were then loaded onto the Discovery XT Autostainer (Ventana Medical Systems). All solutions used for automated immunohistochemistry were from Ventana Medical Systems. Slides were

deparaffinized with xylene and subjected to heat-induced epitope retrieval [tris/borate/EDTA buffer, pH 8.0 to 8.5 (Cell Conditioning 1, Ventana), 60 min at 37°C]. Following automated preincubation steps, rabbit polyclonal anti-PPP2R3B (clone 70) (Aviva Systems Biology) at 0.5 mg/ml in antibody diluent (Ventana Medical Systems) was added for 32 min at 37°C, followed by detection with Omnimap anti-rabbit horseradish peroxidase (HRP) and 3,3-diaminobenzidine. A negative control was performed by the omission of the primary antibody. Slides were counterstained with Gill's hematoxylin no. 1 for 4 min, blued with Bluing Reagent (lithium carbonate solution, Ventana Medical Systems) for 4 min, removed from the autostainer, washed in warm soapy water, rinsed extensively with water, dehydrated through graded alcohols, cleared in xylene, and mounted with Permount. Sections were analyzed by conventional light microscopy. The results were analyzed in a semiquantitative manner (0, absence of nuclear staining; 1+, weak nuclear staining observed at 20x magnification; 2+, moderate nuclear staining not obstructing nuclear details observed at 4x magnification; and 3+, intense nuclear staining obstructing nuclear details). These cutoffs were determined in a study set of 60 primary melanomas regrouped in TMA and then analyzed in the study population composed of 234 annotated primary melanomas grouped in TMAs.

DNA and RNA FISH

DNA FISH for visualization of the X chromosome centromere and RNA FISH for XIST and PPP2R3B RNA were performed on 4-µm consecutive sections of formalin-fixed, paraffin-embedded tissues. Following deparaffinization through toluene and graded alcohol baths, the X chromosome centromere was hybridized with a fluorescent probe from Vysis (cepX SpectrumOrange, Abbott Molecular) according to the manufacturer's instructions. Stellaris RNA FISH probes were purchased from Biosearch Technologies for the detection of XIST and

PPP2R3B RNA according to the manufacturer's instructions. All slides were mounted with medium containing DAPI (Abbott Molecular), and images were captured with a Zeiss AX10 microscope equipped with a CV-M4+ monochrome megapixel camera (Jai Inc). The number of nuclear signals was counted to determine the number of X chromosomes (cepX), number of inactivated X chromosomes (XIST), and actively transcribed *PPP2R3B* alleles (*PPP2R3B*) in at least 100 nuclei of tumor cells per sample.

Cell lines

Early passage melanoma cell lines derived from lymph node metastasis (MM) were provided by G. Ghanem (Institut Jules Bordet, Brussels, Belgium) and cultured in Ham's F10 medium (Wisent) supplemented with 10% heat-inactivated fetal bovine serum (FBS) (Wisent) at 37°C and 5% CO2. All MM cell lines were derived from female melanoma patients. Bimonthly tests for mycoplasma demonstrated the absence of contamination. MM117 cells stably expressing *PPP2R3B* were generated by a Lipofectamine-mediated transfection of pCMV6-*PPP2R3B*-Flag plasmid (OriGene #RC222908), followed by neomycin (0.5 mg/ml) selection of stably expressing clones.

A set of pLKO.1-shRNAplasmid encoding shRNA with a scrambled sequence or sequences targeting human *PPP2R3B* (NM_013239) was purchased from Open Biosystems. After first-round selection in MM57 melanoma cells, shRNA clones sh-*PPP2R3B* TRCN0000006924 (5′-ATGGCGACGAACTTGTGGACG-3′) and sh-*PPP2R3B* TRCN0000011056 (5′TAGAAGGTCGGAATGCTTTGG-3′) designated as Sh-PR70-D and Sh-PR70-F, respectively, were chosen for lentivirus production on the basis of knockdown efficiency following the protocol described in the RNAi Consortium Protocols Section II (The RNA Consortium). Then, these viruses were used to infect MM57 melanoma cells. Stable shRNA-expressing cells were finally selected with puromycin (1 mg/ml) and were used for further analysis.

In vitro cell proliferation assay

MTT assay was used to determine the proliferation rate and calculate the doubling time for the cell lines. Briefly, cells were seeded in 96-well plates (5×10^3 cells per well per 100 μl) in culture medium containing 10% FBS for 24, 48, 72, and 96 hours. At the end of incubation, MTT [20 μl per well of MTT (5 mg/ml) in phosphate-buffered saline (PBS)] was added to each well, and plates were incubated in the dark for 3 hours at 37°C. After removal of the medium, the dye crystals were dissolved with acidified isopropanol and then the absorbance was measured at 590-nm wavelength with a FLUOstar Optima microplate reader (BMG LABTECH). Experiments were repeated three times in quadruplicate wells to ensure the reproducibility of results. The doubling time was calculated for each cell line using the equation $N_t = N_{02tf}$, where N_t is the number of cells at time t, N_0 is the initial number of cells, t is the time in days, and f is the frequency of cell cycles per day.

Cell cycle analysis

Nonsynchronized and nocodazole (200 nM)–synchronized subconfluent cells were harvested and washed twice with PBS. Pellets were resuspended in 1 ml of PBS, fixed in 70% ethanol, and incubated overnight at −20°C. Cells were collected by centrifugation and washed once with PBS, and the pellets were suspended in 0.5 ml of PI (50 μg/ml) containing RNase A (0.1 mg/ml; Sigma). The cell suspension was incubated in the dark for 30 min at room temperature and subsequently analyzed on a BD LSRFortessa flow cytometer for DNA content. The percentage of cells in different phases of the cell cycle was determined using FlowJo version 10.6 software.

For the BrdU-labeling experiment, cells were nocodazole (200 nM)– synchronized for 24 hours. Subsequently, cells were maintained in complete medium for the indicated time periods and

then pulse-labeled with BrdU (10 mM) for 45 min. Thereafter, cells were fixed in 70% ethanol, incubated with BrdU DNA-specific antibody, stained with PI as above, and subjected to flow cytometric analysis.

Spheroid formation assay

For spheroid formation, 1 ml per well of cell suspensions (3×10^3 cells/ml) was dispensed onto the bottom agar layer (1%) in six-well plates. Plates were then incubated for 3 days at 37°C, 5% CO2, and 95% humidity. Images were captured using an AMG-EVOS FL microscope.

Soft agar colony formation assay

Anchorage-independent growth was assessed by colony formation on soft agar. Briefly, cells (5×10^3 cells per well) were suspended in 1.5 ml of 0.35% agar solution in Ham's-F10/10% FBS medium and overlaid onto the bottom agar layer (0.5%) in six-well plates. Top agar was then covered with 1 ml of complete culture medium. Plates were incubated at 37°C and 5% CO2 in a humidified incubator for 3 weeks, and medium was refreshed every 3 to 4 days. Colony formation was observed by light phase-contrast microscope, and the number of colonies greater than 60 μm in diameter was counted using the GelCount colony counting system (Oxford Optronix) according to the manufacturer's instructions. Means and SDs were calculated on the basis of the colony counts from triplicate wells.

In vivo growth assay

Mice were injected subcutaneously with vector-transfected control MM117 cells (2×10^6) on the left flank and cells stably expressing *PPP2R3B* (2×10^6) on the right flank. Two independently isolated clones overexpressing *PPP2R3B* were tested [MM117/*PPP2R3B*-1 (10 mice) and MM117/*PPP2R3B*-2 (5 mice)]. MM57cells (2×10^6) stably expressing sh-*PPP2R3B* were injected

subcutaneously [MM57/sh-D (5 mice) and MM57/sh-F (5 mice)] on the right flank with sh-scramble control-transfected cells on the left flank. Tumor growth was monitored biweekly with a caliper ($L \times W^2/2$). Mice were housed and handled according to the local ethical guidelines of the McGill University (protocol approval no. 2011–7012).

Immunoblotting

For immunoblotting, cells were washed twice with ice-cold PBS and lysed in radioimmunoprecipitation assay buffer (50 mM tris-HCl, 150 nM NaCl, 1mM EDTA, 1mM DTT, 0.1% Tween 20, and protease and phosphatase inhibitors). After 20 min of incubation on ice, samples were sonicated and the lysates were cleared by 10 min of centrifugation at 4°C. Protein concentration was quantitated using a BCA (bicinchoninic acid) protein assay (Pierce). Equal amounts of protein were separated on SDS–polyacrylamide gel electrophoresis (PAGE) and transferred onto polyvinylidene difluoride (PVDF) membranes. Membranes were blocked overnight in tris-buffered saline containing 0.1% Tween 20 and 5% BSA at 4°C. Blots were extensively washed and probed with the primary antibodies followed by HRP-conjugated secondary antibody. Blots were washed extensively and developed with chemiluminescent substrate in the presence of hydrogen peroxide using Immun-Star WesternC Chemiluminescent Kit (Bio-Rad), and imaging was performed with a ChemiDoc XRS System (Bio-Rad). The primary antibodies used were as follows: a rabbit polyclonal anti-PPP2R3B antibody at 1:2000 (ab72027; Abcam), a mouse monoclonal anti-Cdt1 antibody at 1:2000 (SC-365305; Santa Cruz Biotechnology), a rabbit polyclonal anti-Cdc6 antibody at 1:2000 (GTX108979; GeneTex), a rabbit polyclonal anti–pCdc6-Ser54 antibody at 1:2000 (SC-12920R; Santa Cruz Biotechnology), a rabbit polyclonal anti–pCdc6-Ser74 antibody at 1:1000 (SC-12921; Santa Cruz Biotechnology), a rabbit polyclonal anti-Geminin antibody at 1:2000 (#5165;Cell Signaling), a rabbit polyclonal

anti-ORC2 antibody at 1:10000 (#559266; BD Pharmingen), a rabbit polyclonal anti-Rb antibody at 1:2000 (ab6075; Abcam), and a rat monoclonal (LY1/2) anti-tubulin antibody at 1:7000 (ab6160; Abcam).

HaloTag pull-down

HEK293T cells were transfected with HaloTag empty vector or vector encoding Halo-tagged PR70. HaloTag fusion proteins form highly specific and irreversible bonds with the HaloLink Resin. Pull-downs were performed according to the manufacturer's specifications (HaloTag Mammalian Pull-Down Systems, Promega).

Chromatin-binding assay

Cells (2×10^7) were harvested and lysed in 1 ml of lysis buffer containing 100 mM Hepes/KOH (pH7.4), 300 mM sucrose, 100 mM NaCl, 3 mM MgCl2, 0.5% NP-40, 1 mM CaCl2, protease inhibitors [1 mM phenylmethylsulfonyl fluoride, aprotinin (10 μg/ml), and leupeptin (10 μg/ml)], and phosphatase inhibitors (1 mM Na3VO4 and 1 mM NaF). Lysates were incubated on ice for 15 min. Soluble fractions were obtained as supernatant after low-speed centrifugation (400g for 3 min at 4°C). Pellets were washed twice with 1 ml of lysis buffer for 5 min on ice and centrifuged again to obtain a chromatin-enriched fraction. Chromatin pellets were then resuspended in lysis buffer, and the concentration of NaCl was adjusted to 420 mM plus 2% Triton X-100. After 20 min of incubation on ice, samples were sonicated. Equal amounts of protein were separated by SDS-PAGE (10%) and transferred to PVDF membranes and immunoblotted.

Statistical analyses

All values were presented as means ± SEM. IBM SPSS Statistics software (version 23.0; $\alpha < 0.05$) was used for statistical analyses. χ^2 and Fisher's exact tests were used for immunohistochemical

staining. Log-rank was used for survival analyses. Mann-Whitney U test was used for PR70 expression, gender, Xi status, tumor take, and cell lines. Pearson correlation was used to study linear correlation between PR70 expression, tumor growth, and tumorigenicity in vivo.

Supplemental Tables and Figures

Table S1. Patient and sample characteristics.

	Cluster A		Cluster B		Cluster C	
Cluster population (n)	**13**		**16**		**20**	
Age		*13*		*16*		*20*
Median (m, range)	67 (1 - 89)		67 (33 - 93)		63 (43 - 92)	
Sex		*13*		*16*		*20*
Female	11	85%	10	63%	12	60%
Male	2	15%	6	38%	8	40%
Breslow						
Median (m, range)	7 (2.1 - 18.6)		1.45 (0.5 - 17.1)		3.6 (1.8 - 8.2)	
Mitotic rate		*13*		*16*		*20*
Low (between 1 and 6 / mm²)	2	15%	12	75%	10	50%
High (more than 6 / mm²)	11	85%	4	25%	10	50%
BRAF mutation status		***13***		***16***		***20***
Positive	**5**	**38%**	**3**	**19%**	**14**	**70%**
Negative	**8**	**62%**	**13**	**81%**	**6**	**30%**
NRAS mutation status		*13*		*16*		*20*
Positive	2	15%	1	6%	1	5%
Negative	11	85%	15	94%	19	95%
Distant metastasis-free survival		*13*		*16*		*20*
Positive	2	15%	12	75%	15	75%
Negative	11	85%	4	25%	5	25%
Death		*13*		*15*		*19*
Positive	10	77%	6	40%	9	47%
Negative	3	23%	9	60%	10	53%

Fig. S1. Clustering of aCGH profiles

A

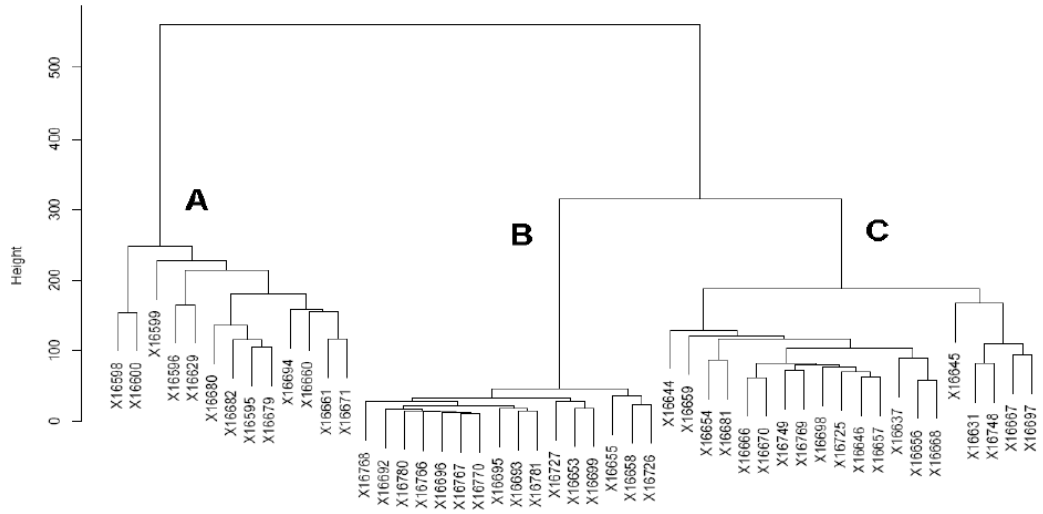

B

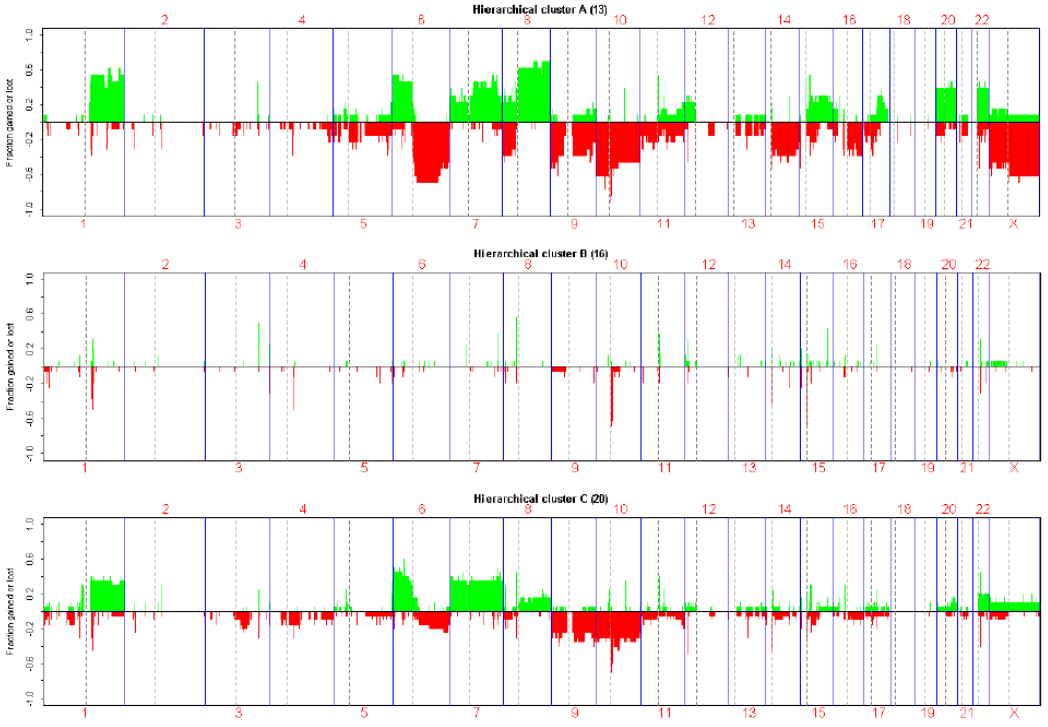

Fig. S2. *PPP2R3B* and PR70 expression in melanoma.

A

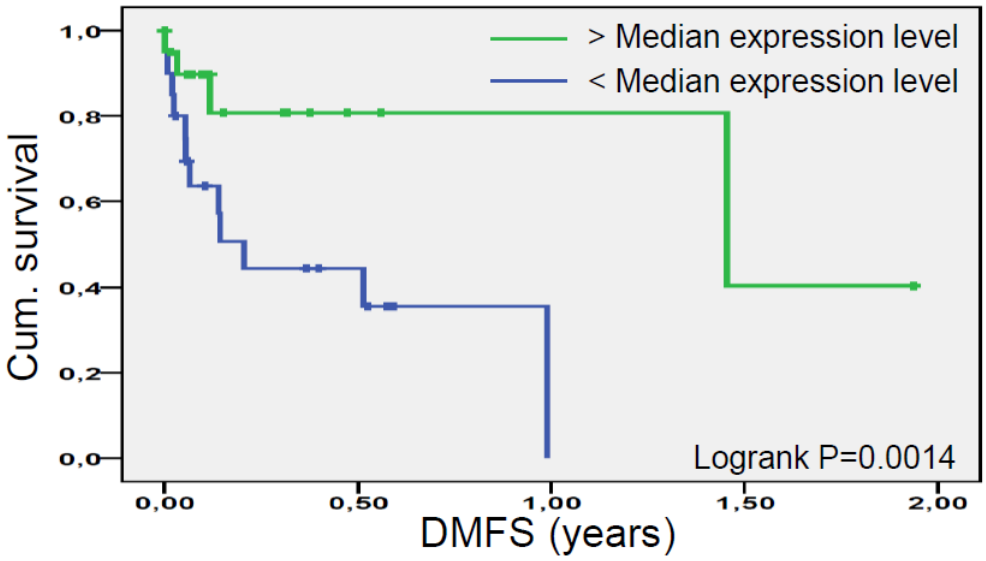

B

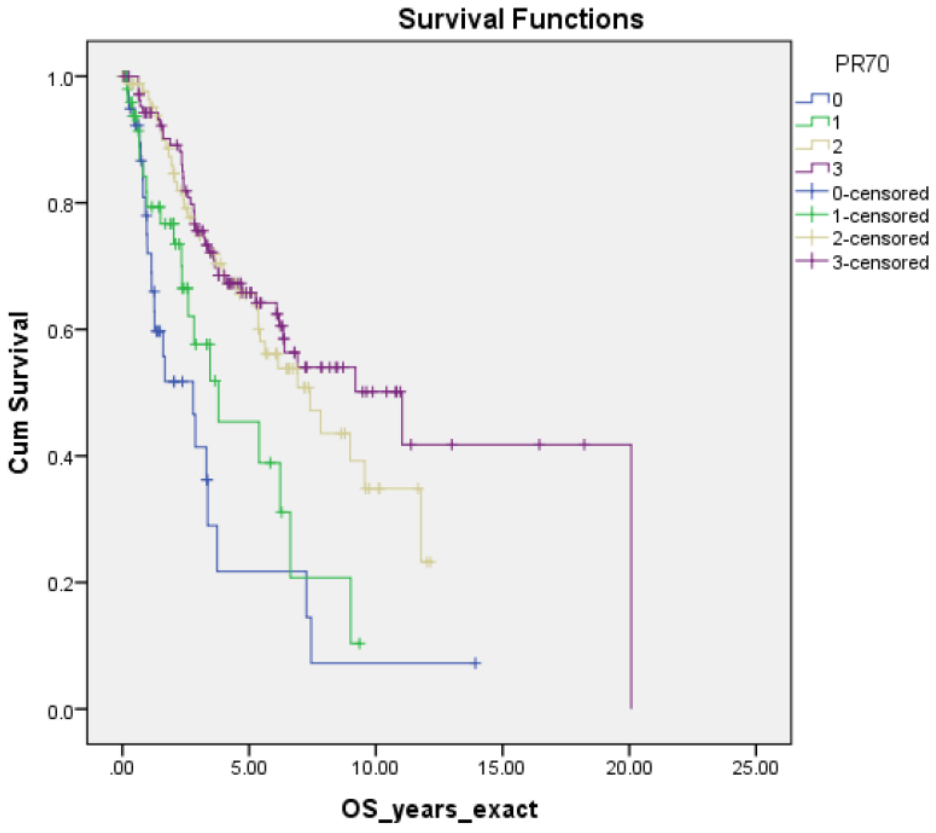

Fig. S3. Schematic presentation of newly identified SNVs in PPP2R3B. Schematic presentation of the PR70 protein and the PPP2R3B gene and coding region SNVs. Five known (open triangles) and two new non-synonymous SNV (black triangles) were identified in 10 pairs of lymph node metastates and normal lymp nodes. The number on brackets identifieds the number of cases in which the SNV was detected. All variants that were indentified in the tumor, were also present in DNA isolated form normal lymph nodes (no involvement of tumor) from the same patient.

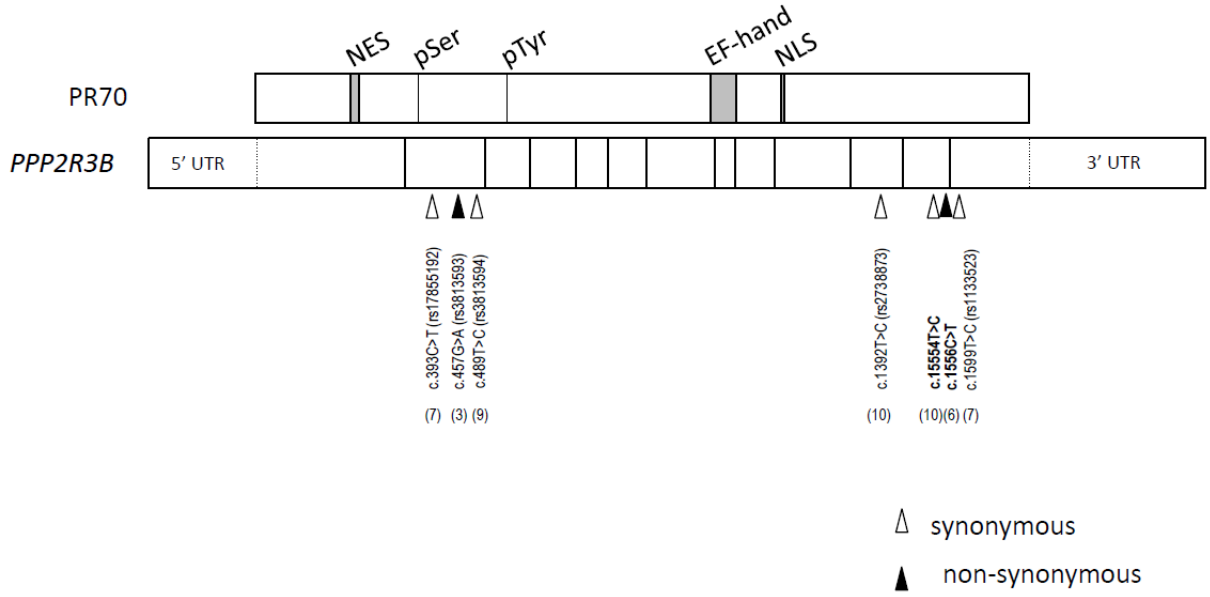

Fig. S4. Effect of PR70 expression on MM117 melanoma cells.

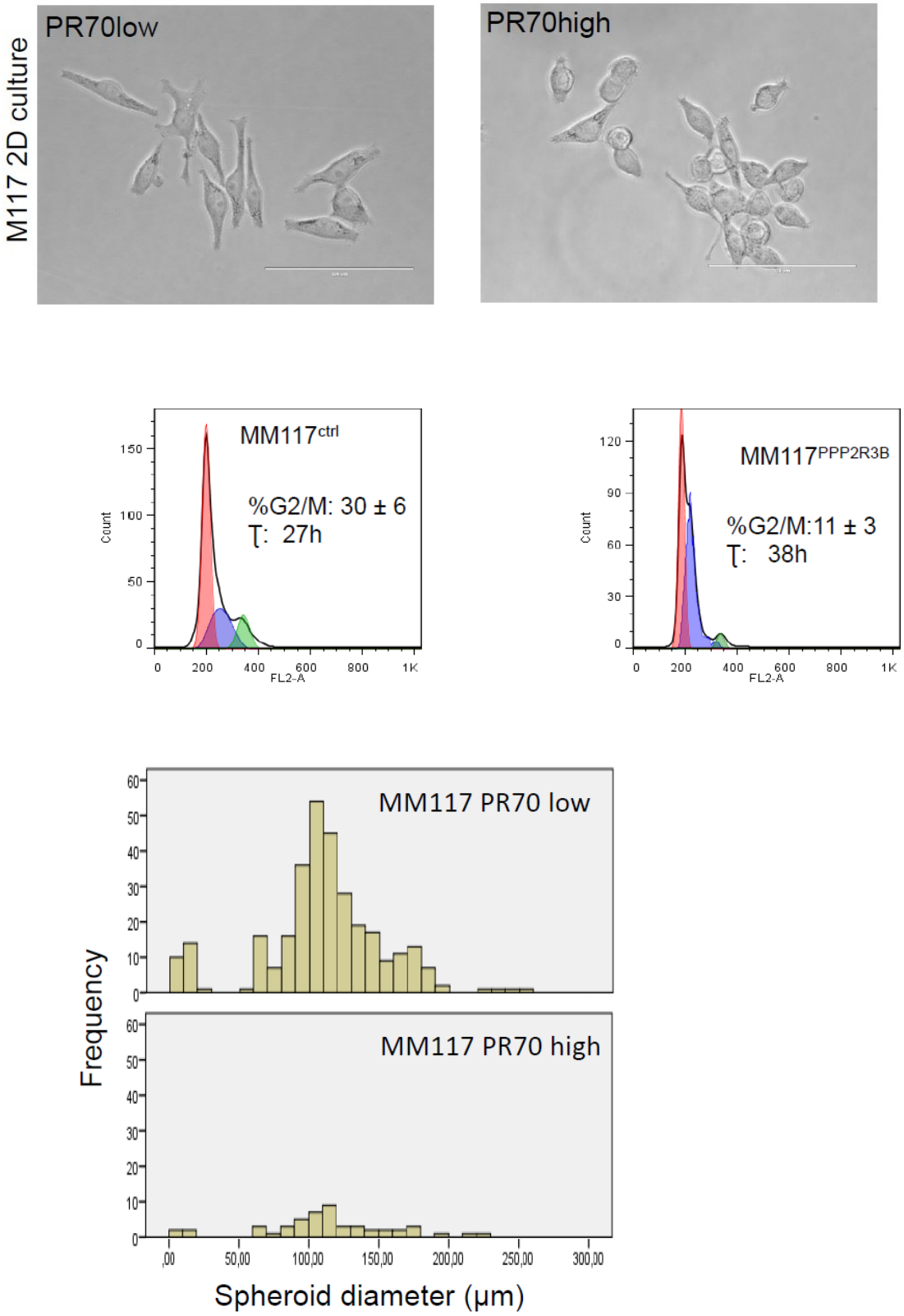

Fig. S5. Effect of PR70 down-regulation on cell morphology.

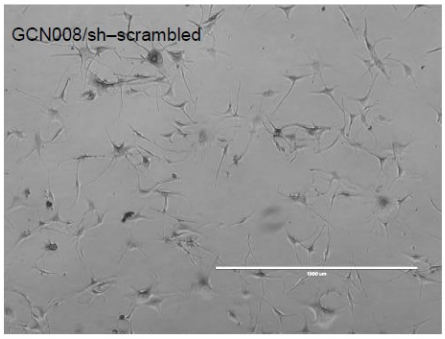

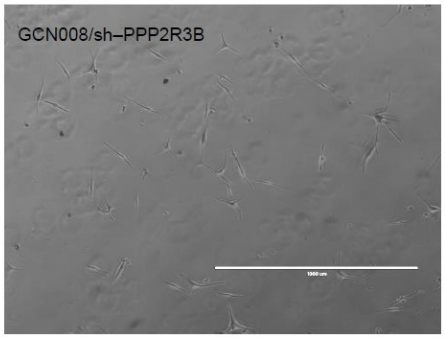

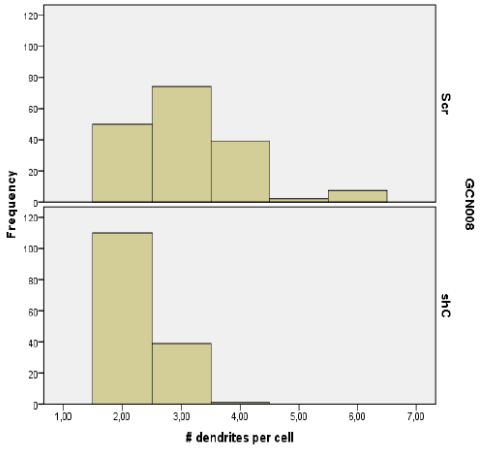

dendrites * GCN008 Crosstabulation

			GCN008		Total
			Scr	shC	
dendrites	2	Count	50	110	160
		% within GCN008	29,1%	73,3%	
	3	Count	74	39	113
		% within GCN008	43,0%	26,0%	
	4	Count	39	1	40
		% within GCN008	22,7%	0,7%	
	5	Count	2	0	2
		% within GCN008	1,2%	0,0%	
	6	Count	7	0	7
		% within GCN008	4,1%	0,0%	
Total		Count	172	150	322
		% within GCN008	100,0%	100,0%	100,0%

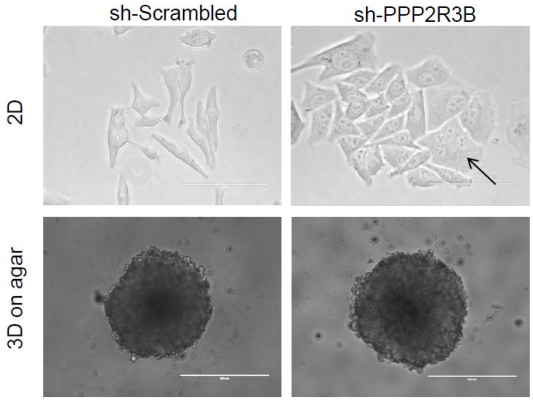

Fig. S6. PR70 expression decreased tumorigenicity of MM117 melanoma cells in mice.

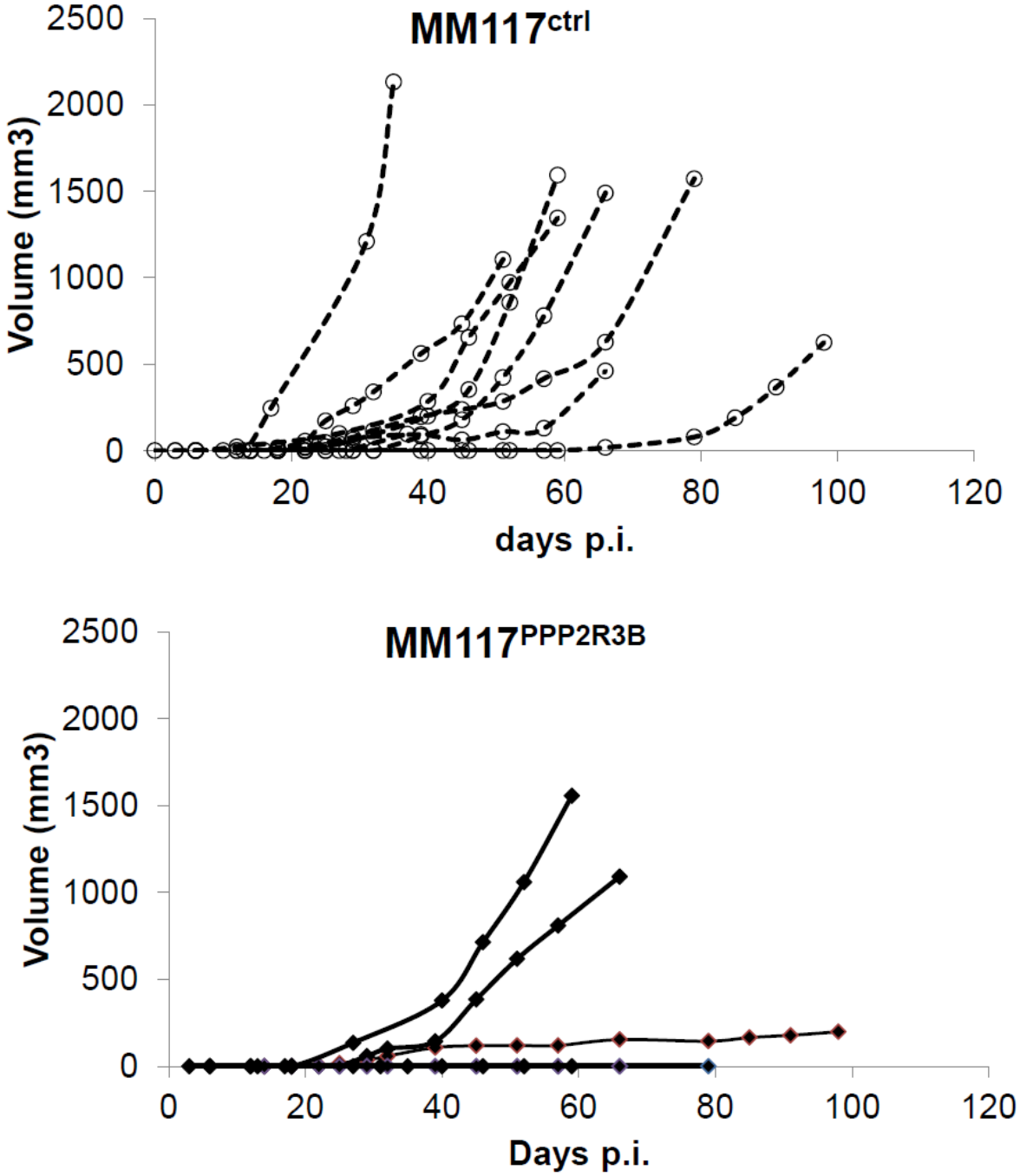

Fig. S7. Decreasing PR70 expression in MM57 melanoma cells increased their in vivo growth capacity.

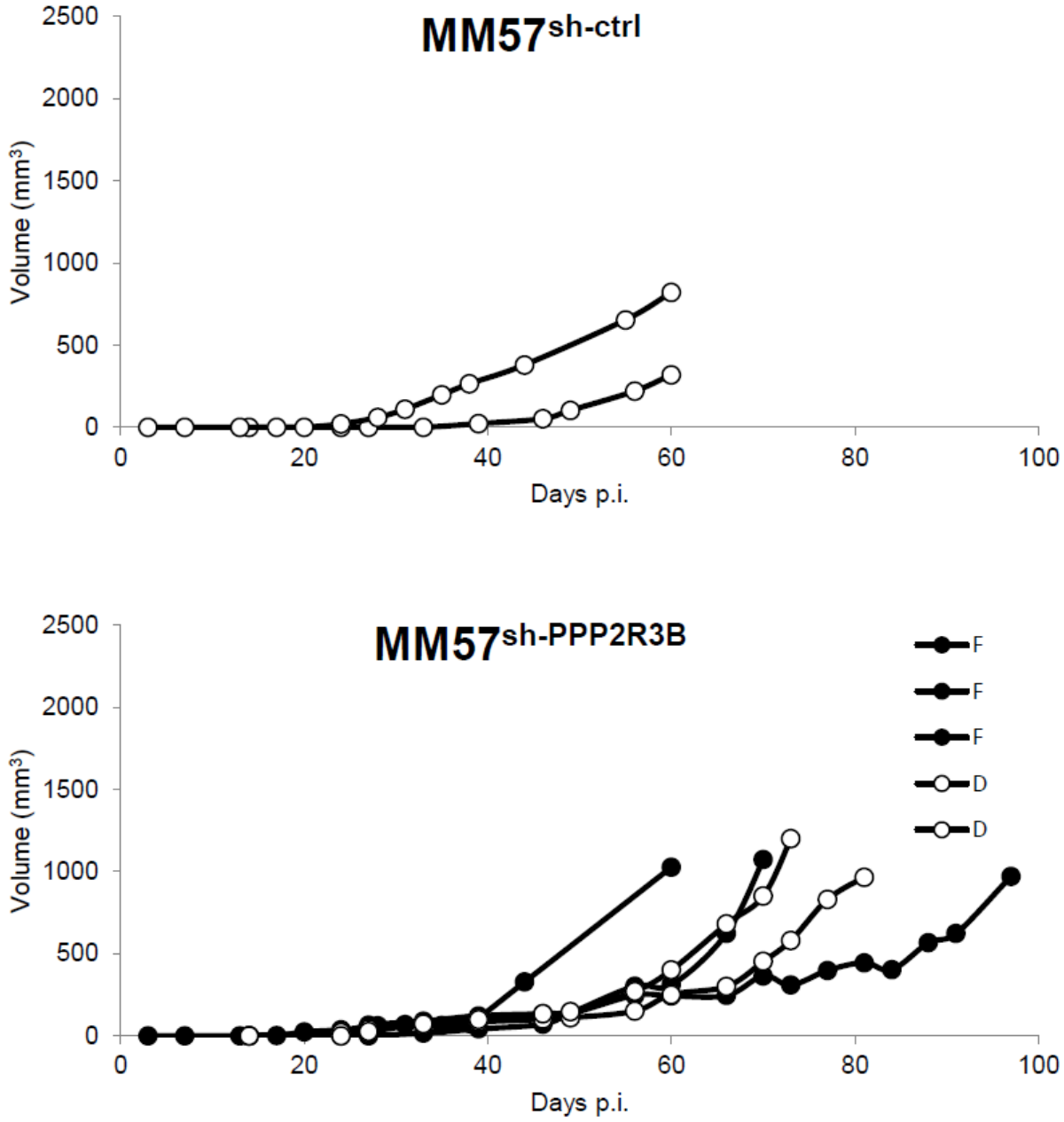

Fig. S8. Schematic presentation of the firing of origins of replications.

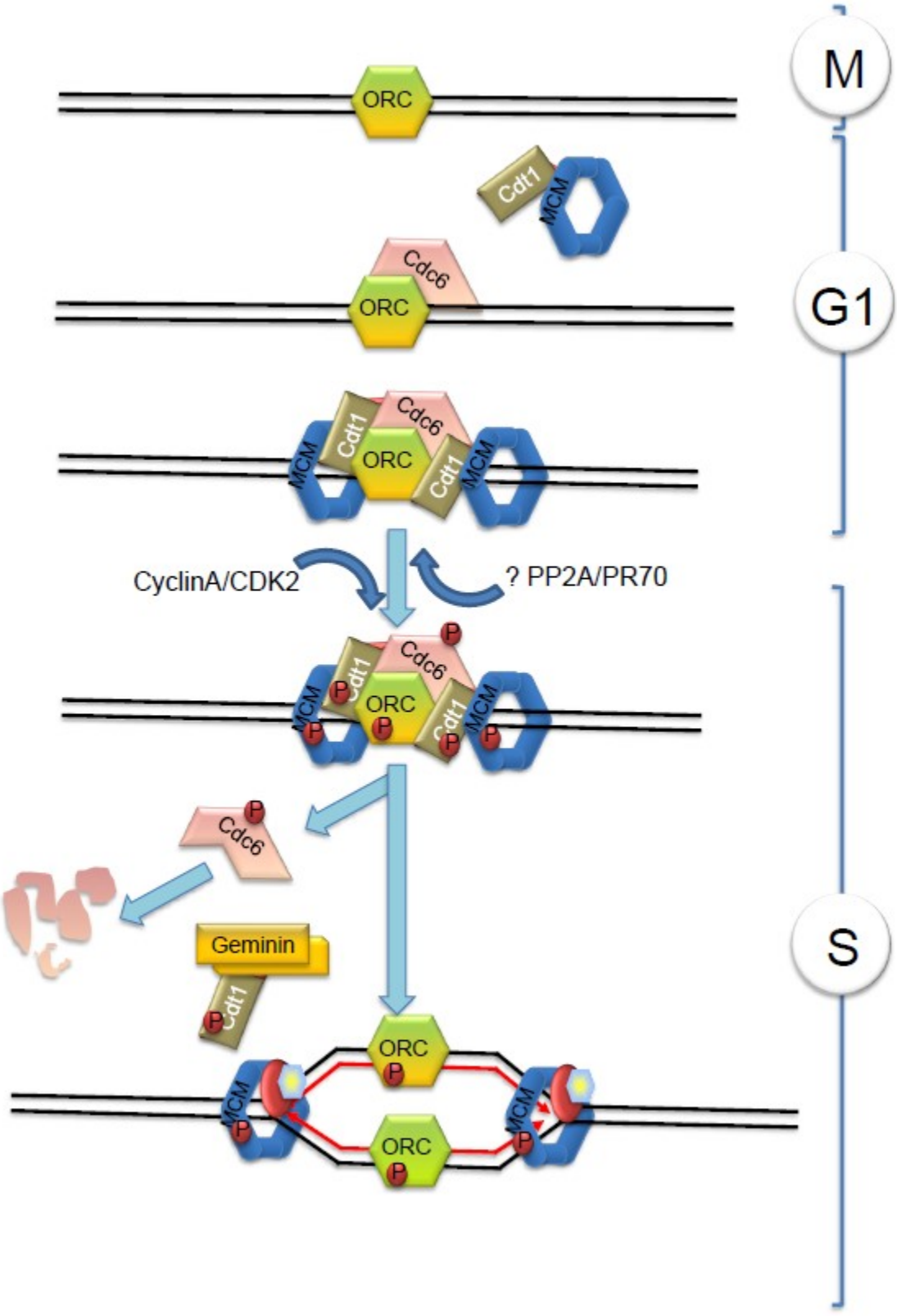

Fig. S9. Flow cytometry cell proliferation data following the release after a nocodazole arrest of MM117 cells with low (MM117^{ctrl}) or high (MM117^{PPP2R3B}) PR70 expression.

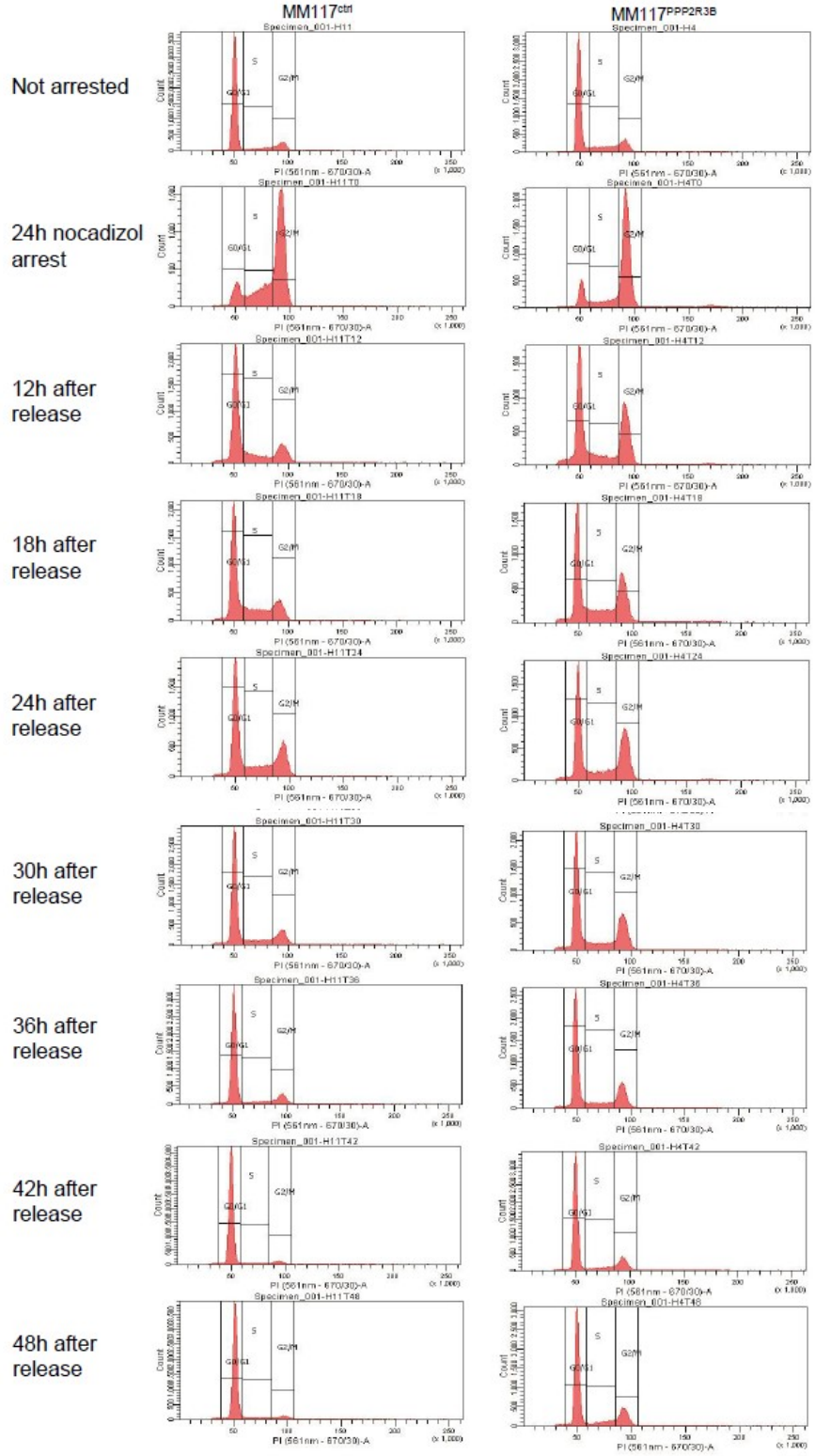

Fig. S10. PR70 dephosphorylates pRb.

A

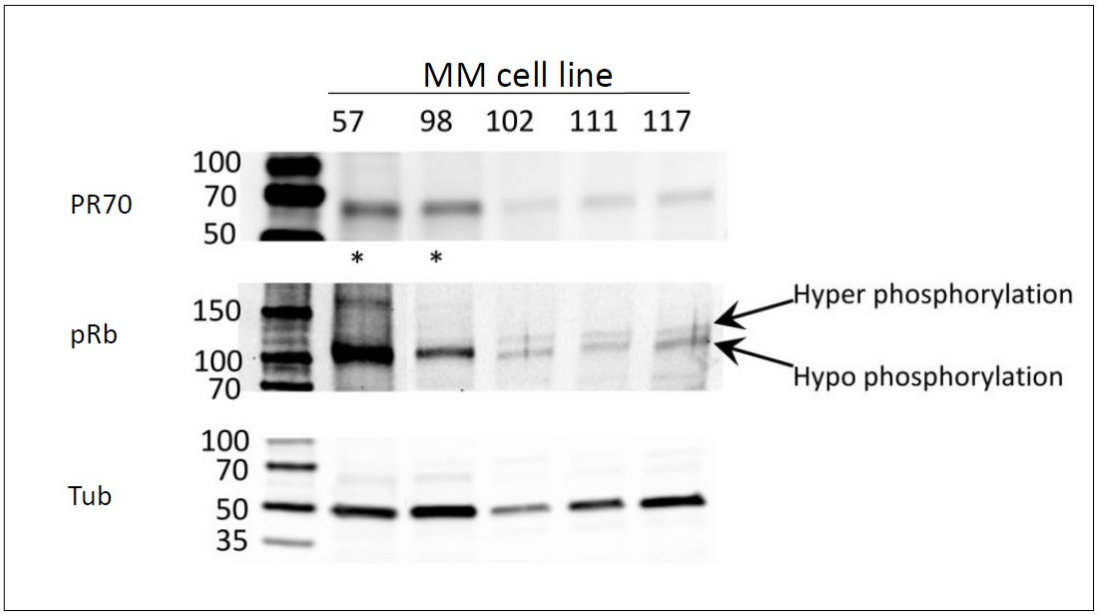

B

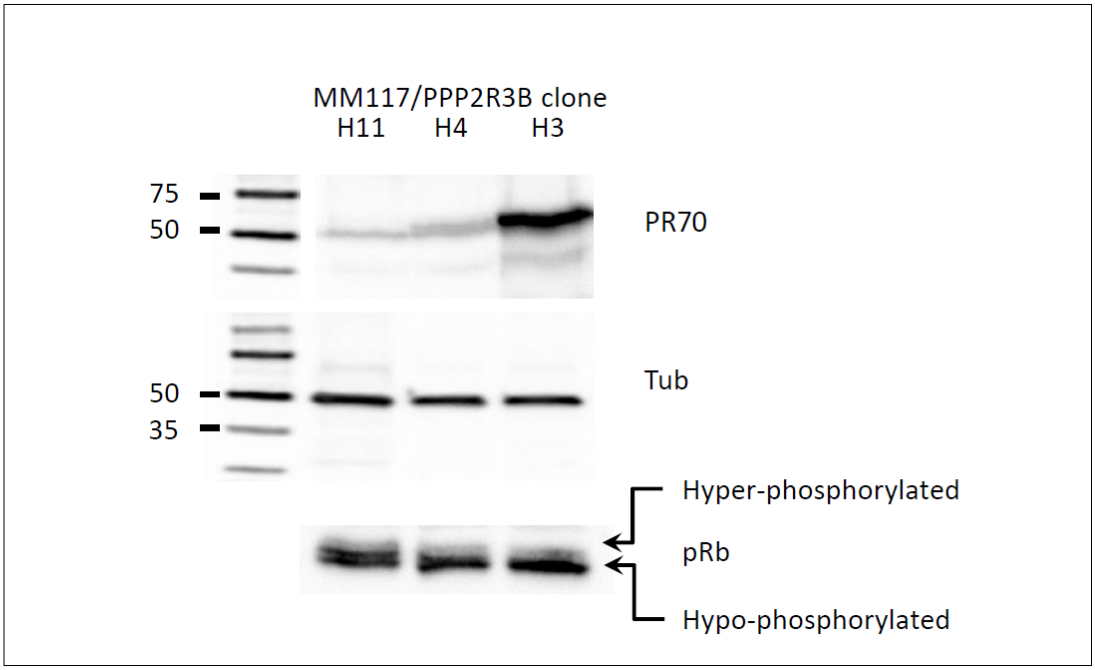

REFERENCES

1. J. S. Weber, Current perspectives on immunotherapy. *Semin. Oncol*. **41**(suppl. 5), S14–S29 (2014).

2. A. M. Menzies, G. V. Long, Systemic treatment for BRAF-mutant melanoma: Where do we go next? *Lancet Oncol.* **15**, e371–e381 (2014).

3. A. Spatz, N. Stock, G. Batist, L. C. van Kempen, The biology of melanoma prognostic factors. *Discov. Med*. **10**, 87–93 (2010).

4. A. Joosse, S. Collette, S. Suciu, T. Nijsten, F. Lejeune, U. R. Kleeberg, J. W. Coebergh, A. M. M. Eggermont, E. de Vries, Superior outcome of women with stage I/II cutaneous melanoma: Pooled analysis of four European Organisation for Research and Treatment of Cancer phase III trials. *J. Clin. Oncol*. **30**, 2240–2247 (2012).

5. A. Joosse, S. Collette, S. Suciu, T. Nijsten, P. M. Patel, U. Keilholz, A. M. M. Eggermont, J. W. Coebergh, E. de Vries, Sex is an independent prognostic indicator for survival and relapse/progression-free survival in metastasized stage III to IV melanoma: A pooled analysis of five European organisation for research and treatment of cancer randomized controlled trials. *J. Clin. Oncol.* **31**, 2337–2346 (2013).

6. L. Carrel, H. F. Willard, X-inactivation profile reveals extensive variability in X-linked gene expression in females. *Nature* **434**, 400–404 (2005).

7. F. Yang, T. Babak, J. Shendure, C. M. Disteche, Global survey of escape from X inactivation by RNA-sequencing in mouse. *Genome Res*. **20**, 614–622 (2010).

8. L. Carrel, H. F. Willard, Heterogeneous gene expression from the inactive X chromosome: An X-linked gene that escapes X inactivation in some human cell lines but is inactivated in others. *Proc. Natl. Acad. Sci. U.S.A.* **96**, 7364–7369 (1999).

9. A. Spatz, C. Borg, J. Feunteun, X-chromosome genetics and human cancer. *Nat. Rev. Cancer* **4**, 617–629 (2004).

10. G. J. Pageau, L. L. Hall, S. Ganesan, D. M. Livingston, J. B. Lawrence, The disappearing Barr body in breast and ovarian cancers. *Nat. Rev. Cancer* **7**, 628–633 (2007).

11. L. A. Forsberg, C. Rasi, N. Malmqvist, H. Davies, S. Pasupulati, G. Pakalapati, J. Sandgren, T. Diaz de Ståhl, A. Zaghlool, V. Giedraitis, L. Lannfelt, J. Score, N. C. P. Cross, D. Absher, E. T. Janson, C. M. Lindgren, A. P. Morris, E. Ingelsson, L. Lind, J. P. Dumanski, Mosaic loss of chromosome Y in peripheral blood is associated with shorter survival and higher risk of cancer. *Nat. Genet*. **46**, 624–628 (2014).

12. R. J. Blaschke, G. Rappold, The pseudoautosomal regions, SHOX and disease. *Curr. Opin. Genet. Dev.* **16**, 233–239 (2006).

13. V. Winnepenninckx, V. Lazar, S. Michiels, P. Dessen, M. Stas, S. R. Alonso, M.-F. Avril, P. L. Ortiz Romero, T. Robert, O. Balacescu, A. M. M. Eggermont, G. Lenoir, A. Sarasin, T. Tursz, J. J. van den Oord, A. Spatz, Melanoma Group of the European Organization for Research and Treatment of Cancer, Gene expression profiling of primary cutaneous melanoma and clinical outcome. *J. Natl. Cancer Inst*. **98**, 472–482 (2006).

14. A. M. Cotton, B. Ge, N. Light, V. Adoue, T. Pastinen, C. J. Brown, Analysis of expressed SNPs identifies variable extents of expression from the human inactive X chromosome. *Genome Biol.* **14**, R122 (2013).

15. P. J. A. Eichhorn, M. P. Creyghton, R. Bernards, Protein phosphatase 2A regulatory subunits and cancer. *Biochim. Biophys. Acta* **1795**, 1–15 (2009).

16. I. Cifola, A. Pietrelli, C. Consolandi, M. Severgnini, E. Mangano, V. Russo, G. De Bellis, C. Battaglia, Comprehensive genomic characterization of cutaneous malignant melanoma cell lines derived from metastatic lesions by whole-exome sequencing and SNP array profiling. *PLOS ONE* **8**, e63597 (2013).

17. A. J. Davis, Z. Yan, B. Martinez, M. C. Mumby, Protein phosphatase 2A is targeted to cell division control protein 6 by a calcium-binding regulatory subunit. *J. Biol. Chem*. **283**, 16104–16114 (2008).

18. J. J. Blow, A. Dutta, Preventing re-replication of chromosomal DNA. *Nat. Rev. Mol. Cell Biol.* **6**, 476–486 (2005).

19. A. Magenta, P. Fasanaro, S. Romani, V. Di Stefano, M. C. Capogrossi, F. Martelli, Protein phosphatase 2A subunit PR70 interacts with pRb and mediates its dephosphorylation. *Mol. Cell. Biol.* **28**, 873–882 (2008).

20. Z. Yan, S. Federov, M. C. Mumby, R. Sanders Williams, PR48, a novel regulatory subunit of protein phosphatase 2A, interacts with Cdc6 and modulates DNA replication in human cells. *Mol. Cell. Biol*. **20**, 1021–1029 (2000).

21. B. O. Petersen, J. Lukas, C. S. Sørensen, J. Bartek, K. Helin, Phosphorylation of mammalian CDC6 by cyclin A/CDK2 regulates its subcellular localization. *EMBO J*. **18**, 396–410 (1999).

22. H. Yim, J.-W. Park, S. U. Woo, S.-T. Kim, L. Liu, C.-H. Lee, S. K. Lee, Phosphorylation of Cdc6 at serine 74, but not at serine 106, drives translocation of Cdc6 to the cytoplasm. *J. Cell. Physiol.* **228**, 1221–1228 (2012).

23. P. Perez-Arnaiz, I. Bruck, D. L. Kaplan, Mcm10 coordinates the timely assembly and activation of the replication fork helicase. *Nucleic Acids Res*. **44**, 315–329 (2016).

24. M. N. Rivera, W. J. Kim, J. Wells, D. R. Driscoll, B. W. Brannigan, M. Han, J. C. Kim, A. P. Feinberg, W. L. Gerald, S. O. Vargas, L. Chin, A. J. Iafrate, D. W. Bell, D. A. Haber, An X chromosome gene, WTX, is commonly inactivated in Wilms tumor. *Science* **315**, 642–645 (2007).

25. G. van Haaften, G. L. Dalgliesh, H. Davies, L. Chen, G. Bignell, C. Greenman, S. Edkins, C. Hardy, S. O'Meara, J. Teague, A. Butler, J. Hinton, C. Latimer, J. Andrews, S. Barthorpe, D. Beare, G. Buck, P. J. Campbell, J. Cole, S. Forbes, M. Jia, D. Jones, C. Y. Kok, C. Leroy, M.-L. Lin, D. J. McBride, M. Maddison, S. Maquire, K. McLay, A. Menzies, T. Mironenko, L. Mulderrig, L. Mudie, E. Pleasance, R. Shepherd, R. Smith, L. Stebbings, P. Stephens, G. Tang, P. S. Tarpey, R. Turner, K. Turrell, J. Varian, S. West, S. Widaa, P. Wray, V. P. Collins, K. Ichimura, S. Law, J. Wong, S. T. Yuen, S. Y. Leung, G. Tonon, R. A. DePinho, Y.-T. Tai, K. C. Anderson, R. J. Kahnoski, A. Massie, S. K. Khoo, B. T. Teh, M. R. Stratton, P. A. Futreal, Somatic mutations of the histone H3K27 demethylase gene *UTX* in human cancer. *Nat. Genet*. **41**, 521–523 (2009).

26. A. H. Berger, A. G. Knudson, P. P. Pandolfi, A continuum model for tumour suppression. *Nature* **476**, 163–169 (2011).

27. B. Stamova, Y. Tian, G. Jickling, C. Bushnell, X. Zhan, D. Liu, B. P. Ander, P. Verro, V. Patel, W. C. Pevec, N. Hedayati, D. L. Dawson, E. C. Jauch, A. Pancioli, J. P. Broderick, F. R. Sharp, The X-chromosome has a different pattern of gene expression in women compared with men with ischemic stroke. *Stroke* **43**, 326–334 (2012).

28. K. Glass, J. Quackenbush, E. K. Silverman, B. Celli, S. I. Rennard, G.-C. Yuan, D. L. DeMeo, Sexually-dimorphic targeting of functionally-related genes in COPD. *BMC Syst. Biol*. **8**, 118 (2014).

29. S.-J. Schramm, G. J. Mann, Melanoma prognosis: A REMARK-based systematic review and bioinformatic analysis of immunohistochemical and gene microarray studies. *Mol. Cancer Ther*. **10**, 1520–1528 (2011).

30. Z. Yan, J. DeGregori, R. Shohet, G. Leone, B. Stillman, J. R. Nevins, R. S. Williams, Cdc6 is regulated by E2F and is essential for DNA replication in mammalian cells. *Proc. Natl. Acad. Sci. U.S.A.* **95**, 3603–3608 (1998).

31. J. A. Curtin, J. Fridlyand, T. Kageshita, H. N. Patel, K. J. Busam, H. Kutzner, K.-H. Cho, S. Aiba, E.-B. Bröcker, P. E. LeBoit, D. Pinkel, B. C. Bastian, Distinct sets of genetic alterations in melanoma. *N. Engl. J. Med*. **353**, 2135–2147 (2005).

32. A. B. Olshen, E. S. Venkatraman, R. Lucito, M. Wigler, Circular binary segmentation for the analysis of array-based DNA copy number data. *Biostatistics* **5**, 557–572 (2004).

33. R. Suzuki, H. Shimodaira, Pvclust: An R package for assessing the uncertainty in hierarchical clustering. *Bioinformatics* **22**, 1540–1542 (2006).

34. S. A. Bustin, V. Benes, J. A. Garson, J. Hellemans, J. Huggett, M. Kubista, R. Mueller, T. Nolan, M. W. Pfaffl, G. L. Shipley, J. Vandesompele, C. T. Wittwer, The MIQE guidelines: Minimum information for publication of quantitative real-time PCR experiments. *Clin. Chem.* **55**, 611–622 (2009).

35. L. M. McShane, D. G. Altman, W. Sauerbrei, S. E. Taube, M. Gion, G. M. Clark, Statistics Subcommittee of the NCI-EORTC Working Group on Cancer Diagnostics, Reporting recommendations for tumor marker prognostic studies (REMARK). *J. Natl. Cancer Inst*. **97**, 1180–1184 (2005)."

Chapter 4- Characterization of FOXP3 isoforms in melanoma

Manuscript in preparation: Redpath M., Elchebly M., M'Boutchou, M.-N., Van Kempen, L., Spatz, A. FOXP3 Isoforms Suppress Proliferation in Melanoma.

Contributions of authors:

Margaret Redpath: Designed and performed the experiments to characterize FOXP3 expression in melanoma cell lines including primer design, cell culture, end point PCR, qPCR, immunofluorescence microscopy and western blotting. Designed and performed BrdU flow cytometry experiments to assess proliferation and cell cycle progression including cloning, lentivirus generation, cell culture and staining of cells. Data analysis, data interpretation and manuscript writing.

Mounib Elchebly: Cell culture, primer design and cloning experiments.

Marie-Noël M'Boutchou: Cell culture and flow cytometry experiments.

Kishanda Vyboh: Cell culture and flow cytometry experiments.

Osama Roshdy: Data analysis and interpretation of FACS experiments

Leon van Kempen: Involved in experimental design, data analysis, data interpretation and manuscript editing.

Alan Spatz: Involved in experimental design and data interpretation.

Introduction

FOXP3 is a member of the *forkhead*/winged-helix family of transcription regulators and is an important transcription factor in T-cell differentiation. It is involved in the generation of natural T-regulatory cells in the thymus and induced T-regulatory cells in the periphery. The human *FOXP3* gene contains an 188 bp 5' untranslated region, a 1293 bp open reading frame and a 388 bp 3' untranslated region (Brunkow et al., 2001). The gene, located on chromosome Xp11.23, contains 11 coding exons and is translated into a 431 amino acid protein. Hemizygous or homozygous germline mutations in *FOXP3* lead to severe, fatal autoimmune disease in mice and humans. Immune dysfunction, polyendocrinopathy, enteropathy and X-linked inheritance (IPEX) is a syndrome associated with autoimmune enteropathy, polyendocrinopathy, atopic dermatitis, and fatal infections. At least 8 different mutations in *FOXP3* have been identified that result in IPEX including premature truncating mutations, frameshift mutations, an amino acid substitution in the forkhead domain and a mutation involving the polyadenylation signal (Bennett et al., 2001a&b). The severe autoimmune responses that result from mutations in *FOXP3* highlight the critical role that this transcription factor plays in regulating cytotoxic T-cells that recognize self-antigens. FOXP3 is also important in curbing lymphocyte activity at the end of a normal physiologic inflammatory response. Interestingly some tumor cells have been shown to take advantage of this immunosuppressive effect by expressing FOXP3 to avoid detection and/or destruction by innate or adaptive anti-tumor immune cells.

It is not known if melanoma cells expressing FOXP3 can lead to modulation of the immune microenvironment. This could have an important effect on patient outcome because the degree of tumor infiltrating lymphocytes (TILs) in primary melanoma tumors has been shown to be a significant prognostic factor. The survival rate at 8 years is 77% for patients with a brisk infiltrate,

compared to 53% for tumors with a non-brisk infiltrate, and 37% for tumors that display no significant infiltrate of TILs (Crowson, Magro, & Mihm, 2006). Nevi tend to have little, if any, infiltrating lymphocytes. Dysplastic-type nevi and radial growth phase melanomas are typically associated with more TILs than other nevi, vertical growth phase melanomas and melanoma metastases (Mourmouras et al., 2007). This peak in TILs in pre-malignant and early malignant melanocytic lesions suggests that immunotolerance is an early event in tumor genesis. Further characterization of the composition of the infiltrate showed that in all lesions the majority of the lymphocytes were CD4+ T-lymphocytes with little to no B-cells and CD8+ cytotoxic T-cells. The mechanism of immunotolerance that develops in melanoma is not known. One way that melanoma cells can evade detection is by downregulating antigen presentation. Cells with high antigenicity will be attacked by the immune system resulting in clonal selection of cells with lower antigenicity. Alternatively, the melanoma cells can release factors that alter the inflammatory infiltrate to promote immune evasion. There are two possible mechanisms by which melanoma cells expressing FOXP3 can modify the tumor microenvironment to evade the immune system. As a transcription factor, FOXP3 can modulate the expression of chemokines/cytokines that have direct suppressive effects on cytotoxic CD8+ T-cells or other innate anti-tumor cells such as natural killer cells. FOXP3 can also prevent a robust anti-tumor response by recruiting and/or stimulating suppressive T-cells, such as T-regulatory cells, to indirectly suppress the anti-melanoma inflammatory cells. In pancreatic cancer, FOXP3 expression in tumor cells was shown to inhibit T-cell proliferation in coculture experiments (Hinz et al., 2007). Given the prognostic importance of TILs in melanoma, it would be useful to know if FOXP3 expression by tumor cells can affect the T-cell infiltrate in the microenvironment of melanoma.

In addition to determining if FOXP3 regulates genes that attract and/or suppress infiltrating

lymphocytes, it is also important to investigate FOXP3's effect on the transcription of other genes involved in the biology of melanoma. The role of FOXP3 as a transcription factor has been most thoroughly characterized in T-regulatory cells with the identification of 5579 targets in the human genome by chromatin immunoprecipitation array profiling (CHIP) (Sadlon 2010). In cancer FOXP3 has been shown to directly repress several oncogenes such as Her2/ErbB2, SKP2, c-Myc and SATB1 (Zuo et al., 2007; Zuo et al., 2009; Wang et al., 2009). In addition to repressing transcription of important oncogenes, FOXP3 also acts as a transcriptional activator of major tumor suppressor genes such as BRCA1, p21, p18 and ARHGAP5 (R. Liu et al., 2009; Li et al., 2013). In breast cancer cell line MCF7, FOXP3 was shown to significantly upregulate 508 genes and downregulate 216 genes (R. Liu et al., 2009). This list of upregulated genes in breast cancer was cross referenced with the genes that were shown to have a CHIP-hit in the Sadlon (2010) paper and that were found to be differentially expressed in primary melanomas (Winnepenninckx et al., 2006 and Harbst et al, 2012) to identify a list of 16 potential FOXP3 gene targets that are relevant to melanoma biology (supplemental figure 1). Additionally, genes involved in epithelial-mesenchymal transition (CDH2, ZEB1), melanocyte differentiation (TYRP1, MITF) and immune suppression/evasion (CTLA4, PDL1) were tested for differential regulation by FOXP3. Given that FOXP3 has been shown to bind to the promoter of more than 5000 genes it is not surprising that FOXP3 has been shown to play different roles in different cell types. Whether FOXP3 behaves as a tumor suppressor or an oncogene in melanoma has yet to be elucidated.

After investigating the effect of full length FOXP3 on these gene targets, it is important to examine if the known isoforms of FOXP3 are associated with a different magnitude or direction or gene expression. In natural T-regulatory cells two isoforms of FOXP3 are typically expressed; full length and a variant lacking exon 3 (FOXP3ΔE3). In addition to these isoforms, several other

splice variants have been discovered in breast cancer cell lines including FOXP3ΔE8, FOXP3ΔE3ΔE4 and FOXP3ΔE3ΔE8 (Zuo et al., 2007). These isoforms have the potential to show differential regulation of gene targets because these exons are found in different functional domains of the protein and contain nuclear import and export signals that can affect subcellular localization.

There are four distinct structural domains of FOXP3. Starting from the amino terminus there is the repressor, zinc finger, leucine zipper and forkhead domains (figure 1). The N-terminal proline-rich domain is important for repression of transcription (Lopes et al., 2006; Ziegler, 2006) and is unique to FOXP3. The remaining 3 domains are common to other members of the FOXP subfamily: FOXP1, FOXP2 and FOXP4 (Lopes et al., 2006). FOXP3 has shown to homo and heterodimerize with other members of the family through the leucine zipper domain (Wang et al., 2003). Coimmunoprecipitation experiments by Lopes et al. revealed that the leucine zipper domain is both necessary and sufficient for homodimerization to occur. The C_2H_2 zinc finger domain, based on the role of zinc fingers in general, it is thought to be involved in protein-DNA interactions. The forkhead domain is responsible for DNA binding and it contains a nuclear localization signal (NLS) (Schubert et al., 2001). Based on the location of the removed exons, the

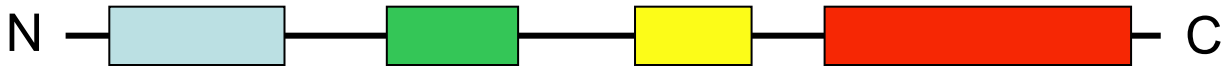

MPNPRPGKPSAPSLALGPSPGASPSWRAAPKASDLLGARGPGGTFQGRDLRGGAHASSSSLNPMPPSQLQLPTLPLVMVAPSGARLGPLPHLQAL
LQDRPHFMHQLSTVDAHARTPVLQVHPLESPAMISLTPPTTATGVFSLKARPGLPPGINVASLEWVSREPALLCTFPNPSAPRKDSTLSAVPQSSYPL
LANGVCKWPGCEKVFEEPEDFLKHCQADHLLDEKGRAQCLLQREMVQSLEQQLVLEKEKLSAMQAHLAGKMALTKASSVASSDKGSCCIVAAGS
QGPVVPAWSGPREAPDSLFAVRRHLWGSHGNSTFPEFLHNMDYFKFHNMRPPFTYATLIRWAILEAPEKQRTLNEIYHWFTRMFAFFRNHPATW
KNAIRHNLSLHKCFVRVESEKGAVWTVDELEFRKKRSQRPSRCSNPTPGP

Figure 1: Schematic diagram and sequence of human FOXP3 protein domains. Blue- proline-rich transcriptional repressor domain (Light blue- general transcription repressor, Dark blue- NFAT transcription repressor); Green- C_2H_2 zinc-finger domain; Leucine zipper domain; Red- forkhead domain; Single underline- nuclear export signals, double underline- nuclear localization signal.

FOXP3ΔE3, FOXP3ΔE3ΔE4 and FOXP3ΔE3ΔE8 isoforms may show differential expression of transcription targets because they contain changes in the protein sequence of the repressor domain compared to FOXP3 full length. The FOXP3ΔE8 variant may show impaired dimerization or a different affinity for bindings partners based on its interruption of the leucine zipper domain. FOXP3ΔE3ΔE4 is a prematurely truncated protein that is hypothesized to lose its DNA-binding capacity secondary to loss of the forkhead domain. Whether or not these isoforms are present in melanoma is not known and their functional significance is unclear.

The isoforms also have the potential to impact the function of the FOXP3 protein by affecting its subcellular localization. It has been shown that the many of the somatic mutations that occur in *FOXP3* in tumors have an effect on subcellular localization. Importantly, localization to the cytoplasm has been demonstrated to abrogate FOXP3's suppressive effect on proliferation (Wang, Liu, Ribick, Zheng, & Liu, 2010). It makes sense that where the transcription factor is situated affects its function. When it is located in the nucleus it is available for gene transcription and when it is in the cytoplasm it can sequester binding partners and prevent them from entering the nucleus. Originally FOXP3 was found to reside exclusively in the nucleus of several different cell types. A nuclear localization signal was identified in exon 12 that was both necessary and sufficient for FOXP3 translocation into the nucleus (Lopes et al., 2006). Another group identified two nuclear export signals and showed that the localization of FOXP3 is cell-line specific (Magg, Mannert, Ellwart, Schmid, & Albert, 2012). They demonstrated that a mutation of the export signals slowed the kinetics of FOXP3 translocation to the cytoplasm and increased the suppressive capacity of T-cells. A double mutant affecting both nuclear export signals remained in the nucleus for as long as the protein was detectable. These findings are pertinent to an isoform-specific effect because the nuclear export signals are located in exons 3 and 8 and thus they are disrupted in the

FOXP3ΔE3, FOXP3ΔE3ΔE4 and FOXP3ΔE3ΔE8 variants (figure 2). Additionally the FOXP3ΔE3ΔE4 isoform does not contain the NLS signal in exon 12 so this isoform may never gain access to the nucleus. It is important to investigate which subcellular compartment the isoforms localize to in melanoma because this impacts protein function.

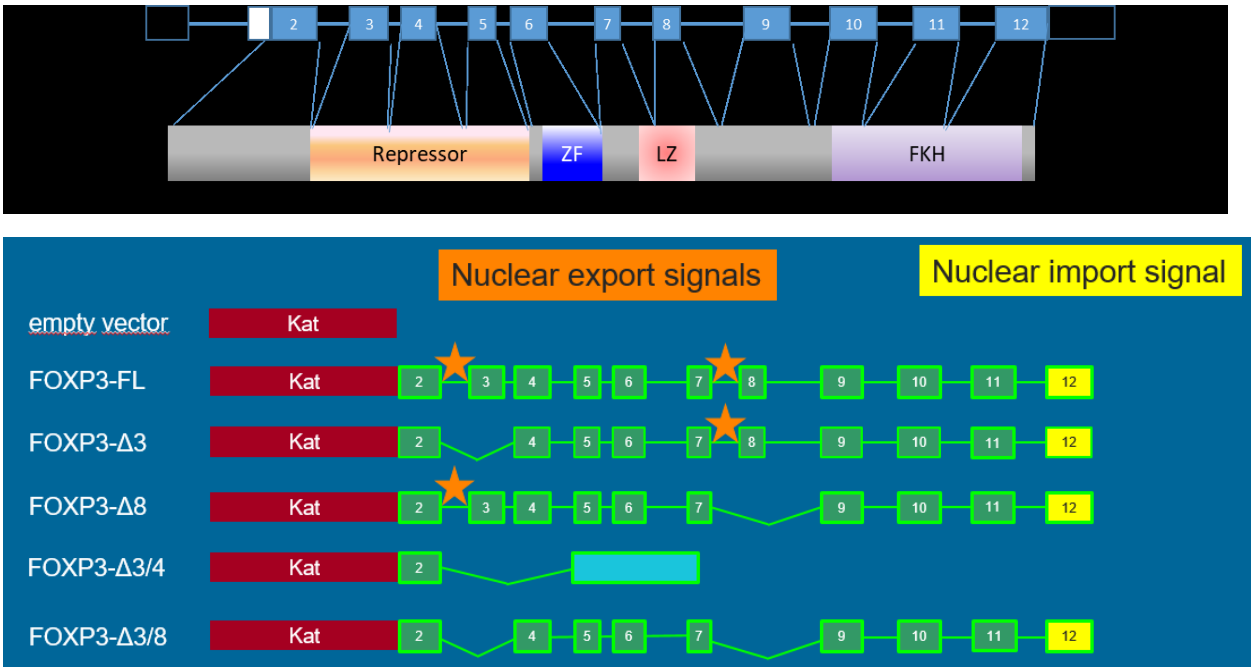

Figure 2: Schematic diagram of Katushka-tagged FOXP3 isoforms with the location of nuclear export signals (orange stars) and nuclear import signals (yellow).

Methods

FOXP3 endogenous mRNA and protein expression in melanoma cell lines:

Cell lines used include cutaneous melanoma cells lines (MM46, MM50, MM57, MM71, MM73, MM74, MM79, MM94, MM102, MM104, MM111, MM117, A375M, DAUV, 451Lu, MV1, MV3, SKMel-28, BLM, M24MET and LMMel34) and uveal melanoma cells lines (OCM-1, UW-1, 92.1, MKT-BR and SP6.5). Cells were cultured in media (DMEM, Ham's F-10 or RPMI 1640 depending on the cell line) containing 10% fetal bovine serum. The cells lines were screened by

end point and qPCR for *FOXP3* mRNA expression levels. RNA was extracted using a Qiagen RNeasy Mini Kit and eluted in 30µLs of RNase-free water. The concentration and purity of RNA was analyzed by using the Thermo Fisher Scientific NanoDrop 100ND-1000 Spectrometer. cDNA was synthesized using a Bio-Rad iScript Select Kit. End point PCR reactions were performed using Bio-Rad iTaq polymerase in a Bio-Rad thermocycler with a total reaction volume of 25µL. qPCR was performed on an Applied Biosystems 7500 Fast Real-Time PCR System in a final volume of 20 µl in a 96-well format. The expression of FOXP3 isoforms in melanoma cell lines was further characterized by Sanger sequencing performed at Genome Quebec. Protein for Western Blots was extracted using radioimmunoprecipitation assay buffer (150 mM NaCl, 50 mM tris (pH 8.0), 1% triton X-100, 1mM DTT, 0.5% Na deoxycholate, 0.1% SDS, aprotinin, leupeptin, PMSF and phosphatase inhibitor mix). Protein concentration was quantitated using a BCA (bicinchoninic acid) protein assay (Pierce). Equal amounts of protein were separated on SDS–polyacrylamide gel electrophoresis (PAGE) and transferred onto polyvinylidene difluoride (PVDF) membranes. Membranes were blocked using 5% milk and probed with the primary antibodies followed by HRP-conjugated secondary antibody. Blots were developed with PerkinElmer Western Blot Chemiluminescence Reagent.

Exogenous localization of FOXP3 isoforms in melanoma:

To observe subcellular localization of FOXP3 by fluorescent microscopy, GFP-tagged FOXP3 constructs were transfected into melanoma cell lines using lipofectamine. Viral constructs of Katushka-tagged FOXP3 isoforms were generated using the Invitrogen Lentiviral Protocol in 293FT cells according to the manufacturer's instructions and infected into melanoma cell lines. Images were captured using an AMG-EVOS FL microscope.

FOXP3 isoform effect on gene targets:

Endogenous FOXP3 and CTLA4 mRNA expression were assessed by qPCR in 29 melanoma cell lines. GFP-tagged-FOXP3 full length was then overexpressed by transfection in two melanoma cell lines (451Lu and MM117) and after 48 hours the cells were harvested and qPCR was run with primers towards sixteen targets of interest (see supplemental figure 1 for list of targets and primer sequences). An additional two cell lines (MM117 and A375M) were infected with all of the Katushka-tagged-FOXP3 isoforms. After 48 hours the cells were harvested and sorted by flow cytometry into low, mid and high expression levels based on median fluorescence intensity. The RNA was extracted, cDNA was prepared and qPCR was run with primers towards five targets of interest (*CDH2*, *ZEB1*, *TYRP1*, *MITF*, *PDL1*) and two reference genes (*HPRT1* and *TBP*).

FOXP3 effect on melanoma cell proliferation and cell cycle progression:

The effect of FOXP3 on cell cycle progression was assessed by a BrdU assay in cell line MM117 transfected with his-myc-tagged FOXP3FL, FOXP3ΔE3, FOXP3ΔE8, FOXP3ΔE3ΔE4 and FOXP3ΔE3ΔE8 isoforms. Supplemental figure 2 shows confirmation of protein expression of the isoforms by Western blot. Supplemental figure 3 shows the gating that was used for the phases of the cell cycle. The effect of FOXP3 on proliferation was assessed using Katushka-tagged FOXP3 isoforms that were infected into cell lines MM117, SKMel-28 and A375M. The infection was performed in triplicate using 6 well plates. After 24hrs the cells are re-infected. 48hrs later BrdU was added for 30 minutes. The cells were then fixed, stained and analyzed on a BD LSRFortessa flow cytometer using FlowJo software using the gating shown in supplemental figure 4.

Results

mRNA and Protein Expression of FOXP3 and CTLA4 In Melanoma:

FOXP3 full length mRNA is expressed in 15 of the 19 cutaneous melanoma cell lines and all 5 of the uveal melanoma cell lines that were tested. The FOXP3ΔE3 isoform is expressed in 16 out of

the 19 cutaneous melanoma cell lines and all of the uveal melanoma cell lines. The FOXP3ΔE3ΔE4 isoform was found in one cutaneous and one uveal melanoma cell line (results are summarized in supplemental figure 5). qPCR shows that the level of expression in the cutaneous melanoma cell lines is generally quite low compared to the uveal melanomas (figure 3). There was no significant

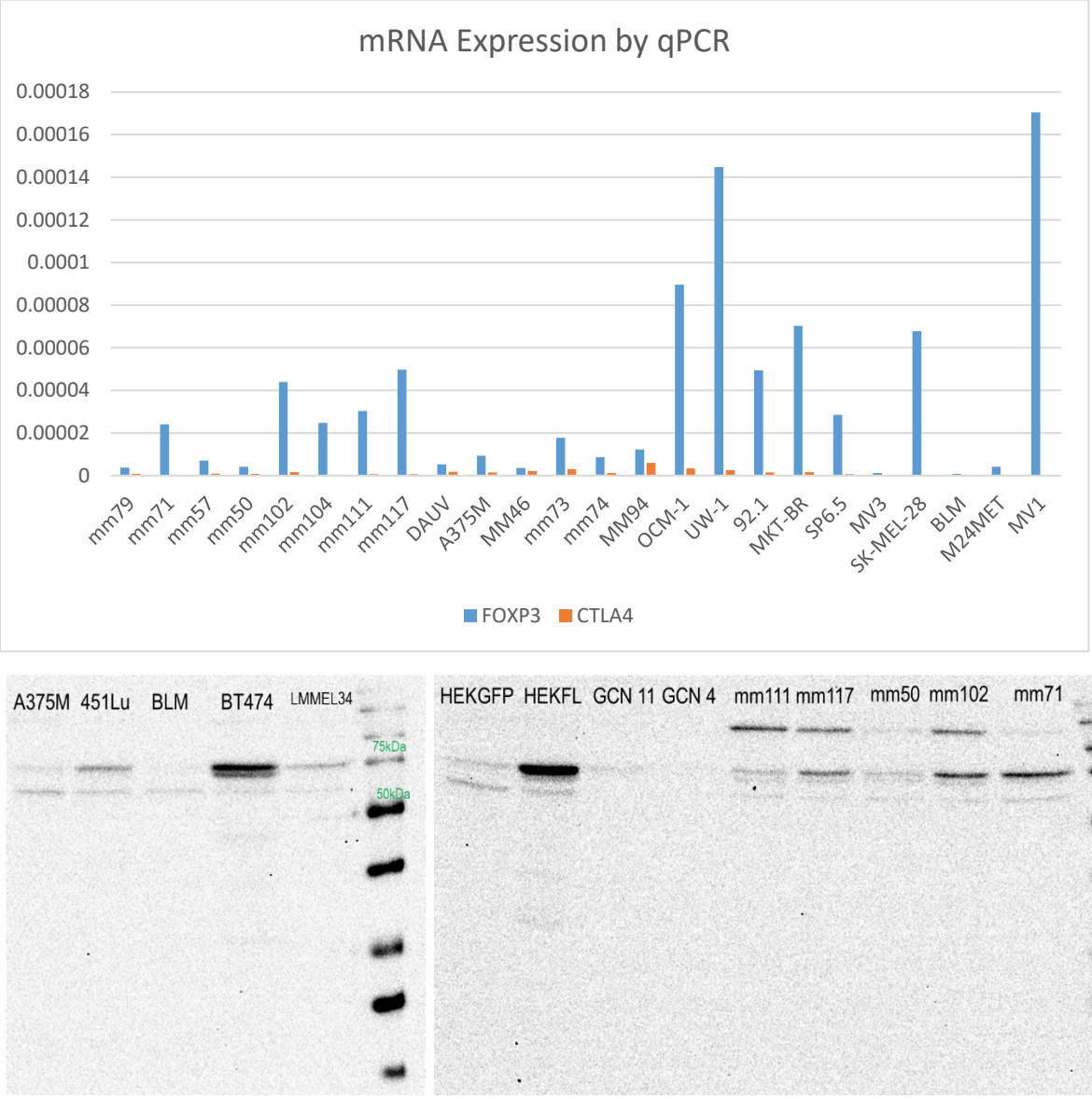

Figure 3: Endogenous FOXP3 mRNA is expressed in the majority of our melanoma cell lines and CTLA4 mRNA expression was negligible in all of the cell lines (top). Endogenous FOXP3 protein (bottom) is expressed at the highest level in breast cancer cell line BT474. In general the melanoma cell lines show a higher level of expression than nevus cells. Exogenous overexpression of GFP-tagged FOXP3FL in HEK293 is also shown.

expression of CTLA4 mRNA in all 24 of the melanoma cells lines tested. FOXP3 endogenous protein expression is shown by Western blot for nevic, melanoma and a breast cancer cell lines in figure 3. Compared to two nevic cell lines (GCN4 and GCN11), seven melanoma cell lines (MM111, MM117, MM50, MM102, MM71, 451Lu and LMMel34) had a higher level of FOXP3 protein expression. Two melanoma cell lines (BLM and A375M) showed negligible expression of FOXP3. Compared to the breast cancer cell line BT474, FOXP3 protein levels were lower in melanoma. CTLA4 protein levels were tested in six melanoma cells lines and in keeping with the mRNA results little, if any, endogenous expression was observed (supplemental figure 6).

Subcellular Localization of Foxp3 Isoforms:

Using HEK293 transfected with FOXP3FL fused to GFP we confirmed the previously reported finding that FOXP3 localizes to the nucleus in this cell line. We observed persistent nuclear expression throughout the 72 hours that these cells were in culture. Using three melanoma cell lines (A375M, MM117 and 451Lu) transfected with FOXP3FL, similar nuclear localization was observed for up to 144 hours (figure 4). A375M infected with katushka-tagged isoforms showed that all of the variants localized to the nucleus and remained nuclear for at least 40 hours (figure 4). The FOXP3ΔE3ΔE4 variant had a unique clustered distribution in the nucleus compared to the other isoforms that showed a more homogeneous or diffuse localization pattern.

Foxp3 Effect on Transcriptional Targets:

When FOXP3FL was transfected into cell lines 451Lu and MM117 there was no significant difference in the levels of mRNA expression of the 16 genes that were tested compared to empty vector transfection. This was thought to be due to the low efficiency of transfection. To enrich the proportion of FOXP3-positive cells cell sorting was then performed prior to analysis. The gene

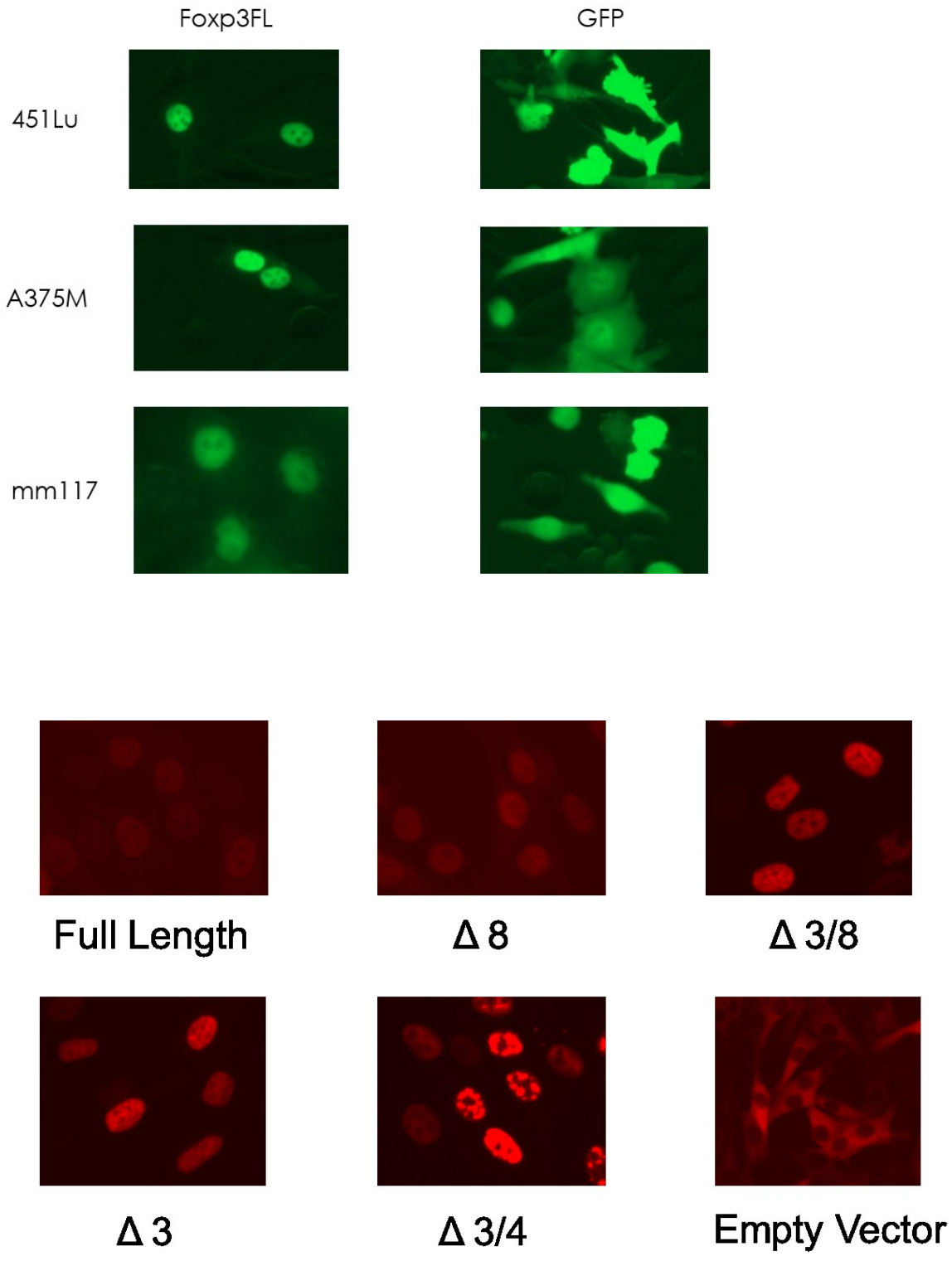

Figure 4: Melanoma cell lines A375, MM117 and 451Lu transfected with GFP-fused Foxp3FL showed nuclear localization of FOXP3 (top left) compared to empty GFP vector control (top right) that is distributed throughout the nucleus and cytoplasm. Exogenous expression of all of the isoforms in cell line A375M showed nuclear localization as well (bottom).

targets showed isoform- and cell line-specific differences in expression (supplemental figure 7). Some of the FOXP3 variants showed a dose-dependent difference in the levels of PDL1 mRNA expression levels in SKMel-28. We decided to test if this results in differences in expression at the protein level. There was a trend for some of the isoforms to increase PDL1 protein expression in melanoma cell line SKMel-28 but these differences were not significant. This lack of significance could be secondary to relatively low endogenous levels of PDL1 in melanoma so the experiments were repeated in a breast cancer cell line that has a higher baseline expression level of PDL1, MDA-MB-436. Overexpression of FOXP3FL, FOXP3ΔE3, FOXP3ΔE8 and FOXP3ΔE3ΔE8 isoforms were observed to increase PDL1 protein expression in this cell line (figure 5).

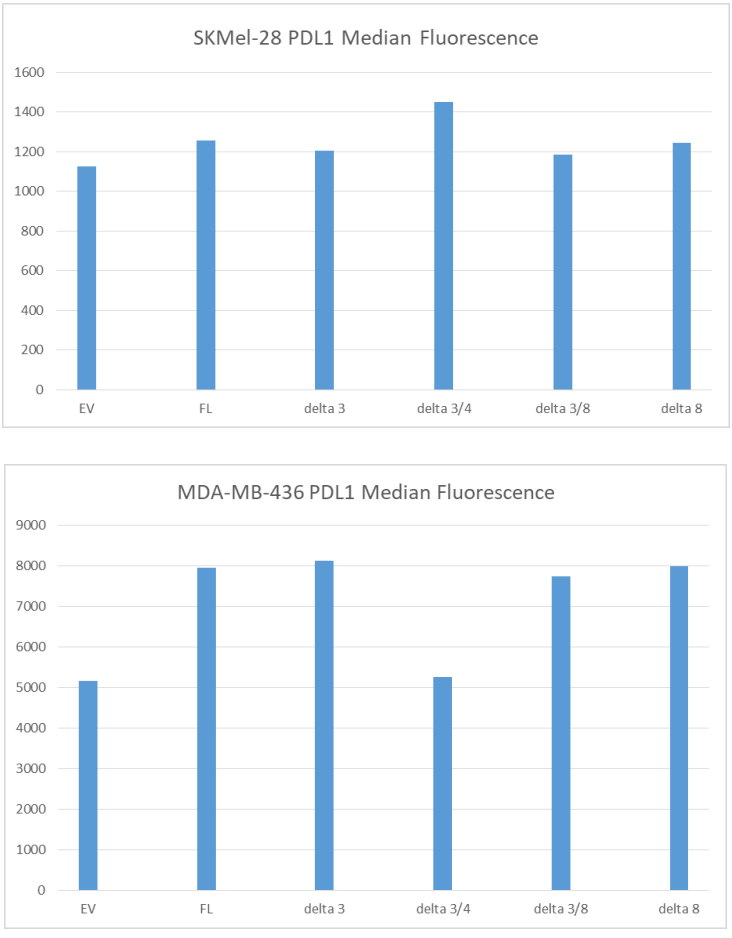

Figure 5- Overexpression of the FOXP3 isoform is associated with a mild non-significant increase in PDL1 protein expression by flow cytometry in SKMel28 (top). FOXP3 isoform overexpression was found to increase median PDL1 fluorescence by flow cytometry in MDA-MB-436 (bottom).

Foxp3 Effect on Proliferation:

BrdU proliferation assays were performed on melanoma cell line MM117 transfected with FOXP3 full length. Overexpression of N-terminal GFP-tagged FOXP3FL led to a 50% reduction in the proportion of cells in the S-phase of the cell cycle compared to the empty vector control (18% vs 37% respectively). To ensure that the location of the tag does not interfere with the suppressive effect, the experiment was repeated with a C-terminal his-myc-tagged FOXP3FL and similarly resulted in a relative decrease in the S-phase population (supplemental figure 8). Transfection of all of the katushka-tagged isoforms, except FOXP3ΔE3ΔE4, demonstrated a shift to an increased proportion of cells in the G0/G1-phase compared to the S-phase (figure 6). The FOXP3ΔE3 variant appeared to have the strongest effect on delaying progression to the S-phase.

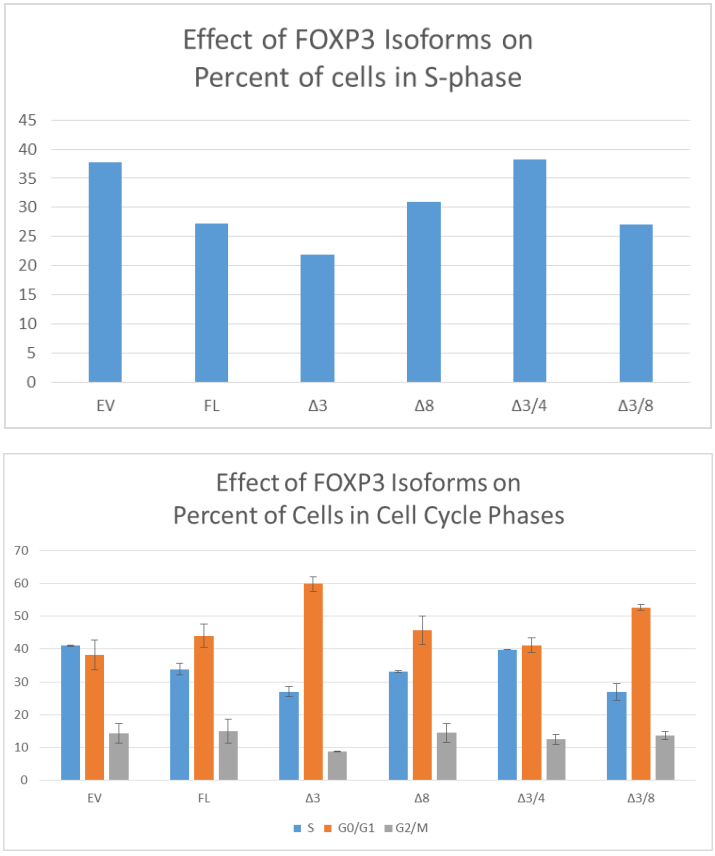

Figure 6: Exogenous overexpression of FOXP3 shows a decrease in the percent of cells in S-phase of the cell cycle for all of the isoforms except FOXP3ΔE3ΔE4 (top). Similarly, overexpression of all of the FOXP3 isoforms leads to a relative accumulation of cells in G0/G1 phase of the cell cycle (bottom).

The FOXP3 isoforms were then overexpressed in MM117 and A375M cell lines. The percentage of BrdU positive cells was used to assess the rate of proliferation. Overexpression of all of the FOXP3 isoforms in melanoma cell lines MM117 and A375M led to a decrease in proliferation compared to the empty vector control (figure 7). The cells were then subdivided into four populations based on the degree of FOXP3 overexpression as measured by the intensity of katushka fluorescence. A dose-dependent inhibitory effect was shown for cells with katushka negative, low, medium and high expression levels.

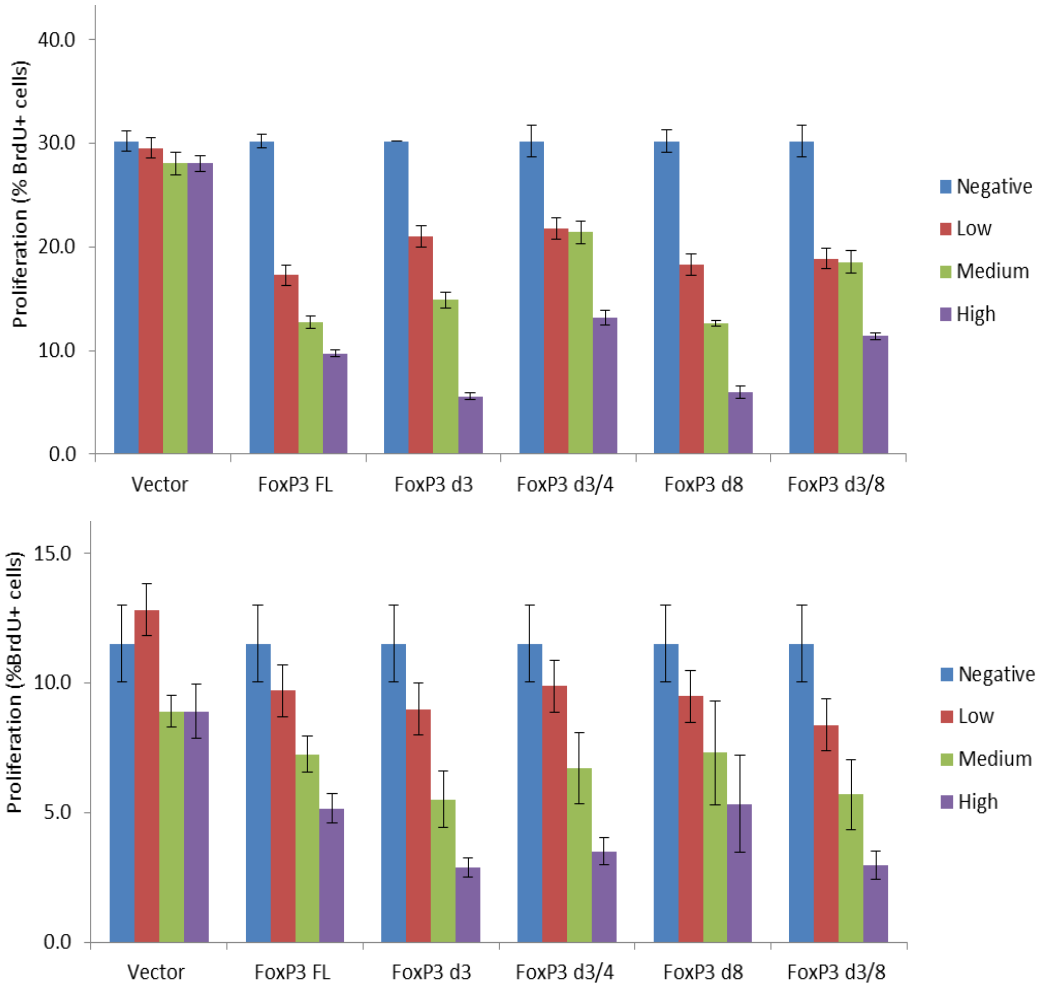

Figure 7: All of the FOXP3 isoforms show a dose-dependent decrease in proliferation in cell lines MM117 (top) and A375M (bottom).

Discussion:

While studying the role of FOXP3 on the immune system it was observed that germline heterozygous mutations of *FOXP3* are associated with an increased incidence of cancer. This serendipitous observation inspired future experiments that recognized the relevance of *FOXP3* in murine cancer. FOXP3 was then proven to be an equally important player in human oncology acting as a tumor suppressor in breast, prostate and ovarian cancer, and an oncogene in pancreatic and gastric cancers. The behaviour of FOXP3 in melanoma, and whether or not it was even expressed in melanocytic tumors, was not known. Our objective was to characterize the role of FOXP3 in melanoma. We detected FOXP3 expression on the mRNA and protein level in the majority of our cell lines. In addition to proving that it is expressed in melanoma, it was important to determine what compartment of the cell it is found in since others had shown that the localization of FOXP3 is cell type specific and that cytoplasmic expression abolishes its tumor suppressive effects. We determined that FOXP3 expression is nuclear in melanoma in three independent cells lines. The isoforms of FOXP3 differ from each other with regards to the presence of previously described nuclear import and export signals so we further investigated whether the localization of FOXP3 is isoform specific. Interestingly we found that all of the isoforms localized to the nucleus, including the FOXP3ΔE3ΔE4 variant that does not contain any of the localization signals. It was unexpected to find the FOXP3ΔE3ΔE4 variant in the nucleus because it does not contain the nuclear import signal that was previously shown to be required for import. A possible explanation for this is that this truncated variant of the protein may be able to passively diffuse across the nuclear membrane, unlike the other heavier isoforms that require active transport. If in fact the FOXP3ΔE3ΔE4 variant can passively diffuse across the membrane, the fact that this protein was not equally distributed between the nuclear and cytoplasmic compartments suggests that it may be

binding to transcription factors, cofactors or other protein partners that are contributing to its nuclear sequestration. Further studies are necessary to see what the FOXP3ΔE3ΔE4 variant is binding to because whatever is keeping this variant in the nucleus could be the key to determining why all of the other isoforms also remain in the nucleus in melanoma cells despite containing nuclear export signals.

After determining that the FOXP3 isoforms localize to the nucleus, where they can act as transcription factors, we decided to explore their effects on the transcription of genes involved in different aspects of melanoma biology. The transcriptional regulation of genes by FOXP3 was found to be isoform- and cell line-specific. Further research is required to determine if this is due to variations in the affinity for, and availability of, different cofactors and binding partners. We observed a trend in the increase of PDL1 protein expression *in vitro* that was significant in breast cancer cell line MDA-MB-436, but not did not reach significance in melanoma cell line SKMel-28. Increased PDL1 expression in breast cancer cells has been shown to be associated with an increase in tumor infiltrating cells and a good prognosis in certain subtypes of breast cancer by one group (Kim et al., 2017). Conversely, another group showed that PDL1 expression in breast cancer cells is associated with an increase in T-regulatory cells and a poor prognosis (Li et al., 2016). Given these conflicting associations, it would be interesting to test the effect of overexpression of FOXP3 on the amount and composition of the infiltrating T-cells. If FOXP3 is capable of modulating the immune microenvironment this could have important implications for its use as a prognostic marker of disease and/or a predictive marker of response to immuno-oncologic therapies.

The final objective was to investigate FOXP3's effect on melanoma cell proliferation. Mitotic rate is one of the strongest independent prognostic factors in melanoma and we

demonstrated that FOXP3 full length overexpression correlates with a dose-dependent decrease in proliferation in two independent melanoma cell lines, suggesting that it can behave as a tumor suppressor in melanoma. One of the cell lines harbors a BRAF V600E mutation while the other is wildtype for BRAF suggesting that this effect is independent of BRAF mutation status. FOXP3 full length was also shown to decrease the percentage of cells in the S-phase of the cell cycle. This is a significant finding because a reduced fraction of cells in the S-phase has also been shown to be an independent prognostic factor in melanoma that is associated with increased survival (Crowson et al., 2006). Interestingly, despite differences in the sequence of the repressor and leucine zipper domains the FOXP3ΔE3, FOXP3ΔE8 and FOXP3ΔE3ΔE8 variants showed similar dose-dependent suppressive effects on the rate of proliferation and cell cycle progression. This suggests that the anti-proliferative effects of FOXP3 are independent of exons 3 and 8. FOXP3ΔE3ΔE4 overexpression was comparable to empty vector and did not result is a relative accumulation of cells in the G0/G1 phase of the cell cycle. Given that the FOXP3ΔE3ΔE4 variant is a truncated protein missing all four of the main functional domains of this protein, this lack of effect is not surprising. What is intriguing though is that high levels of the FOXP3ΔE3ΔE4 isoform were found to inhibit proliferation. Whether this is due to sequestering of other proteins or some other mechanism requires further investigation.

The significance of FOXP3 inducing a dose-dependent effect on proliferation in melanoma is related to the potential for drug therapies that increase FOXP3 expression to suppress tumor growth *in vivo*. Candidate drugs are treatments that either increase the transcription/translation of *FOXP3* or that increase the stability of the protein. FOXP3 has been shown to have a short half-life of two hours and the degree of FOXP3 phosphorylation, acetylation and ubiquination have all been shown to impact its rate of turnover (Morawski, Mehra, Chen, Bhatti, & Wells, 2013). Drugs

that alter these post translational modifications towards increased acetylation, decreased ubiquination and decreased phosphorylation increase the stability and the magnitude of the suppressive activity of FOXP3 and have the potential to restore its anti-proliferative effect in tumors with low levels of FOXP3 expression (Morawski et al., 2013; Van Loosdregt et al., 2010; Van Loosdregt et al., 2013). Lysine deacetylase inhibitors such as Trichostatin A, Vorinostat or even less toxic options like vitamin B3 have the potential to boost FOXP3 levels by increasing protein acetylation (Van Loosdregt et al., 2011). Seliciclib is an example of a drug that can increase FOXP3 expression by inhibiting FOXP3 phosphorylation by cyclin-dependent kinase 2 (Morawski et al., 2013). Doxorubicin and anisomycin are two other therapies worth investigating in melanoma since they have been shown to increase FOXP3 levels in breast cancer (Jung et al., 2010; Y. Liu, Wang, Li, Zheng, & Liu, 2009). Some of these treatments have already been tested in melanoma patients and it would be worthwhile to investigate if FOXP3 can be used as a predictive marker of therapeutic response.

Supplemental Figures

Gene Name	Forward Primer	Tm	Reverse Primer	Tm
RAP1A	ACTTACAGGACCTGAGGGAACA(	60.9	CCTGCTCTTTGCCAACTACTCG	63.5
S100A4	CAGAACTAAAGGAGCTGCTGAC(	61.8	CTTGGAAGTCCACCTCGTTGTC	63.2
HBEGF	TGTATCCACGGACCAGCTGCTA	65.1	TGCTCCTCCTTGTTTGGTGTGG	66.7
FOXP4	CCAGGATGTTCGCCTATTTCCG	66.8	TTTGGCGGTCTCCGCTTCTGAT	69.3
IL15	AACAGAAGCCAACTGGGTGAAT(	64.6	CTCCAAGAGAAAGCACTTCATTGC	63.7
IL11	GGACCACAACCTGGATTCCCTG	67.1	AGTAGGTCCGCTCGCAGCCTT	66.8
MCL1	CCAAGAAAGCTGCATCGAACCAT	66.7	CAGCACATTCCTGATGCCACCT	66.8
BCL2L1	GCCACTTACCTGAATGACCACC	62.9	AACCAGCGGTTGAAGCGTTCCT	68.3
ARHGAP5	CTCCAGGATCTGGTTACAGCTG	61.2	GTCTTGGTCAGTTTTATTCCCGC	63.1
RASA4	GCTGAAGGACTTCATCACCAAGC	64.6	TTGCCCTTGGTCCTGTGGATGA	69.1
CTNNA1	GGACCTGCTTTCGGAGTACATG	63.1	CTGAAACGTGGTCCATGACAGC	65.1
BMF	CAGTGGCAACATCAAGCAGAGG	65.3	GCAAGGTTGTGCAGGAAGAGGA	66.0
TYRP1	TCTCAATGGCGAGTGGTCTGTG	65.9	CCTGTGGTTCAGGAAGACGTTG	64.2
AIM1L	TCACCAACTGGCTGACCTACAG	62.6	GCCTGCTTTCATGTCCTCCACA	66.9
BCL2L1	CATTCAGTGACCTGACATCCC	60.4	CTGCTGCATTGTTCCCATAGA	61.2
CDKN1A	AGGTGGACCTGGAGACTCTCAG	62.2	TCCTCTTGGAGAAGATCAGCCG	65.2

Supplemental Figure 1: List of qPCR targets with primer sequences and melting temperatures

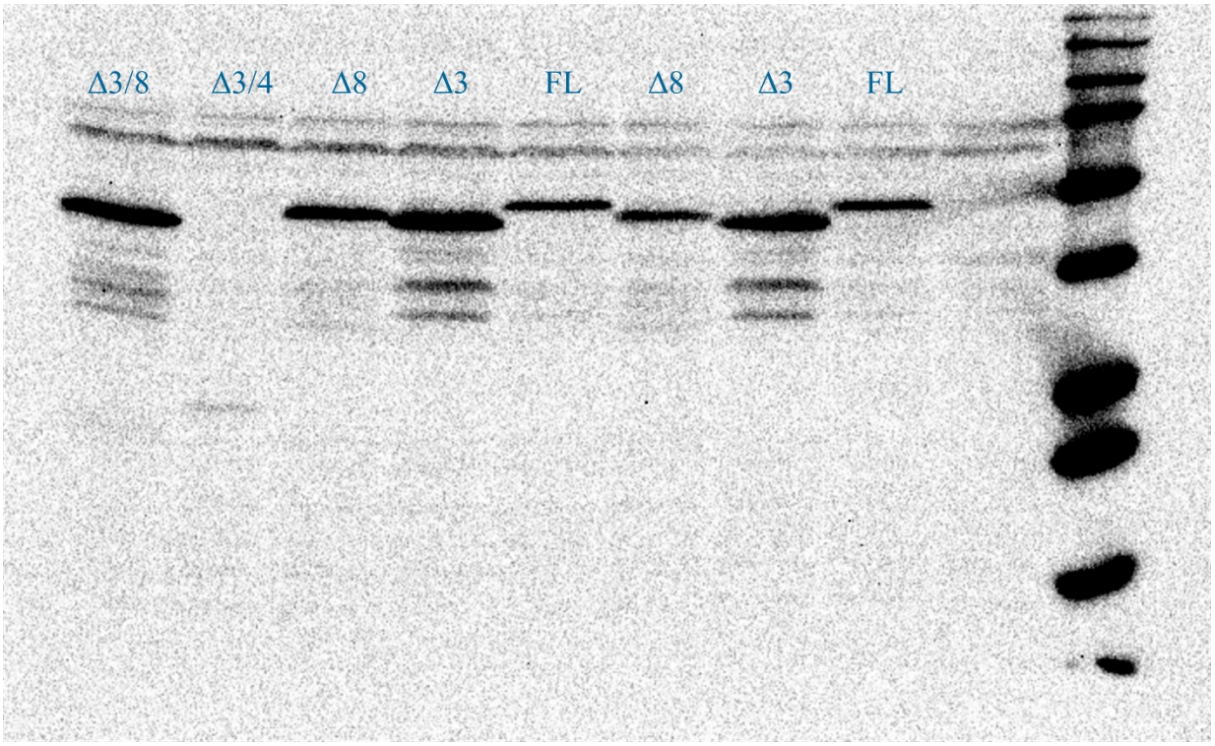

Supplemental Figure 2: Western blot of exogenous overexpression of his-myc-tagged FOXP3 isoforms used for BrdU cell cycle analysis assay. The proteins bound both anti-myc (shown here) and anti-FOXP3 antibodies.

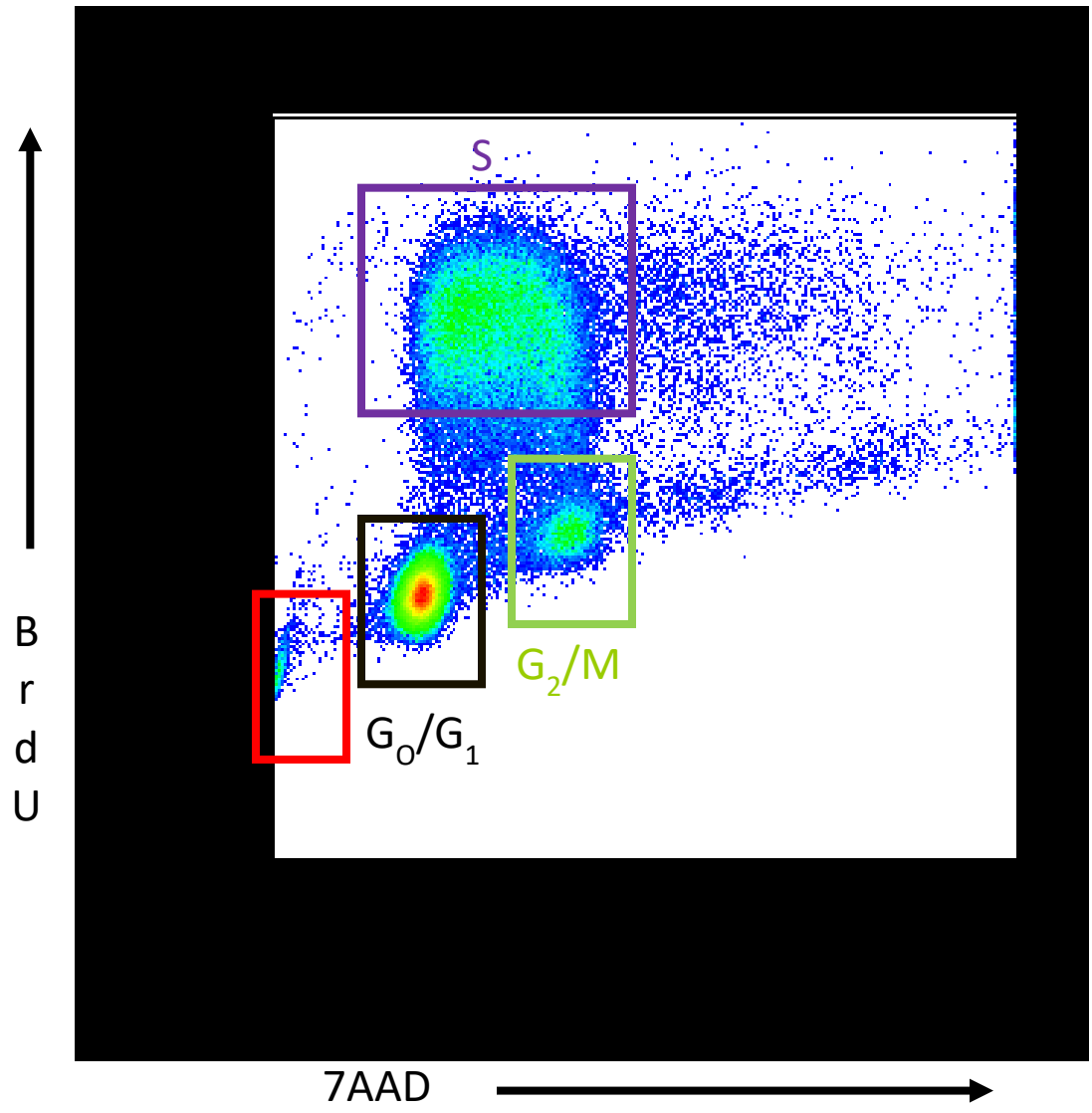

Supplemental Figure 3- Gating for BrdU cell cycle phase anaylsis

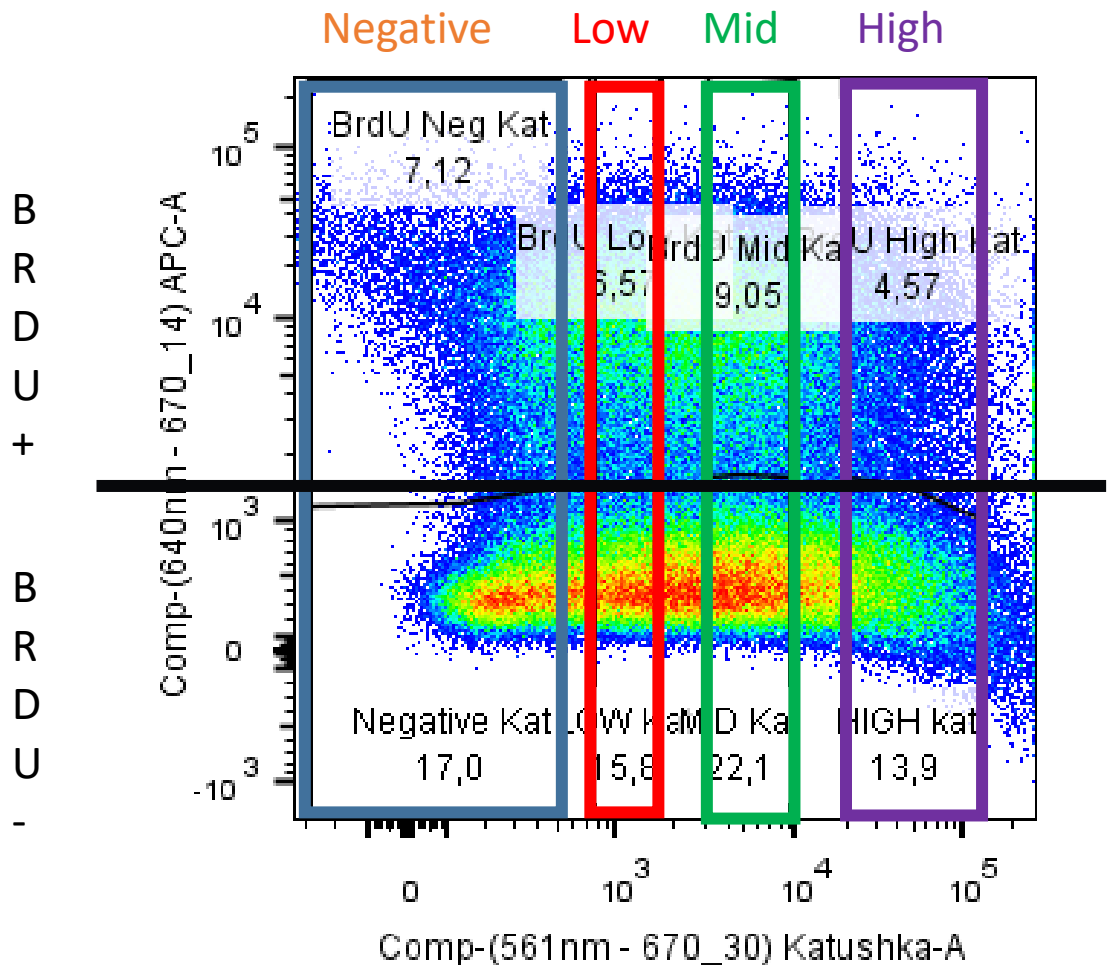

Supplemental Figure 4: Gating for BrdU Proliferation Assay. The black line represents the cut-off on the vertical axis for BrdU positive cells. The blue box represent the FOXP3 negative population of cells. The red, green and pruple boxes contain cells with low, moderate and high levels of FOXP3 protein expression respectively. Rate of proliferation = Number of cells that are BrdU positive / Total number of cells

Full length	Δ3	Δ3,4	no expression
mm71	mm71	mm104	MV3
mm57	mm57	OCM-1	BLM
mm50	mm50		M24-MET
mm104	mm104		
mm111	mm111		
mm117	mm117		
mm73	mm73		
A375M	A375M		
OCM-1	OCM-1		
OCM-1-CX	OCM-1-CX		
UW-1	UW-1		
UW-1-CX	UW-1-CX		
92.1	92.1		
92.1-CX	92.1-CX		
MKT-BR	MKT-BR		
MKT-BR-CX	MKT-BR-CX		
SP6.5	SP6.5		
SP6.5-CX	SP6.5-CX		
MV1	MV1		
mm79	mm79		
SK-MEL-28	SK-MEL-28		
DAUV	DAUV		
mm46	mm46		
mm102	mm102		
mm94	mm94		
	mm74		

Supplemental Figure 5: Summary of end point PCR results screening for FOXP3 Isoform Expression in Melanoma Cell lines

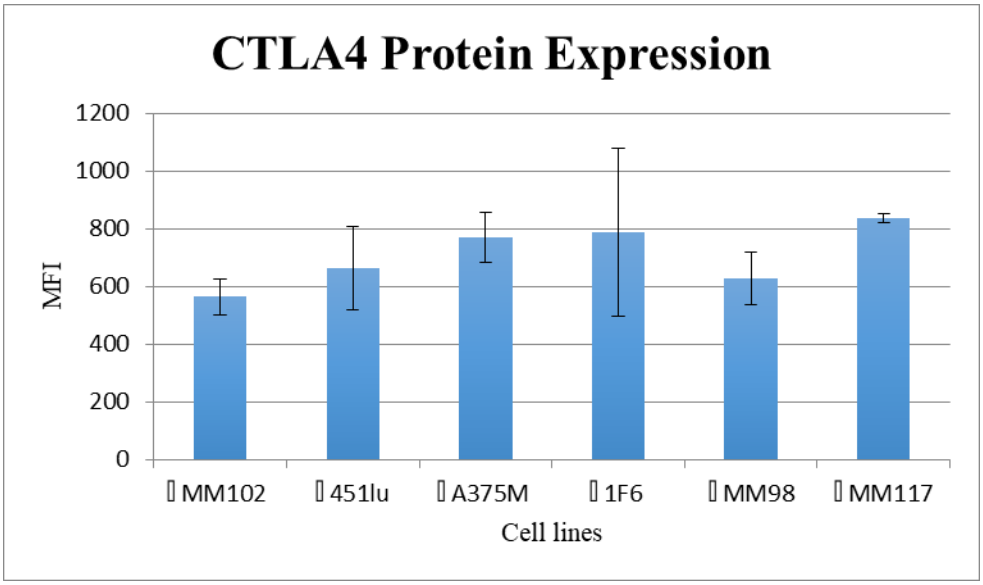

Supplemental Figure 6: Six melanoma cells lines express low to negligible CTLA4 protein levels by FACS analysis

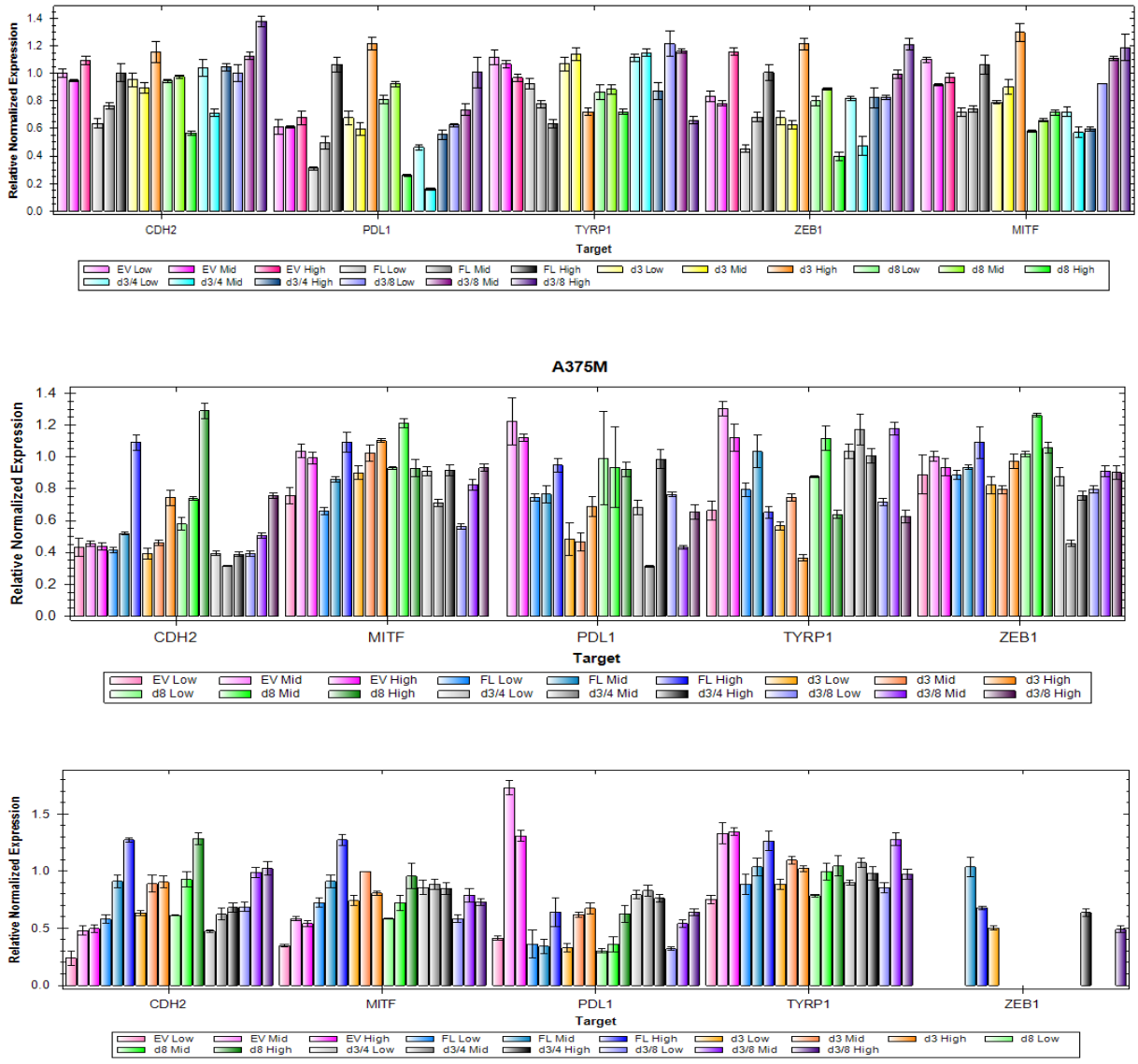

Supplemental figure 7: Normalized qPCR mRNA expression of putative gene targets of FOXP3 in SKMel-28 (top), A375M (middle) and MM117 (bottom) cells sorted into low, medium and high levels of FOXP3 isoform overexpression.

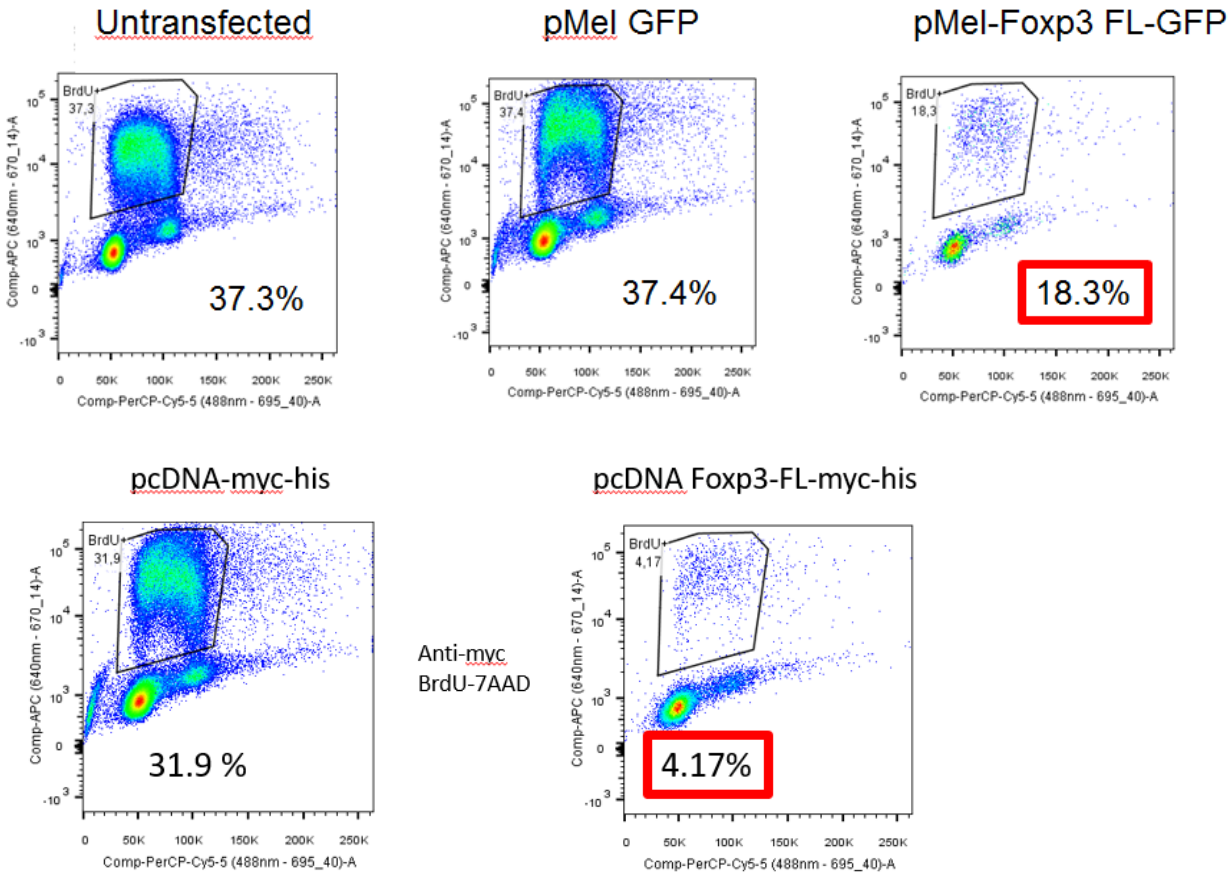

Supplemental figure 8: Both N-terminal (top) and C-terminal (bottom) tagged full length FOXP3 overexpression leads to decreased percentage of cells in S-phase compared to empty vector control.

References

Bennett, C.L., Brunkow, M.E., Ramsdell, F., O'Briant, K.C., Zhu, Q., Fuleihan, R.L., …, Chance, P.F. (2001a). A rare polyadenylation signal mutation of the FOXP3 gene (AAUAAA–>AAUGAA) leads to the IPEX syndrome. *Immunogenetics, 53*, 435-439.

Bennett, C.L., Christie, J., Ramsdell, F., Brunkow, M.E., Ferguson, P.J., Whitesell, L., …, Ochs, H.D. (2001b). The immune dysregulation, polyendocrinopathy, enteropathy, X-linked syndrome (IPEX) is caused by mutations of FOXP3. *Nat Genet, 27*(1), 20-21.

Brunkow, M.E., Jeffery, E.W., Hjerrild, K.A., Paeper, B., Clark, L.B., Yasayko, S.A., ..., Ramsdell F. (2001). *Nat Genet, 27*(1), 68-73.

Crowson, A.N., Magro, C.M., & Mihm M.C. (2006). Prognosticators of melanoma, the melanoma report, and the sentinel lymph node. *Mod Pathol, 19*, Suppl 2:S71-87.

Harbst, K., Staaf, J., Lauss, M., Karlsson, A., Måsbäck, A., Johansson, I., … Jönsson, G. (2012). Molecular Profiling Reveals Low- and High-Grade Forms of Primary Melanoma. *Clinical Cancer Research: An Official Journal of the American Association for Cancer Research*, *18*(15), 4026–4036.

Hinz, S., Pagerols-Raluy, L., Oberg, H-H., Ammerpohl, O., Grussel, S., Sipos, B., … Kalthoff, H. (2007). Foxp3 expression in pancreatic carcinoma cells as a novel mechanism of immune evasion in cancer. *Cancer Res., 67*(17), 8344-50.

Kim, A., Lee, S. J., Kim, Y. K., Park, W. Y., Park, D. Y., Kim, J. Y., … Choi, K. U. (2017). Programmed death-ligand 1 (PD-L1) expression in tumour cell and tumour infiltrating lymphocytes of HER2-positive breast cancer and its prognostic value. *Scientific Reports*, *7*, 11671.

Li, W., Katoh, H., Wang, L., Yu, X., Du, Z., Yan, X., … Liu, Y. (2013). *FOXP3* Regulates Sensitivity of Cancer Cells to Irradiation by Transcriptional Repression of *BRCA1*. *Cancer Research*, *73*(7), 10.1158/0008–5472.CAN–12–2481. http://doi.org/10.1158/0008-5472.CAN-12-2481

Li, Z., Dong, P., Ren, M., Song, Y., Qian, X., Yang, Y., … Liu, F. (2016). PD-L1 Expression Is Associated with Tumor FOXP3^{+} Regulatory T-Cell Infiltration of Breast Cancer and Poor Prognosis of Patient. *Journal of Cancer*, *7*(7), 784–793.

Liu, R., Wang, L., Chen, G., Katoh, H., Chen, C., Liu, Y., & Zheng, P. (2009). FOXP3 Up-regulates *p21* Expression by Site-specific Inhibition of Histone Deacetylase 2/4 Association to the Locus. *Cancer Research*, *69*(6), 2252–2259.

Liu, Y., Wang, Y., Li, W., Zheng, P., & Liu, Y. (2009). ATF2 and c-Jun-Mediated Induction of FoxP3 for Experimental Therapy of Mammary Tumor in the Mouse. *Cancer Research*, *69*(14), 5954–5960.

Lopes, J.E., Torgerson, T.R., Schubert, L.A., Anover, S.D., Ocheltree, E.L., Ochs, H.D., & Ziegler, S.F. (2006). Analysis of FOXP3 reveals multiple domains required for its function as a transcriptional repressor. *J Immunol, 177*(5), 3133-42.

Magg, T., Mannert, J., Ellwart, J.W., Schmid, I., & Albert, M.H. (2012). Subcellular localization of FOXP3 in human regulatory and nonregulatory T cells. *Eur J Immunol, 42*(6), 1627-1638.

Morawski, P. A., Mehra, P., Chen, C., Bhatti, T., & Wells, A. D. (2013). Foxp3 Protein Stability Is Regulated by Cyclin-dependent Kinase 2. *The Journal of Biological Chemistry, 288*(34), 24494–24502.

Mourmouras, V., Fimiani, M., Rubegni, P., Epistolato, M.C., Malagnino, V., Cardone, C., …,

Miracco, C. (2007). Evaluation of tumour-infiltrating CD4+CD25+FOXP3+ regulatory T cells in human cutaneous benign and atypical naevi, melanomas and melanoma metastases. *Br J Dermatol, 157*(3), 531-9.

Sadlon, T.J., Wilkinson, B.G., Pederson, S., Brown, C.Y., Bresatz, S., Gargett, T., … Barry, S.C. (2010). Genome-wide identification of human FOXP3 target genes in natural regulatory T cells. *J Immunol, 185*(2), 1071-81.

Schubert, L.A., Jeffery, E., Zhang, Y., Ramsdell, F., & Ziegler S.F. (2001). Scurfin (FOXP3) acts as a repressor of transcription and regulates T cell activation. *J Biol Chem, 276*(40), 37672-37679.

Van Loosdregt, J., Vercoulen, Y., Guichelaar, T., Gent, Y. Y., Beekman, J. M., van Beekum, O., ..., Coffer, P. J. (2010). Regulation of Treg functionality by acetylation-mediated Foxp3 protein stabilization. *Blood,* 115(5), 965-974.

Van Loosdregt, J., Brunen, D., Fleskens, V., Pals, C. E. G. M., Lam, E. W. F., & Coffer, P. J. (2011). Rapid Temporal Control of Foxp3 Protein Degradation by Sirtuin-1. *PLoS ONE*, *6*(4), e19047.

Van Loosdregt, J., Fleskens, V., Fu, J., Brenkman, A. B., Bekker, C. P. J., Pals, C. E. G. M., … Coffer, P. J. (2013). Stabilization of the Transcription Factor Foxp3 by the Deubiquitinase USP7 Increases Treg-Cell-Suppressive Capacity. *Immunity*, *39*(2), 259–271.

Wang, B., Lin, D., Li, C., & Tucker, P. (2003). Multiple domains define the expression and regulatory properties of Foxp1 forkhead transcriptional repressors. *J Biol Chem, 278*(27), 24259-24268.

Wang, L., Liu, R., Li, W., Chen, C., Katoh, H., Chen, G.Y., …, Zheng, P. (2009) Somatic single

hits inactivate the X-linked tumor suppressor *FOXP3* in the Prostate. *Cancer Cell, 16*(4), 336-346.

Wang, L., Liu, R., Ribick, M., Zheng, P., & Liu, Y. (2010). *FOXP3* as X-linked Tumor Suppressor. *Discovery Medicine*, *10*(53), 322–328.

Winnepenninckx, V., Lazar, V., Michiels, S., Dessen, P., Stas, M., Alonso, S.R., ..., Spatz, A. (2006) Gene Expression Profiling of Primary Cutaneous Melanoma and Clinical Outcome. *J Natl Cancer Inst, 98*(7), 472-82.

Ziegler, S.F. (2006). FOXP3: of mice and men. *Annu Rev Immunol, 24*, 209-26.

Zuo, T., Liu, R., Zhang, H., Chang, X., Liu, Y., Wang, L., … Liu, Y. (2007a). FOXP3 is a novel transcriptional repressor for the breast cancer oncogene SKP2. *The Journal of Clinical Investigation, 117(12), 3765–3773.*

Zuo, T., Wang, L., Morrison, C., Chang, X., Zhang, H., Li, W., … Liu, Y. (2007b). FOXP3 is an X-linked breast cancer suppressor gene and an important repressor of the *HER2/ErbB2* oncogene. *Cell, 129*(7), 1275–1286.

Chapter 5- Overall conclusion and discussion

The unexplained observation that men have a higher incidence and worse prognosis of melanoma is intriguing because unraveling the mechanisms that contribute to this sex effect will provide insight into the pathophysiology of this aggressive and poorly understood malignancy. Ultimately this information can potentially lead to a better understanding of how to prevent and/or control this disease in both men and women. One of the most obvious differences between melanoma cells in men and women is the baseline number of X chromosomes they contain. The main objective of this project was to explore the X chromosome as an explanation for some of the differences in the behavior of melanoma between the sexes. It is now clear that the X chromosome affects the biology of melanoma. Females who have lost an X chromosome in their tumors have an unfavorable outcome relative to females with two X chromosomes. We showed that a somatic loss of one X chromosome occurs in approximately a quarter of female melanoma patients and is associated with a shorter period of distant metastasis-free survival. In addition to proving that loss of an entire X chromosome is prognostically relevant, a decrease or loss of expression of two specific genes on the X chromosome, *PPP2R3B* and *FOXP3,* have been demonstrated to impact the pathophysiology of melanoma.

In human melanomas, PR70 mRNA and protein expression levels correlate with distant metastasis-free and overall survival respectively. The tumor suppressive role of PR70 in melanoma was further proven by xenograft experiments. PR70 overexpression was shown to decrease both tumorigenicity in mice and colony formation in soft agar, compared to knock down of PR70 that displayed the opposite effect. The proliferation rate of melanoma cells was related to the expression of PR70 in six different situations. Endogenous PR70 expression levels were observed to have a positive correlation with doubling time in a panel of melanoma cells lines. Exogenous

overexpression of PR70 showed a decrease in the rate of proliferation of melanoma cells. Correspondingly, in the xenograft tumors that developed in the mice, higher levels of PR70 were associated with a lower rate of tumor growth and a lower mitotic rate by PH3 immunostaining. And lastly, ex vivo human tumor tissue showed an inverse correlation between PR70 and PH3 staining.

Exogenous FOXP3 was also shown to have an inhibitory effect on melanoma cell proliferation. Overexpression of all five of the known isoforms, FOXP3FL, FOXP3ΔE3, FOXP3ΔE8, FOXP3ΔE3ΔE4 and FOXP3ΔE3ΔE8, showed a similar dose-dependent decrease in proliferation. Cell cycle analysis demonstrated that overexpression of all of the isoforms, except FOXP3ΔE3ΔE4, resulted in an increase in the percent of cells in the G0/G1 phase of the cell cycle. Similarly, PR70 expression also resulted in an accumulation of cells in the G0/G1 phase of the cell cycle. The significance of this finding is that FOXP3 and PR70 have an impact on one of the strongest prognostic factors in melanoma, mitotic rate.

Now that we have identified FOXP3 and PR70 as having important suppressive effects on cell proliferation and cell cycle progression, the next logical question is how these genes/proteins are dysregulated in melanoma. In men a single mutation has the potential to inactivate FOXP3. Human prostate cancers often harbor somatic *FOXP3* deletions or missense mutations that lead to reduced expression levels compared to benign prostatic epithelial cells in the same patient (Wang et al., 2009). Since *FOXP3* is subject to inactivation, a single mutation in *FOXP3* can be equally debilitating to women, due to selective inactivation of the X chromosome containing the wildtype allele. Somatic mutations and deletions of *FOXP3* are common in human breast cancers and analysis of mammary carcinomas that develop in mice with heterozygous *FOXP3* mutations showed skewed X-inactivation of the X chromosome with the wild-type *FOXP3* allele in all cases

(Zuo et al., 2007). Unlike other tumors, *FOXP3* gene mutations have not been shown to occur in human melanoma (Tan et al., 2012). Similarly, mutations in the *PPP2R3B* gene do not appear to contribute to its altered expression levels in melanoma. Of the 167 human samples that we sequenced only one was found to contain an inactivating mutation in *PPP2R3B.* Further research is required to better understand the mechanisms of downregulation of *PPP2R3B* and *FOXP3* in melanoma given that somatic mutations are rare. *PPP2R3B* has been shown to have a high rate of DNA methylation in primary melanoma cells compared to normal human melanocytes (Duan et al., 2018). Methylation of DNA is one mechanism of downregulating tumor suppressor genes that could contribute to lower levels of PR70 expression.

Even though it is not yet known how *PPP2R3B* and *FOXP3* are downregulated in melanoma, therapies that upregulate their expression have the potential to be effective strategies to control melanoma. As previously described, therapies that increase the stability of FOXP3 by increasing protein acetylation and decreasing protein phosphorylation and ubiquination have been shown to increase the suppressive activity of FOXP3. Interestingly, some of the agents that have been shown to increase the transcription or stability of the FOXP3 protein, such as Vorinostat and TGFβ, have also been shown to activate PP2A activity (Perrotti & Neviani, 2013). This naturally elicits the question of whether FOXP3 and PR70 directly or indirectly influence each other. Currently there is no evidence that FOXP3 regulates the transcription of *PPP2R3B* directly or indirectly through the transcription of other proteins involved in its regulation. Preliminary data (not shown) found no effect of FOXP3 overexpression on PR70 mRNA levels. Further studies are necessary to determine if FOXP3's stability can be increased through dephosphorylation by PR70. This mechanism is conceivable since cyclin dependent kinase 2 (CDK2) has also been shown to

decrease the stability of FOXP3 by phosphorylating it and PR70 shares other protein targets with CDK2, such as CDC6 (Morawski et al., 2013).

It is also possible that the relationship between FOXP3 and PR70 is more complex than a direct interaction. We showed that FOXP3 has an inhibitory effect on cell cycle progression and others have shown that FOXP3 overexpression downregulates the expression of cyclin dependent kinases and upregulates the expression of cyclin dependent kinase inhibitors (Zhang & Sun, 2010; Liu et al., 2009). PR70 has been shown by us, and others, to interfere with the initiation of transcription through dephosphorylation of cyclin dependent kinase targets such as CDC6. Thus FOXP3 and PR70 may have a synergistic inhibitory effect on cell cycle progression by hindering cyclin dependent kinases by decreasing their transcription, increasing the expression of their inhibitors and by decreasing the phosphorylation of their target proteins.

Even if FOXP3 and PR70 are not acting on the same pathway, the fact that they both decrease proliferation without impacting ERK activation means that they have the potential to complement anti-BRAF therapies (Zhang & Sun, 2010; unpublished data). New combinations of drugs are continuously being tested in clinical trials to achieve the fastest, most complete and durable anti-tumor response. We have identified FOXP3 and PR70 as having important suppressive effects on cell proliferation and cell cycle progression with the hope that novel therapies can be developed that take advantage of upregulating these proteins as effective strategies to combat melanoma. Treatments targeting these X-linked proteins have the potential to narrow the sex-specific discrepancies in prognosis that exist in melanoma today and more importantly to improve the survival of both men and women with this tenacious disease.

Chapter 6- Contribution to the field

Through this research two new prognostic factors have been identified in melanoma. The first marker of poor prognosis is a loss of an X-chromosome which has been shown to be associated with a distant metastasis-free survival of less than 3 years in females. The number of X-chromosomes in a patient's melanoma cells can be determined by hybridizing X-centromere probes to a slide using fluorescent in situ hybridization (FISH). Testing by FISH is ideal because compared to other techniques it is cheaper, faster and can be performed on readily available formalin-fixed paraffin embedded (FFPE) tissue. Using FISH to establish the number of X-chromosomes in a melanoma sample can easily be incorporated as an adjunct test in the clinical setting to help stratify a patient's relative risk of progression of disease and help guide clinical management decisions.

The second prognostic factor uncovered in this research is PR70. Increasing levels of both *PPP2R3B* mRNA and PR70 protein expression are associated with a better prognosis for melanoma patients. mRNA can be extracted from FFPE material and was shown to correlate with distant metastasis-free survival as a continuous variable. Protein levels of PR70 can be semi-quantitatively assessed by IHC which is another simple and relatively inexpensive adjunct test that can be performed to help predict the clinical outcome for melanoma patients.

In addition to identifying prognostic factors, the other main contribution of this project was the discovery of new X-linked tumor suppressor genes in melanoma. FOXP3 and its isoforms were identified as putative tumor suppressor proteins in melanoma based on their ability to decrease cell proliferation. PR70 was proven to behave as an important tumor suppressor in melanoma by delaying cell cycle progression through the G1 to S phase checkpoint and inhibiting cell proliferation through dephosphorylation of CDC6 and pRb. This work has paved the way to

investigate if PR70's inhibitory effect on cell proliferation and cell cycle progression can be targeted therapeutically and if expression levels can be used as a predictive marker of response to treatment.

References

Bailey, P., Chang, D.K., Nones, K., Johns, A.L., Patch, A.M., Gingras, M.C., … Grimmond, S.M. (2016). Genomic analyses identify molecular subtypes of pancreatic cancer. *Nature, 531*(7592), 47-52.

Chaligné, R., Popova, T., Mendoza-Parra, M.-A., Saleem, M.-A. M., Gentien, D., Ban, K., … Heard, E. (2015). The inactive X chromosome is epigenetically unstable and transcriptionally labile in breast cancer. *Genome Research*, *25*(4), 488–503.

Davis, A. J., Yan, Z., Martinez, B., & Mumby, M. C. (2008). Protein Phosphatase 2A Is Targeted to Cell Division Control Protein 6 by a Calcium-binding Regulatory Subunit. *The Journal of Biological Chemistry*, *283*(23), 16104–16114.

Duan, H., Jiang, K., Wei, D., Zhang, L., Cheng, D., Lv, M., … He, A. (2018). Identification of epigenetically altered genes and potential gene targets in melanoma using bioinformatic methods. *OncoTargets and Therapy*, *11*, 9–15.

Dunford, A., Weinstock, D. M., Savova, V., Schumacher, S. E., Cleary, J. P., Yoda, A., … Lane, A. A. (2017). Tumor suppressor genes that escape from X-inactivation contribute to cancer sex bias. *Nature Genetics*, *49*(1), 10–16.

O'Connor, C.M., Perl, A., Leonard, D., Sangodkar, J., & Narla, G. (2018). Therapeutic targeting of PP2A. *Int J Biochem Cell Biol, 96,* 182-193.

Edgren, G., Liang, L., Adami, H., & Chang, E. (2012). Enigmatic sex disparities in cancer incidence. *European Journal of Epidemiology, 27*(3), 187-196.

Ji J., Zöller B., Sundquist J., & Sundquist K. (2016). Risk of solid tumors and hematological malignancy in persons with Turner and Klinefelter syndromes: A national cohort study. *Int. J. Cancer 139*, 754–758.

Kaneko, S., & Li, X. (2018). X chromosome protects against bladder cancer in females via a *KDM6A*-dependent epigenetic mechanism. *Science Advances*, *4*(6), eaar5598.

Kauko, O. & Westermarck, J. (2018). Non-genomic mechanisms of protein phosphatase 2A (PP2A) regulation in cancer. *Int J Biochem Cell Biol, 96,* 157-164.

Li, X., Zhang, Y., Zheng, L., Liu, M., Chen, C. D., & Jiang, H. (2018). UTX is an escape from X-inactivation tumor-suppressor in B cell lymphoma. *Nature Communications*, *9*, 2720.

Liu, Y., Wang, Y., Li, W., Zheng, P., & Liu, Y. (2009). ATF2 and c-Jun-Mediated Induction of FoxP3 for Experimental Therapy of Mammary Tumor in the Mouse. *Cancer Research*, *69*(14), 5954–5960.

Magenta, A., Fasanaro, P., Romani, S., Di Stefano, V., Capogrossi, M. C., & Martelli, F. (2008). Protein Phosphatase 2A Subunit PR70 Interacts with pRb and Mediates Its Dephosphorylation. *Molecular and Cellular Biology*, *28*(2), 873–882.

Meeusen, B. & Janssens, V. (2018). Tumor suppressive protein phosphatases in human cancer: Emerging targets for therapeutic intervention and tumor stratification. *Int J Biochem Cell Biol., 96,* 98-134.

Miller, V. M. (2014). Why are sex and gender important to basic physiology and translational and individualized medicine? *American Journal of Physiology - Heart and Circulatory Physiology*, *306*(6), H781–H788.

Morawski, P. A., Mehra, P., Chen, C., Bhatti, T., & Wells, A. D. (2013). Foxp3 Protein Stability Is Regulated by Cyclin-dependent Kinase 2. *The Journal of Biological Chemistry, 288*(34), 24494–24502.

Ozbalkan, Z., Bagişlar, S., Kiraz, S., Akyerli, C.B., Ozer, H.T., Yavuz, S., …, Ozçelik T. (2005).

Skewed X chromosome inactivation in blood cells of women with scleroderma. *Arthritis Rheum*, *52*(5), 1564-1570.

Perrotti, D. & Neviani, P. (2013). Protein phosphatase 2A: a target for anticancer therapy. *Lancet Oncol, 14,* e229–38.

Rivera, M.N., Kim, W.J., Wells, J., Driscoll, D.R., Brannigan, B.W., Han, M., …, Haber, D.A. (2007). An X chromosome gene, WTX, is commonly inactivated in Wilms tumor. *Science, 315*(5812), 642-5.

Sharabi, A., Kasper, I., & Tsokos, G. C. (2018). The serine/threonine protein phosphatase 2A controls autoimmunity. *Clin Immunol, 186*, 38-42.

Spatz, A., Stock, N., Batist, G., & van Kempen, L.C. (2010). The biology of melanoma prognostic factors. *Discov Med*, *10*(50), 87-93.

Tan, B., Behran, A., Anaka M, Vella, L., Cebon, J., Mariadason, J. M., & Chen, W. (2012). FOXP3 is not mutated in human melanoma. *Pigment Cell Melanoma Res. 25*, 398–400.

Van Haaften, G., Dalgliesh, G. L., Davies, H., Chen, L., Bignell, G., Greenman, C., … Futreal, P. A. (2009). Somatic mutations of the histone H3K27 demethylase, *UTX*, in human cancer. *Nature Genetics*, *41*(5), 521–523.

Wang, L., Liu, R., Li, W., Chen, C., Katoh, H., Chen, G.Y., …, Zheng, P. (2009) Somatic single hits inactivate the X-linked tumor suppressor *FOXP3* in the Prostate. *Cancer Cell, 16*(4), 336-346.

Wizemann, T.M., & Pardue, M.L., editors. Institute of Medicine (US) Committee on Understanding the Biology of Sex and Gender Differences. Exploring the Biological Contributions to Human Health: Does Sex Matter? Washington (DC): National

Academies Press (US); 2001. 2, Every Cell Has a Sex. Available from: https://www.ncbi.nlm.nih.gov/books/NBK222291/

Zhang, H-Y. & Sun, H. Up-regulation of Foxp3 inhibits cell proliferation, migration and invasion in epithelial ovarian cancer. (2010). *Cancer Letters, 287*(1), 91–97.

Zuo, T., Wang, L., Morrison, C., Chang, X., Zhang, H., Li, W., … Liu, Y. (2007). FOXP3 is an X-linked breast cancer suppressor gene and an important repressor of the HER2/ErbB2 oncogene. Cell, 129(7), 1275–1286.